Project Number: ME-MWR-1234

DYNAMIC MODELING OF WOODEN BASEBALL BATS

A Major Qualifying Project Report

Submitted to the Faculty

of the

WORCESTER POLYTECHNIC INSTITUTE

in partial fulfillment of the requirements for the

Degree of Bachelor of Science

in Mechanical Engineering

by

Ryan Lawrence

_____

Dennis Proulx

_____

Erica Stults

_____

Date: April 30, 2009

Approved:

_____

Prof. Mark W. Richman, Advisor

Abstract

The objective of this project is to develop a dynamic model that predicts the performance of wooden baseball bats. The model is sensitive to the manner in which the mass is distributed throughout out the bat as measured by its total mass, its moment of inertia, and the axial location of the center of its center of mass. Using these properties of the bat, we employ rigid body dynamics and the effects of inelastic bat/ball collisions to investigate how the outgoing ball velocity is affected by changes in the mass distribution of the bat, the minimum and maximum radii of the bat, and the locations along the bat of minimum and maximum radii. The results are influenced by the coefficient of restitution between the bat and the ball, the angular velocity of the swing, and the dynamic dependence of the angular velocity of the swing on the moment of inertia of the bat. Ultimately, we highlight how adjustments to the shape of the bat might improve the outgoing velocity of the ball.

Table of Contents

Table of Figures

List of Nomenclature

A, B, C, D: Non-dimensional constants to determine radial profile of cubic bat

d: Distance from the knob to the center of rotation of the bat before collision

d': Distance from the knob to the center of rotation of the bat after collision

e: Coefficient of restitution of the bat-ball collision

f, g, k: Constants determined by the boundary conditions of the cupping analysis

h: Depth of cup

I_c: Moment of inertia about the axial center of mass of the bat

J_c: Non-dimensional moment of inertia about the axial center of mass of the bat

I_o: Moment of inertia about x=0 of the bat

J_o: Non-dimensional moment of inertia about x=0 of the bat

I_R: Moment of inertia about the center of rotation, x=-d

J_R: Non-dimensional moment of inertia about the center of rotation, x=-d

L: Length of baseball bat

m_1: Mass of baseball bat

M_1: Non-dimensional mass of baseball bat

m_2: Mass of the baseball

M: Non-dimensional mass (m_1/m_2)

P: Axial location of R_{MIN}

Q: Axial location of R_{MAX}

r: The sum of r_1 and r_0, divided by the length, L

r_0: Radius of the bat at x=0

R_0: Non-dimensional radius of the bat at x=0

r_1: Radius of the bat at x=L

R_1: Non-dimensional radius of the bat at x=L

R_c: Maximum radius of the cup

r_i: Cup radius as a function of x

r_{MAX}: Maximum radius of the baseball bat

R_{MAX}: Non-dimensional maximum radius of the baseball bat

r_{MIN}: Minimum radius of the baseball bat

R_{MIN}: Non-dimensional minimum radius of the baseball bat

t: Time required for swing of baseball bat

T: Torque applied

r(x): Radial profile of baseball bat, in terms of x

v_1: Linear velocity of the impact point of the bat before impact

v'_1: Linear velocity of the impact point of the bat after impact

V_1: Non-dimensional linear velocity of the impact point of the bat before impact

V'_1: Non-dimensional linear velocity of the impact point of the bat after impact

v_2: Velocity of the baseball prior to impact

v'_2: Velocity of the baseball after impact

V_2: Non-dimensional velocity of the baseball prior to impact

V'_2: Non-dimensional velocity of the baseball after impact

v_c: Linear velocity of the center of mass of the bat before impact

v'_c: Linear velocity of the center of mass of the bat after impact

V_c: Non-dimensional linear velocity of the center of mass of the bat before impact

V'_c: Non-dimensional linear velocity of the center of mass of the bat after impact

v_{MAX}: Maximum outgoing ball velocity

V_{MAX}: Non-dimensional maximum outgoing ball velocity

x: Distance measured along the bat from the knob

X: Non-dimensional distance measured along baseball bat from the knob

$\bar{x}$: Axial location of the center of mass of the baseball bat

$\bar{X}$: Non-dimensional axial location of the center of mass of the baseball bat

x_{MAX}: Location of impact which produces maximum v'_2

X_{MAX}: Non-dimensional location of impact which produces maximum v'_2

y: Distance from the center of mass of the bat to impact location

Y: Non-dimensional distance from the center of mass of the bat to impact location

y_{MAX}: Location of impact which produces v_{MAX}

Y_{MAX}: Non-dimensional location of impact which produces V_{MAX}

z: Axis representing the depth into the bat from the barrel end

α: Angular acceleration of baseball bat

θ: Angular displacement of the baseball bat

ρ: Density of baseball bat

ω: Angular velocity of the baseball bat before impact

ω': Angular velocity of the baseball bat after impact

ω_0: Angular velocity resultant from the linear acceleration effects of the swing

Ω: Non-dimensional angular velocity of the baseball bat before impact

Ω': Non-dimensional angular velocity of the baseball bat after impact

Executive Summary

The purpose of this project was to construct and apply a rigid-body dynamic model of a bat-ball collision in order to determine and optimize the performance of wooden baseball bats. The bat radial profile was modeled as a cubic polynomial in order to capture the general shape of a typical bat and yet yield a simple mathematical model that could easily be manipulated. Our preliminary analysis was based on total bat mass and mass distribution throughout the bat. Variances of bat mass, center of mass, and moment of inertia were explored for a range of bat shapes. These analyses carried over to the dynamic modeling of performance. Maximum ball exit speed and optimal impact location were graphically analyzed by varying the geometric profile of a bat. Finally, we expanded upon our simple dynamic model by considering how swing speed is affected by moment of inertia about the center of rotation. This allowed us to account for the competing effects of effective mass and swing speed on outgoing ball velocity. Finally, using our complete model we analyzed the popular practice of “cupping” the barrel-end of the bat to comment on the net effect.

We first defined bat mass, center of mass, and moment of inertia in terms of the length, density, and radial profile of any given bat. We then defined our cubic bat profile in terms of four parameters A, B, C, and D, such that each parameter is a coefficient in the four-term cubic function. Combining our equations for bat mass, center of mass, and moment of inertia with our cubic function, we developed these properties as functions of A, B, C, and D. These expressions can be evaluated for any given cubic radial profile. This procedure serves as the foundation of our model.

Our dynamic model of the bat-ball collision was based on four physical equations: conservation of linear momentum, conservation of angular momentum, the definition of the coefficient of restitution, and the relationship between the velocity of the bat's mass center and the velocity of the impact point. The bat mass, mass center, and moment of inertia are requisite quantities that are calculated in the manner described previously. Solving our system of four equations, we calculated four quantities: the outgoing ball velocity v_2'; the velocity of the bat center of mass just after collision v_c'; the velocity of the impact point on the bat just after collision v_1'; and the angular velocity of the bat just after collision ω'. Each was found in terms of pitched ball speed v_2, coefficient of restitution e, initial angular velocity ω, distance from bat knob to center of rotation d, and distance from bat center of mass to impact point y, and the calculated mass, center of mass, and the moment of inertia of the bat.

Finally, we incorporated into our model the effect of moment of inertia on angular velocity of the bat. This allowed us to compare the net effects of geometrical changes, as increased mass, which tends to increase ball output velocity, is often accompanied by a decrease in bat angular velocity, which tends to diminish the outgoing ball speed. Our refined model allowed us to thoughtfully analyze cases in which a small amount of material is removed from the barrel-end. This is a popular practice in baseball today, but it does not provide a clear, intuitive advantage over a standard bat. From our analysis we concluded that there is a near linear decrease in the outgoing ball velocity as the depth of the cup is increased. Although this decrease is slight, if hitting power is the only consideration, cupping results in a negative effect and should not be utilized. However, with an increase in cup depth, the angular velocity of the bat, or the swing speed, is

increased. Therefore, cupping the bat will provide an advantage if a faster swing is sought. These competing effects must be considered by the individual batter, as personal preference will determine the appropriate use of the cupping technique.

Chapter 1 Introduction

Every baseball player knows when they've hit the ball just right: the sound from the bat is different; the ball seems to fly with a little more speed; and the batter feels nothing as the bat head plows through the oncoming pitch. Although the player might not be able to explain this phenomenon, physics provides an explanation for this "sweet spot." The difference in sound occurs due to the proximity to nodes of the first two vibration modes. The high exit velocity of the ball is a result of the large transfer of momentum that occurs where combined effects of both the effective mass and linear velocity of the bat are highest. The special feel associated with the sweet spot is a consequence of low vibration energy and the angular and linear forces canceling one another at the location of the hands. Although the locations of these phenomena are slightly different and vary from bat to bat, they do occur for impacts in a similar area and their effects combine to form what is commonly referred to as the "sweet spot".

While hitting a ball on the sweet spot results in the optimum performance and feel, outside of a laboratory, the collision between bat and ball often occurs away from this optimal zone. This reality leads to the question of how the performance of a bat should be quantified. Is it best to have large hitting power in a relatively large zone; or is it more useful to have a bat with less peak power and a much larger effective hit zone? This can only be answered by the player. A homerun hitter may prefer more power in a small zone, whereas a contact hitter could require the opposite. Whatever the desired qualities, bats can be designed to suit a particular player's needs.

1.1 Review of Previous Work

The simplest way to model the collision between a baseball and a bat is a linear, one-dimensional model. By only taking into account the masses and initial velocities of the bat and ball, conservation of momentum and energy allow for easy calculation of the resultant velocities. This model, however straightforward, is essentially useless for calculating the exit velocities of the bat and ball in a real world application. To make this model more useful, a coefficient of restitution can be used to describe the energy lost as heat and vibrations during the collision. The effective mass of the bat must also be considered, as the collision normally takes place away from the center of mass (Cross 2008b, Russell 2008b).

As Cross sets up a simple model for the collision between bat and ball, Russell (2003) brings experimental values into the equation. College or professional hitters can produce a maximum force upwards of 8000 lbs on the ball. Russell (2008b) then goes on to optimize bat weight against swing speed in order to produce the highest ball exit velocities.

More important than the bat mass, however, is the bat moment of inertia. Sometimes referenced as the swing weight, the moment of inertia dictates how heavy the bat will feel when swung and is affected by the distribution of mass. Bats with higher moments of inertia, though harder to swing, will produce more effective collisions and larger batted ball speeds (Russell 2008a).

Bahill (2004) takes this concept further and applies it to the selection of the proper bat for any individual. By having the individual swing bats of different masses and moments of inertia and measuring the linear velocity of the sweet spot, the optimal

arrangement can be found. The sweet spot for this experiment was not a calculated location, but simply a defined point 29 or 26 inches from the knob for adults and children, respectively.

Similar experiments were conducted by Fleisig et. al. (2002) as a means to regulate the performance of bats. By using a three-dimensional motion analysis system, the bat could be tracked throughout a swing to determine maximum velocity and where it occurred. By loading the bats with extra mass in either the handle or the barrel, it was determined from resultant swing speed data that it was in fact the moment of inertia of the bats, not their total mass that determined the maximum swing speed.

A bat with large moment of inertia will produce a more effective and therefore more powerful collision with the ball; but the bat with large moment of inertia will be harder to accelerate to the same swing speed as a bat with low moment of inertia. Some players, such as Sammy Sosa in 2003, feel that the increased swing speed associated with a lower moment of inertia bat gives them an advantage (Russell 2004b). By drilling out the inside of a wooden bat's barrel and replacing the heavy wood with much lighter cork, the moment of inertia of the bat is decreased, allowing for larger swing speeds. Purely in terms of batted ball speed, this change is negligible. The increased bat speed is offset by a less effective collision with the ball. However, there are benefits to a lower moment of inertia bat. For a professional ball player, the removal of 1.5 oz from the barrel end "means being able to watch the ball travel an additional 5-6 feet before having to commit to a swing" (Russell 2004b). There is also a psychological advantage.

In order to characterize the performance of baseball bats, the effects of impacts all along the barrel of the bat must be considered. By holding bat properties and initial

velocities (both linear and angular) constant, impacts can be compared according to impact location. Since a bat is swung with some angular velocity, the linear velocity of any point on the bat is directly proportional to that point's distance from the handle. Therefore, the linear velocity is greatest at the end of the barrel. This location however, does not produce the greatest batted ball speed. Since the end of the barrel is located away from the center of mass of the bat, the impact with the ball produces a rotation in the bat about this center of mass, as well as linear recoil. Therefore, the effective mass of a collision at the end of the bat is less than a collision near the center of mass. It is where these two effects combine that the greatest batted ball speeds are produced (Nathan 2002, Cross 1999).

While a rigid body model of the ball bat collision is useful, it fails to consider important effects resulting from the flexibility of the bat. Vibrations traveling through the bat due to the collision with the ball not only affect what the batter feels, but also how much energy is transferred to the ball. When the ball impacts the bat in the region between the nodes of the first two vibration modes, the rigid body approximation yields accurate results for ball exit velocity. However, when the impact occurs away from this region, and these modes of vibration are excited, the rigid body approximation is no longer valid, as large amounts of energy are stored in the bat as vibrations and less energy is transferred to the ball (Nathan 2000, Cross 1999).

Some hitting coaches teach that a tighter grip can result in a higher batted ball speed. This supposedly reduces the vibrations in the bat and therefore imparts more energy on the ball. Research by Nathan et. al. (2000) has shown that by the time the first waves have reached the handle and returned to the barrel, the collision between ball and

bat is over. Both experiments and calculations have shown that the collision is independent of the method of support at either end, as long as the collision takes place away from the ends (Nathan 2000, Cross 1999, Russell 2005b).

Players associate the sweet spot of a bat not only with the optimal performance, but also with the distinct feel of an impact there. A collision occurring on the sweet spot will result in a significant reduction in sting felt by the batter on the hands. Two separate effects contribute to this phenomenon.

Any collision occurring at the center of percussion of a body will result in zero net force at the pivot. Although the pivot of a bat at the time of impact is shown by Russell (2004a) to be beyond the end of the handle and off the axis of the bat, the concept is useful in determining forces acting on the hands at this instant. When a baseball impacts the bat in the sweet spot, the combined linear recoil and moment about the center of mass cancel to produce a point on the handle with zero net force (Russell 2005c).

The other effect producing a sting in the batter's hands is the vibrations excited by the collision. Cross (1998a) argues that the first two modes of vibration are large enough to produce pain in the hands. Adair (1998) argues that the fundamental mode is solely responsible for the stinging sensation by reason of biometrics. He argues that the frequencies of all other modes are too high to be detected by receptors in the hands. Regardless, any collision occurring near the nodes of these two modes will reduce the overall vibration, and therefore sting, felt in the batter's hands (Russell 2004a).

Research by Stronge et. al. (2003) has been done into the flight of the ball and how to obtain maximum hit distance by means of modifying the swing of the bat. Based upon the initial velocity and spin of the incident pitch, it can be determined exactly how

to strike the ball to achieve optimal distance. The lift and drag that act on the ball during flight are considered, as well as the friction and energy transfer of oblique collisions.

Significant research by Axtell et. al. (2001) has also gone into the materials used for the construction of baseball bats. Comparisons considering durability, performance and feel are done and recommendations for improving existing bats are made.

1.2 Further Work to Perform

Baseball bat performance is an important consideration for players at all levels of the game. In the MLB, where players compete for multi-million dollar contracts and national championships, even a small batting advantage can have big payoffs. It is important that a player select a bat which provides an optimal balance of swing speed and effective mass.

From a design standpoint, we seek a systematic way to compare various bat geometries in order to tailor mass and moment of inertia to a particular player. According to our findings, there is currently no research in this area of bat design. Most efforts in the field have gone into describing the bat-ball impact in terms of energy transfer and vibration analysis. There has been no major study of how the shape of a baseball bat affects its performance.

The goal of this project is to create a mathematical model for the bat-ball collision which predicts bat performance as a function of geometry. This model will be used to analyze the effect of geometrical changes on the resulting performance. Ultimately, we seek to optimize bat performance by systematically investigating several radial profiles.

Chapter 2 Geometry and Mass Distribution of Wooden Bats

Here we consider the properties of the baseball bat that will appear in our dynamic model. The property that most baseball players consider is the mass of the bat. To calculate this mass we must know the density of the material from which the bat was made, ρ, the length of the bat, *L*, and the radial profile of the bat, *r(x)*, in terms of the distance, *x*, along the bat. Using these properties we can determine the total mass, m_1, of a bat with any radial profile.

$$m_1 = \int_0^L \rho\pi r(x)^2\, dx \tag{1}$$

The second property to consider is the location of the center of mass of the bat, $\bar{x}$. This is found through the first moment of the mass. The first moment of the mass is equal to the product of the mass and the location of the center of mass. This results in the equation for the center of mass:

$$\bar{x} = \int_0^L \frac{\rho\pi}{m_1} x r(x)^2\, dx \tag{2}$$

Following the center of mass, we shall consider the moment of inertia about the end of the bat, I_0. This is equal to the second moment of mass about point 0.

$$I_0 = \int_0^L \rho\pi x^2 r(x)^2 dx \tag{3}$$

Aside from the moment of inertia about the end of the bat, the moment of inertia about the center of mass, I_c, is also important to consider. The value of I_c can be found by using the parallel axis theorem; this can be accomplished by subtracting the product of the squared distance from the knob to the center of mass and the mass from the moment

of inertia about x=0. The distance to the center of mass is already known, $\bar{x}$, so the equation of the moment of inertia about the center of mass is given by:

$$I_c = \int_0^L (x - \bar{x})^2 \rho \pi r(x)^2 dx \tag{4}$$

These equations can be used to calculate properties for a bat of any known radial profile, material density, and length.

For proper analysis and comparisons in later models, these properties are used primarily in their non-dimensional form. The following lengths are non-dimensionalized by dividing by the length of the bat, L:

$$Y = \frac{y}{L} \; ; \; R = \frac{r}{L} \text{; and } X = \frac{x}{L} \quad . \tag{5}$$

An equation to non-dimensionalize the mass of the bat to be used in later linear and cubic models is

$$M_1 = \frac{m_1}{\rho \pi L^3} \quad . \tag{6}$$

The center of mass, $\bar{x}$, can also be non-dimensionalized. Because of the method by which it is derived, it cannot simply be non-dimensionalized by dividing by the length of the bat.

$$\bar{X} = \frac{m_1 \bar{x}}{\rho \pi L^4} \tag{7}$$

The last term that needs to be non-dimensionalized is the moment of inertia about the center of mass. For use in the linear and cubic models, the non-dimensionalized value of the moment of inertia about the knob is

$$J_0 = \frac{30 I_0}{\rho \pi L^5} \quad . \tag{8}$$

Using each of these non-dimensional terms we can non-dimensionalize all equations that have been derived previously. These equations are then used in our later comparisons.

To create a non-dimensionalize variable M for mass in the case of the rigid body dynamic equations, the mass of the bat, m_1, is divided by the mass of the ball, m_2. The equation to non-dimensionalize the moment of inertia in the rigid body dynamics equations, the following equation is used.

$$J_c = \frac{I_c}{m_1 L^2} \tag{9}$$

In terms of the qualities defined here, equation (1) gives us the dimensionless mass

$$M_1 = \int_0^1 R^2(X)dX \quad ; \tag{10}$$

Equation (2) gives the dimensionless axial location of the center of mass

$$\bar{X} = \int_0^1 XR^2(X)dX \quad ; \tag{11}$$

And equation (3) gives the dimensionless moment of inertia about the (X=0) end of the bat

$$J_0 = \int_0^1 X^2R^2(X)dX \quad . \tag{12}$$

2.1 Cubic Profile

A cubic profile was chosen to represent the radial profile of the baseball bat. The radius, *r*, is taken to be a function of the distance along the bat, *x*, starting at the knob. The length of the bat is taken to be *L*, and *x* therefore has a range of 0 to *L*. The global minimum radius is denoted as r_0 and the global maximum radius is denoted as r_1.

Figure 2.1: Cubic Radial Profile

The function *r(x)* can be expressed as:

$$r(x) = a + bx + cx^2 + dx^3 \tag{13}$$

where *a*, *b*, *c* and *d* are constants that determine the shape of the profile, and therefore the bat. The distance along the bat, *x*, and the radius, *r*, can be non-dimensionalized by dividing by the overall bat length, *L*.

$$X = \frac{x}{L} \tag{14}$$

$$R = \frac{r}{L} \tag{15}$$

The non-dimensional radial profile, *R*, can be written as a function of the non-dimensional length, *X*. The non-dimensional radius as a function of location on the bat is therefore:

$$R(X) = AX + BX + CX^2 + DX^3 \tag{16}$$

The constants *A*, *B*, *C* and *D* determine the shape of the profile, and therefore the bat. Four boundary conditions must be specified to obtain a particular bat shape. For this investigation, the boundary conditions that will be used are a minimum (R_{min}) and maximum (R_{max}) radius, and the locations at which the minimum *(R_{min}=R(P))* and maximum (R_{max}=R(Q)) occur on the bat, where *P* is the coordinate in *X* at which the minimum radius exists, and *Q* is the coordinate in *X* at which the maximum radius exists.

These points can be used to solve for the constants *A*, *B*, *C* and *D* by differentiating equation (16) with respect to *X* and setting the derivative equal to 0. By substituting (R_{min}=*R(P)*) and (R_{max}=*R(Q)*) into the non-dimensional radial profile, equation (16), the constants *A*, *B*, *C* and *D* can be determined.

$$D = \frac{2(P-Q)(R_{max} - R_{min})}{Q^4 - 4Q^3P + 8PQ^3 - 5P^4 - 6QP^2 + 6P^3} \tag{17}$$

$$C = \frac{3D(Q^2 - P^2)}{2(P-Q)} \tag{18}$$

$$B = \frac{3DP(P^2 - Q^2 - P)}{P-Q} \tag{19}$$

$$A = R_{min} - BP - CP^2 - DP^3 \tag{20}$$

The non-dimensional mass, center of mass and moment of inertia about the knob can all be calculated by substituting the non-dimensional radius profile into the non-dimensional equations derived in Section 1.

The non-dimensional mass of the bat, M_1, is given by substituting equation (16) into equation (10). M_1 is therefore:

$$M_1 = A^2 + AB + \frac{(2AC+B^2)}{3} + \frac{(AD+BC)}{2} + \frac{(2BD+C^2)}{5} + \frac{CD}{3} + \frac{D^2}{7} \tag{21}$$

The non-dimensional center of mass of the bat, $\bar{X}$, is given by substituting equation (16) into equation (11). $\bar{X}$ is therefore:

$$\bar{X} = \frac{1}{M_1}\left[\frac{A^2}{2} + \frac{2AB}{3} + \frac{(2AC+B^2)}{4} + \frac{(2AD+2BC)}{5} + \frac{(2BD+C^2)}{6} + \frac{2CD}{7} + \frac{D^2}{8}\right] \tag{22}$$

The non-dimensional moment of inertia of the bat about the knob, J_0, is given by substituting equation (16) into equation (12). J_0 is therefore:

$$J_0 = \frac{A^2}{3} + \frac{AB}{2} + \frac{(2AC+B^2)}{5} + \frac{(AD+BC)}{3} + \frac{(2BD+C^2)}{7} + \frac{CD}{4} + \frac{D^2}{9} \tag{23}$$

2.2 A Special Case: Linear Radial Profile

A special case of this mathematical model of a baseball bat is the example of a linear radial profile. This model represents the simplest case in which the radius varies with distance along the bat. It can be used to compare the various effects of changing one property of the bat while holding all others constant.

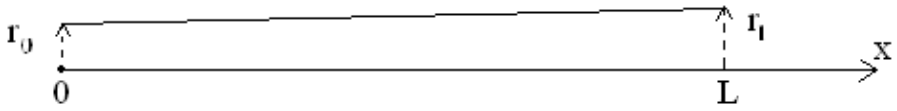

Figure 2.2: Linear Radial Profile

The dimensional radius of the bat at the knob end is denoted as r_0, and the radius of the far end of the bat is denoted by r_1. The length of this bat is defined as the variable L. The function that defines the linear profile of the radius of the bat is given by:

$$r(x) = r_0 + rx \tag{24}$$

where r is defined by equation (25).

$$r = \frac{r_1 + r_0}{L} \tag{25}$$

The first property of this bat to be calculated is the mass of the bat. This can be found by substituting equation (24) into equation (1). After integration this will be simplified to

$$m_1 = \rho\pi L^3 \left(\frac{r_0^2}{L^2} + \frac{r_0 r}{L} + \frac{r^2}{3}\right) \quad . \tag{26}$$

At this point the equation can be non-dimensionalized according to definitions (5) and (6) to use in later comparisons.

$$M_1 = \frac{1}{3}(R_1^2 + R_0 R_1 + R_0^2) \tag{27}$$

Another important quality to consider is the location $\bar{x}$ of the center of mass of the bat as the minimum and maximum radii change. After substituting equation (1) into equation (2) we obtain

$$\bar{x} = \left(\frac{\rho\pi L^4}{12m_1}\right)\left(\frac{6r_0^2}{L^2} + \frac{8r_0 r}{L} + 3r_0\right) \quad . \tag{28}$$

This equation can also be non-dimensionalized according to definition (7) to smooth the progress of later comparisons; the non-dimensional values of r_0 and r_1 must also be substituted. This results in a non-dimensional for the center of mass dependent on the non-dimensional radii.

$$\bar{X} = \frac{1}{12M_1}(R_0^2 + 2R_0R_1 + 3R_1^2) \tag{29}$$

An additional quantity to consider is the moment of inertia of the bat. The moment of inertia about the end of the bat in this linear model is defined as

$$I_0 = \left(\frac{\rho\pi L^5}{30}\right)\left(\frac{10r_0^2}{L^2} + \frac{15r_0 r}{L} + 6r^2\right) \quad . \tag{30}$$

To ease in later comparison, this equation can be non-dimensionalized according to equations (5) and (8). With the value of the non-dimensional moment of inertia from equation (8) and the non-dimensional radii at the knob and tip substituted into the equation, the non-dimensional equation can be derived.

$$J_0 = R_0^2 + 3R_0R_1 + 6R_1^2 \tag{31}$$

Equations (27), (29), and (31) can be plotted and compared in several ways to help find the optimal characteristics of a baseball bat.

The first effect we examined is that of holding the mass of the bat constant while adjusting the magnitude of the radius at the knob end of the bat. Figure 2.3 shows the variation of the dimensionless radius $R_1 = \frac{r_1}{L}$ at x = L with the corresponding radius

$R_0 = \frac{r_0}{L}$ at x = 0 for M_1 = 0.0006, 0.0008, 0.0010, 0.0012, and 0.0014. These values of M_1 were found by inputting maximum and minimum acceptable values of ρ, L, and m_1 into Equation (6). As R_0 increases, R_1 must decrease to maintain a constant mass, as expected. Figure 2.3 also demonstrates that for fixed values of R_0, R_1 increases as M_1 increases, as expected.

The second relationship that is considered is the location $\bar{X}$ of the center of mass of the bat as R_0 is changed and the overall mass of the bat M_1 is held constant, which is demonstrated in Figure 2.4. The values of non-dimensional mass used are the same values used for the previous example. The location of the center of mass when R_0 is at its maximum is 0.25 for each value of non-dimensional mass. Similarly, the location of the center of mass when R_0 is zero is 0.75 for all values of mass analyzed. This indicates that the center of mass in each case varies from three quarters the distance along the bat to one quarter the distance along the bat. The only difference in each case with different mass is the maximum values of R_1 and R_0. Excepting the minimum and maximum values of R_0, at a fixed value of R_0, the axial location of the center of mass is located closer to the knob for decreasing values of mass.

The last analysis that is performed while holding non-dimensional mass M_1 fixed, shown in Figure 2.5, is examining the moment of inertia about the knob end of the bat, J_0. As R_0 increases, the value of J_0 decreases for each fixed M_1. Also, for a fixed value of R_0, the value of J_0 decreases as M_1 increases.

Similar graphs were created to compare the effects of holding the non-dimensional moment of inertia of the bat constant, shown in Figure 2.6. The values of J_0 that were used for these graphs were found by inputting reasonable maximum and

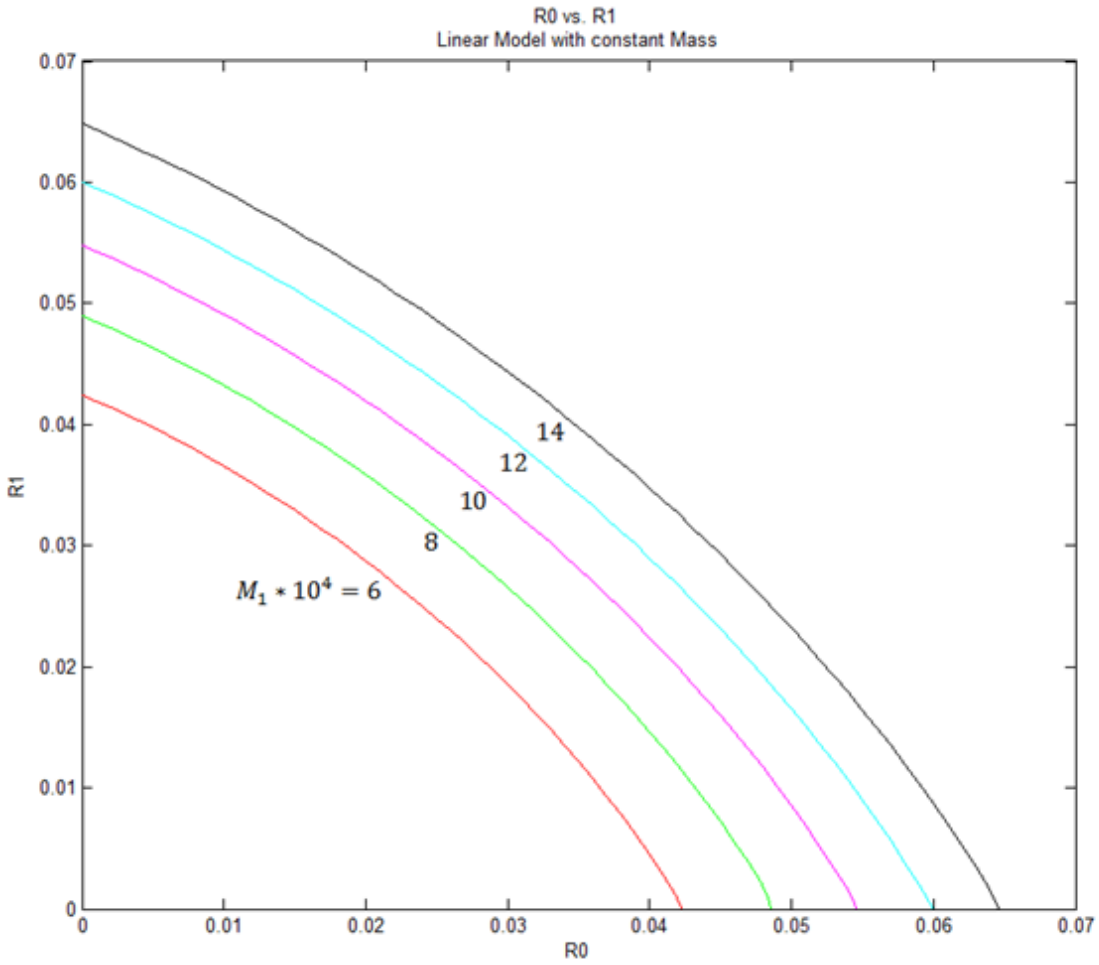

Figure 2.3: Variation of R_1 with R_0 for linear model for M_1 = 0.0006, 0.0008, 0.0010, 0.0012, and 0.0014. (MATLAB code 1, Appendix A)

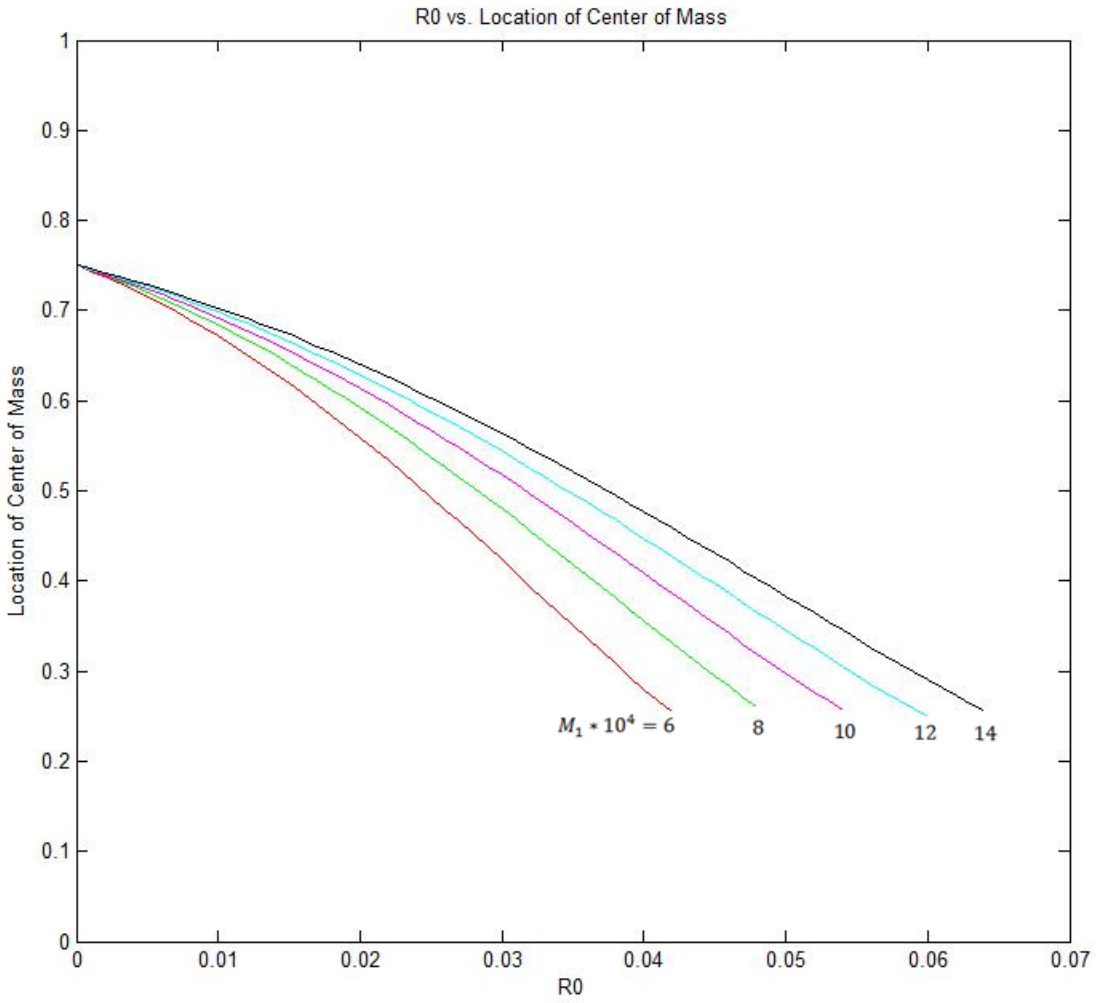

Figure 2.4: Variation of $\bar{X}$ with R_0 for linear model for M_1 = 0.0006, 0.0008, 0.0010, 0.0012, and 0.0014. (MATLAB code 2, Appendix A)

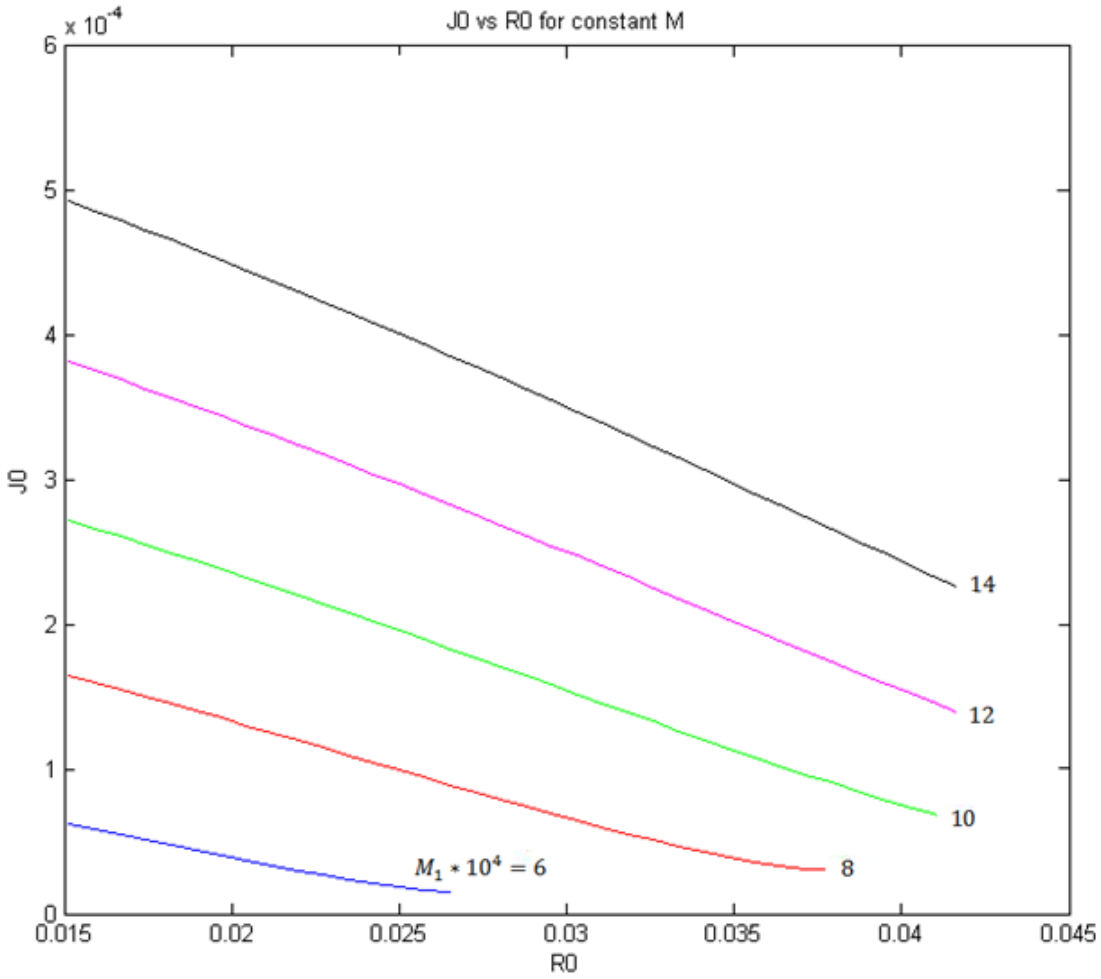

Figure 2.5: Variation of J_0 with R_0 for linear model for M_1 = 0.0002, 0.0004, 0.0006, 0.0008, and 0.0010. (MATLAB code 3, Appendix A)

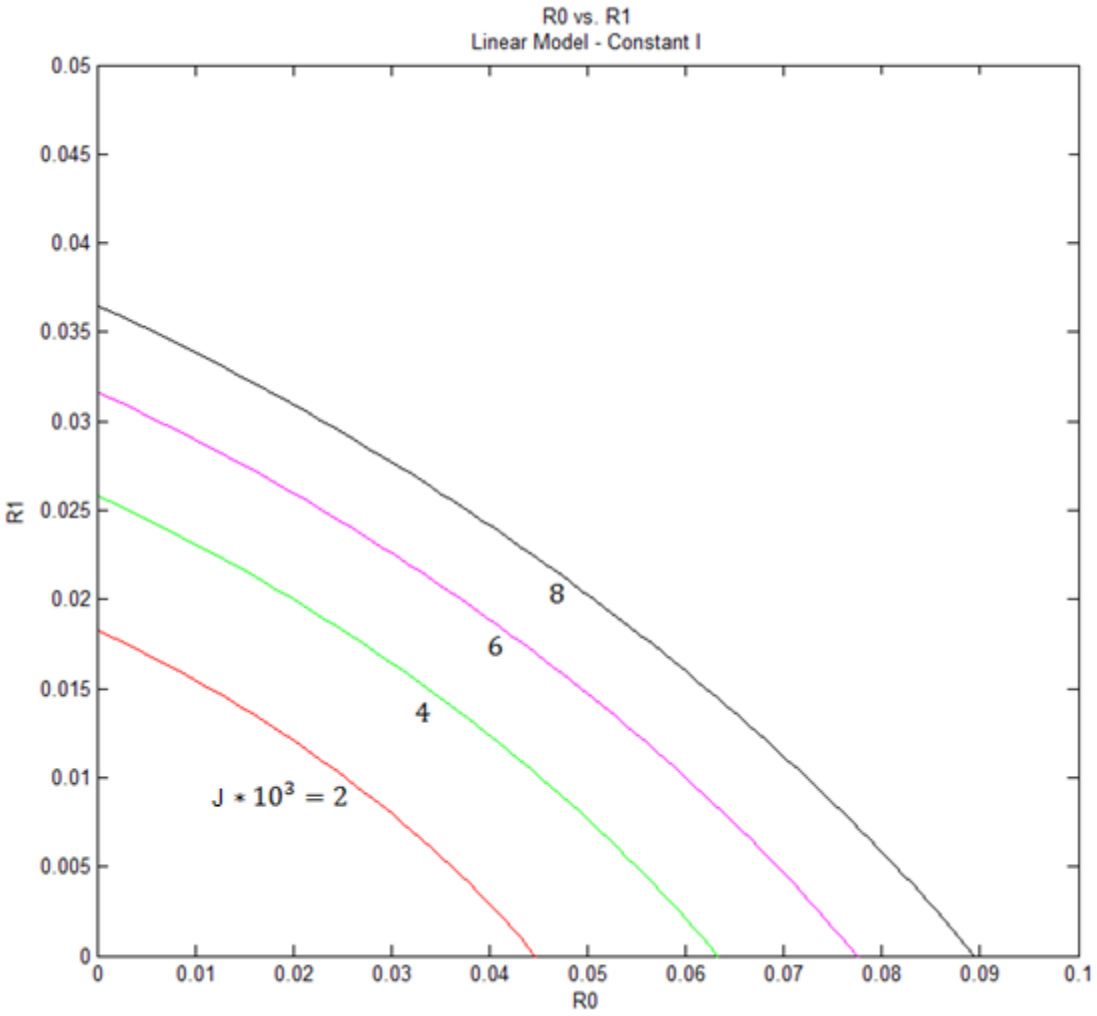

Figure 2.6: Variation of R_1 with R_0 for linear model for J_0 = 0.002, 0.004, 0.006, and 0.008. (MATLAB code 4, Appendix A)

minimum values of ρ, L, and m_1 into equation (8). These values are 0.002, 0.004, 0.006, and 0.008. As expected, the relationship between R_0 and R_1 while holding J_0 constant is very similar to the relationship while holding M_1 constant. As R_0 decreases, R_1 must increase to maintain a constant J_0. A difference that can be noted is that the maximum value of R_0 is not the same as the maximum value of R_1. This is because R_1 has a much greater effect on J_0 than does R_0. At a fixed value of R_0, R_1 increases as J_0 increases.

The relationship between R_0 and $\bar{X}$ is analyzed in Figure 2.7 for constant J_0. As with the case of constant M_1, the location of the center of mass is the same value for each value of J_0 when R_0 is equal to zero. This is also true when R_1 is equal to zero. As with the model in which mass is held fixed, when R_0 is held constant, the axial location of the center of mass moves closer to the knob as the value of the J_0 decreases.

The last graph created for the linear model for the case of constant J_0 is R_0 versus M_1, shown in Figure 2.8. To maintain a constant J_0, the mass of the bat increases as R_0 increases. Also, as J_0 increases the maximum value of R_0 increases. At a fixed value of R_0, the mass increases as J_0 increases.

2.3 A Special Case of the Cubic Profile: Zero Slopes at the Ends

As a special case of the general cubic profile given in equation (16), the locations of the zero slopes (that is the location of the minimum and maximum radius) are taken to be at the ends. Therefore, P=0 and Q=1. These profiles will be examined by first holding mass fixed and varying the end radii, and then by holding the moment of inertia fixed and varying the end radii. These calculations are all completed in non-dimensional terms, but can be easily converted back into dimensional form.

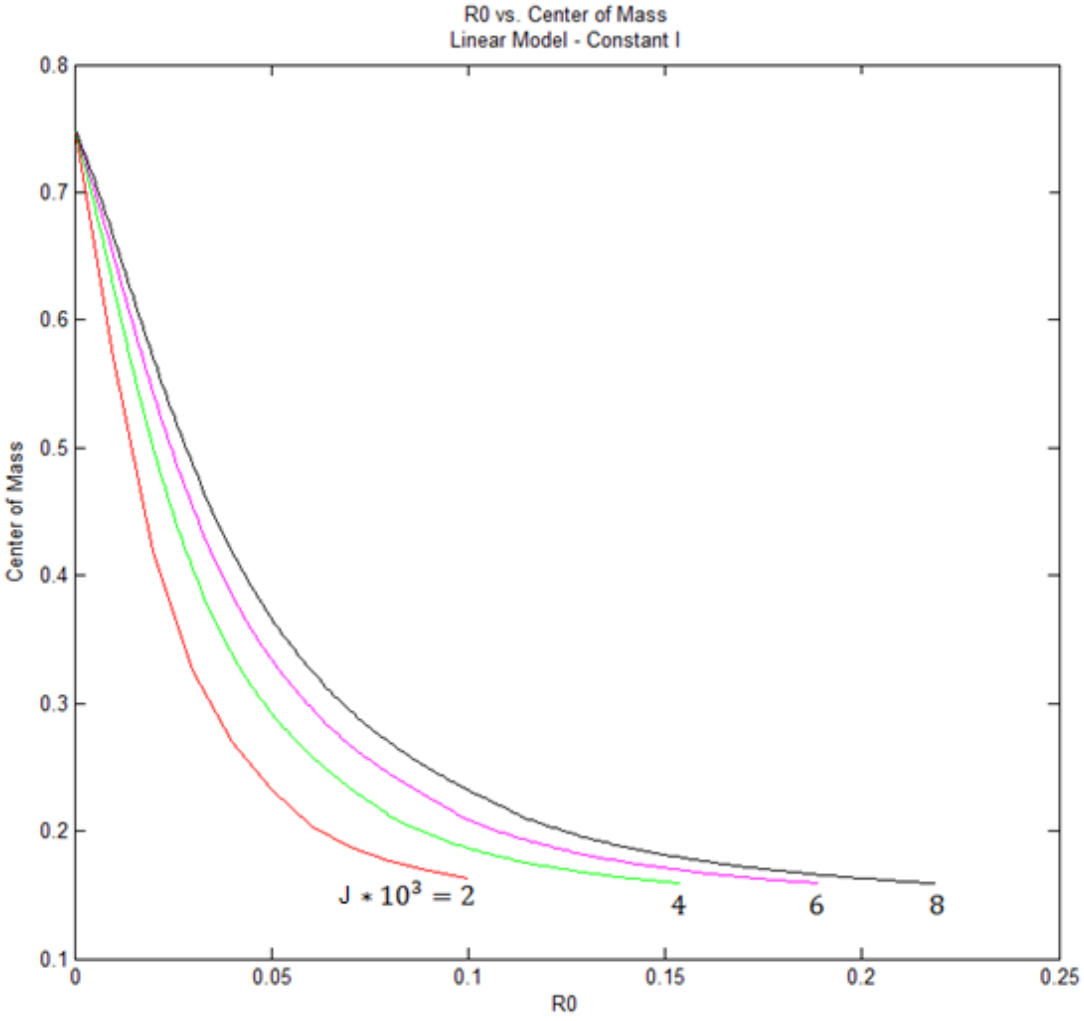

Figure 2.7: Variation of $\bar{X}$ with R_0 for linear model for J_0 = 0.002, 0.004, 0.006, and 0.008. (MATLAB code 5, Appendix A)

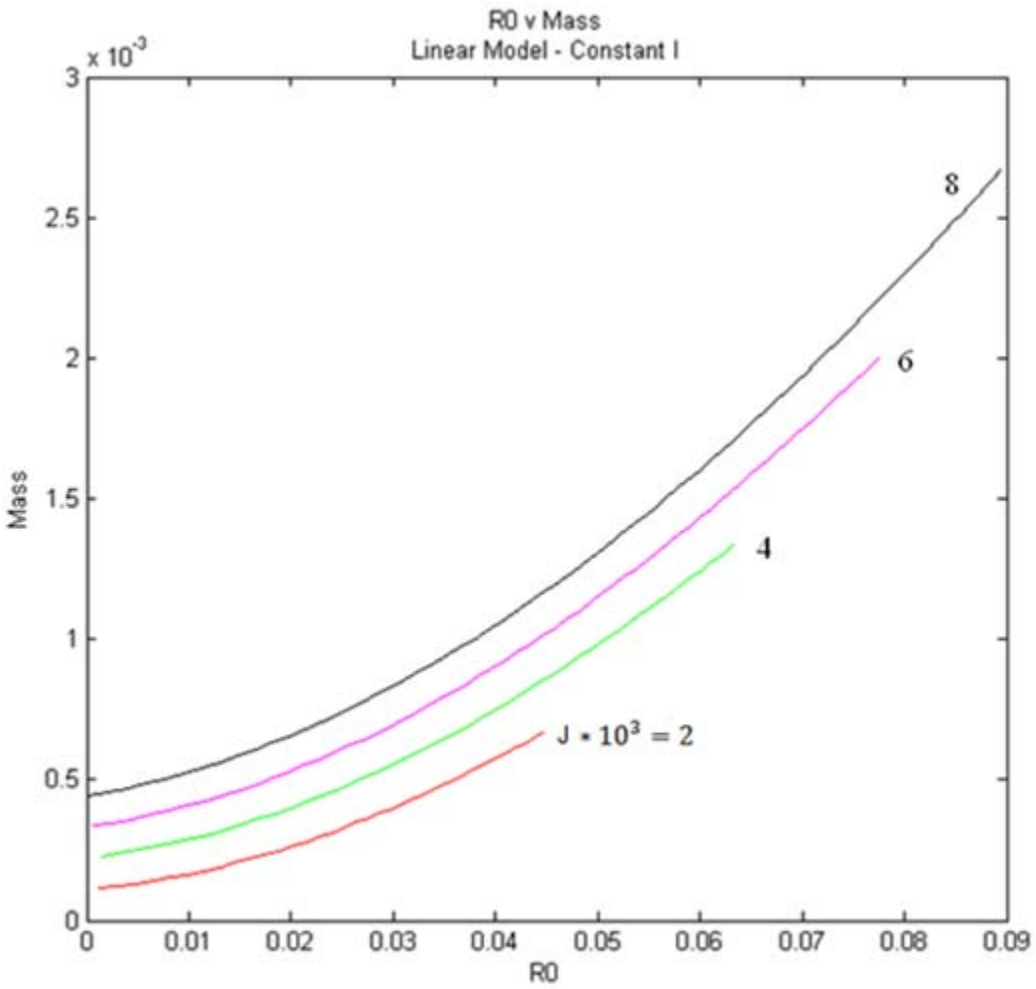

Figure 2.8: Variation of M_1 with R_0 for linear model for J_0 = 0.002, 0.004, 0.006, and 0.008. (MATLAB code 6, Appendix A)

With P=0 and Q=1, equation (16) simplifies to:

$$R(X) = A + CX^2 - \frac{2}{3}CX^3 \tag{32}$$

Equations for non-dimensional mass, M_1, non-dimensional location of the center of mass, $\overline{X}$, and non-dimensional moment of inertia about the knob, I_0, can be obtained by substituting equation (32) into equations (10), (11) and (12). These substitutions result in:

$$M_1 = A^2 + \frac{1}{3}AC + \frac{13}{315}C^2 \tag{33}$$

$$\bar{X} = \frac{1}{M_1}\left(\frac{1}{2}A^2 + \frac{7}{30}AC + \frac{2}{63}C^2\right) \tag{34}$$

$$J_0 = \frac{1}{3}A^2 + \frac{8}{45}AC + \frac{29}{1134}C^2 \tag{35}$$

Since the minimum radius (R_{min}) will be taken to occur at the handle (X=0), the value of A is always A=R_{min}=R_0. The value of the radius at the barrel end will given as R_{max}=R_1. In the plots used to illustrate the effects of changing parameters, the value of the radius at the barrel end could become lower than the radius at the handle end. However, the radius of the handle end will always be denoted as R_0 and the radius at the barrel end will always be denoted as R_1 for this special case.

The mass of a baseball bat is usually one of the two defining characteristics, along with the length, that are important to a player. For this reason, we take a bat of constant length, in this case 33 inches, and fix the mass. For simplicity of calculations, we work in non-dimensional values. For each value of non-dimensional mass, the barrel radius R_1 is taken to be a function of R_0. This value of R_1, as well as the center of mass, $\overline{X}$, and the moment of inertia about the knob, J_0, are plotted against R_0 for fixed values of M_1.

In Figure 2.9, R_1 is plotted as a function of R_0 for typical values of M_1. These values, M_1=0.0006, 0.0008, 0.0010, 0.0012, and 0.0014, are all within a reasonable range of values calculated by equation (10) for typical bat shapes. It is clearly seen that for a constant M_1, as R_0 increases, the value of R_1 decreases. That is, in order to maintain constant mass of the bat, as the handle radius is increases, the barrel radius must be decreased. It is also clear that for fixed values of R_0, the value of R_1 increases with increasing M_1. That is, if the handle radius is held constant and the mass is increased, the barrel radius must increase as well. It is important to note that the graphs of R_1 versus R_0 for fixed M_1 are symmetric about R_1=R_0, as expected.

In Figure 2.10, the non-dimensional center of mass is plotted against R_0 for the same fixed values of M_1. Note that R_0 was taken from 0 to a maximum value of $\sqrt{4M}$, since any calculation with R_0 greater than this maximum value will have an imaginary component. It is obvious that with increasing R_0 and constant M_1, the location of the center of mass decreases, that is, the location of the center of mass moves towards the knob. This is to be expected, as for a fixed mass, when the handle radius increases, the barrel radius must decrease, as seen in Figure 2.9. Therefore, the mass becomes more concentrated at the handle end, producing the expected effect. We also see that for a fixed value of R_0, as M_1 increases, the location of the center of mass will also increase. This is expected, as with a fixed handle radius, any increase in mass must increase the barrel radius, also seen in Figure 2.9, therefore concentrating the mass closer to the barrel. Lastly, we see that for a handle radius of zero, the location of the center of mass will always be in the same place, independent of mass.

Figure 2.11 illustrates variations in the non-dimensional moment of inertia, J_0,

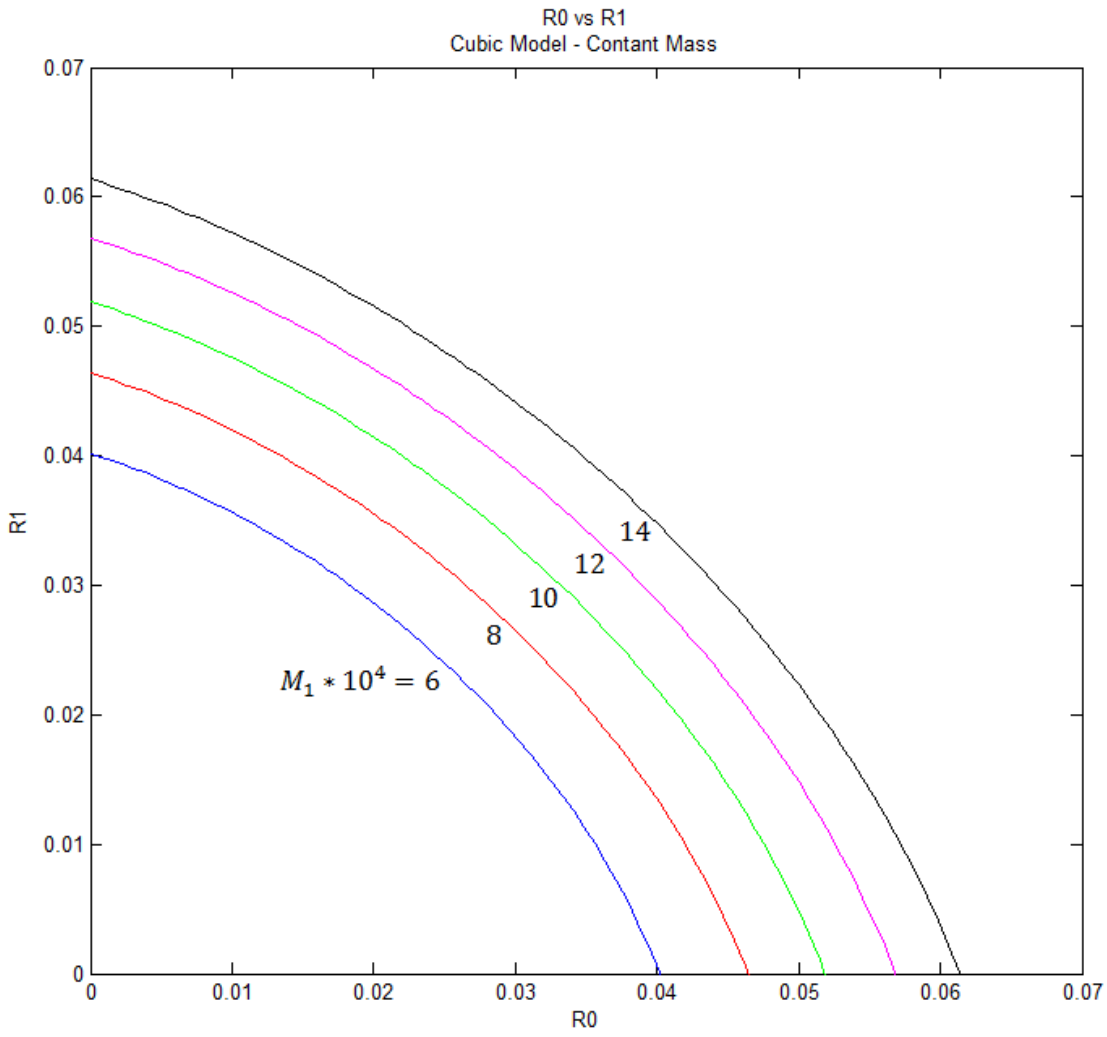

Figure 2.9: Barrel Radius R_1 as a function of Handle Radius R_0 for values of M_1=0.0006, 0.0008, 0.0010, 0.0012, and 0.0014 (MATLAB code 7, Appendix A)

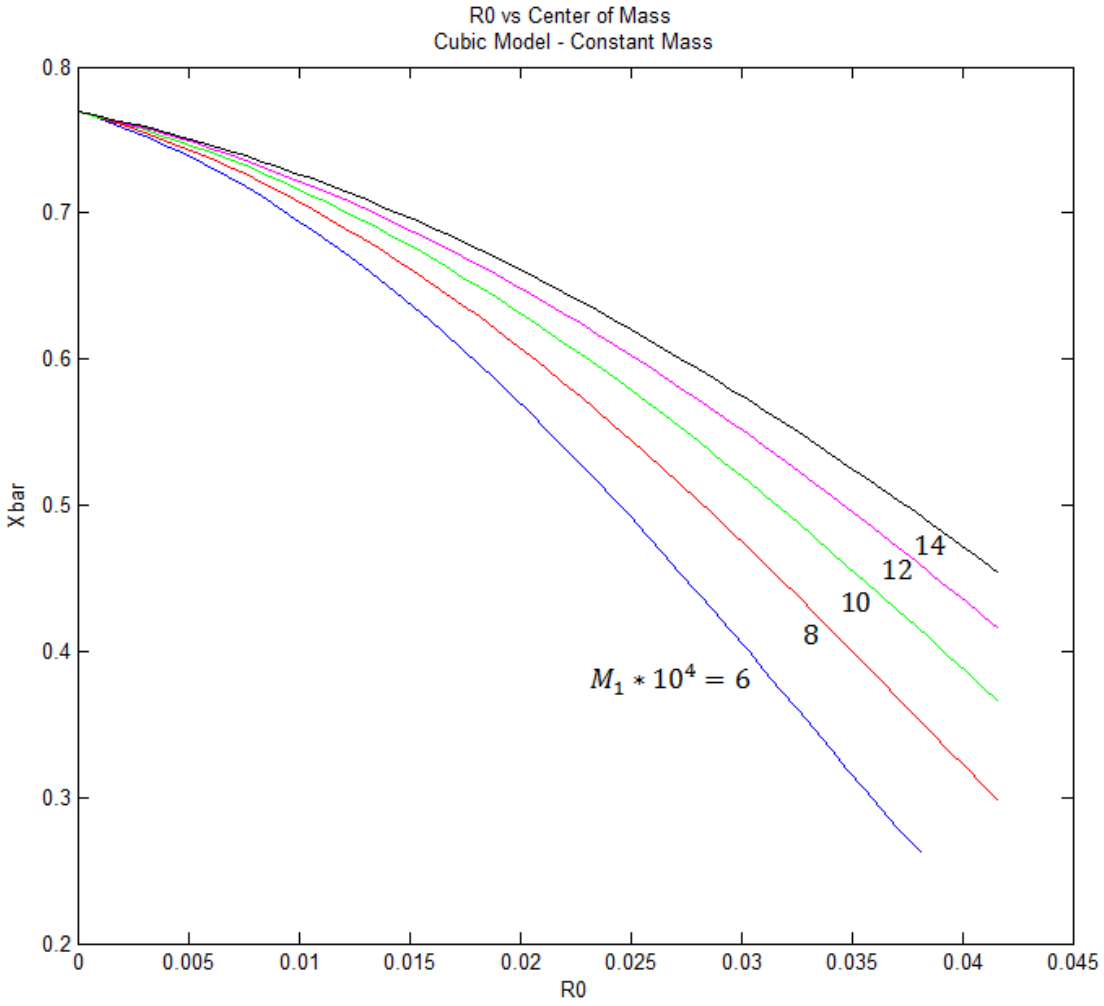

Figure 2.10: Location of center of mass $\bar{X}$ as a function of Handle Radius R_0 for values of M_1=0.0006, 0.0008, 0.0010, 0.0012, and 0.0014 (MATLAB code 8, Appendix A)

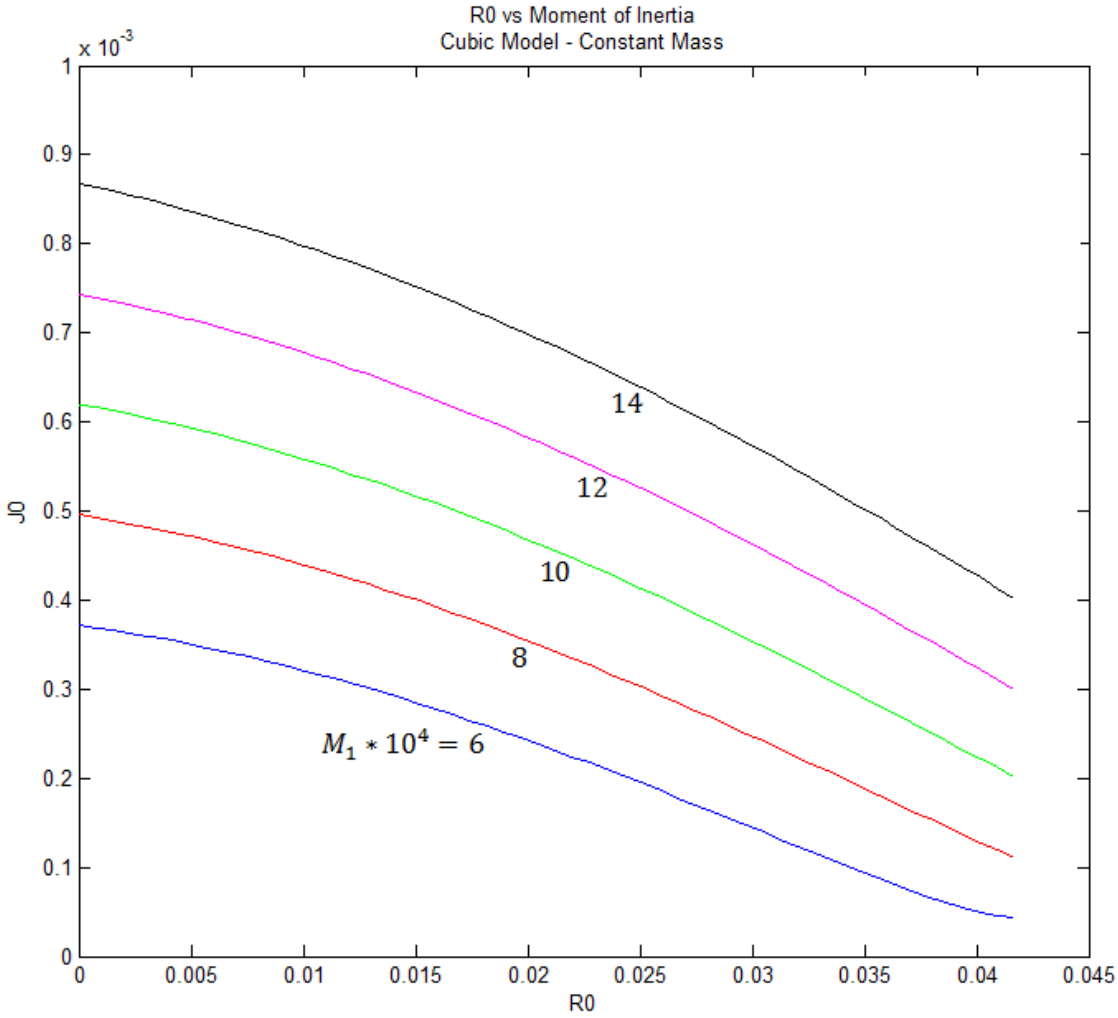

Figure 2.11: Moment of Inertia about the Knob, J_0, as a function of Handle Radius R_0 for values of M_1=0.0006, 0.0008, 0.0010, 0.0012, and 0.0014 (MATLAB code 9, Appendix A)

about the knob end of the bat for fixed values of M_1=0.0006, 0.0008, 0.0010, 0.0012, and 0.0014, and varying handle radius, R_0. Note that R_0 was taken from 0 to a maximum value of $\sqrt{4M}$, since any calculation with R_0 greater than this maximum value will have an imaginary component. As expected, with increasing handle radius, the moment of inertia about the knob decreases. As the handle radius increases and mass is held constant, the barrel radius must decrease, as seen in Figure 2.9. Therefore, with a higher concentration of mass closer to the handle, the moment of inertia about the handle must decrease. We also see that for a fixed handle radius, as mass increases, the moment of inertia increases. This is expected because the increase of mass must occur towards the barrel end in order to maintain the fixed value of R_0, so moment of inertia about the handle will increase with increased mass.

Though not commonly listed as a specification for a baseball bat, the moment of inertia (I_0) about the knob is important in determining how fast a player can swing the bat. Later in this paper, we will also illustrate the effects of moment of inertia on the exit velocity of the baseball after impact with the bat. We take a bat of constant length, in this case 33 inches, and fix the moment of inertia about the knob end. For simplicity of calculations, we work in non-dimensional values. For each value of non-dimensional moment of inertia, the barrel radius R_1 is taken to be a function of R_0. This value of R_1, as well as the center of mass, $\overline{X}$, and the non-dimensional mass of the bat, M_1, are plotted versus R_0 for fixed values of J_0.

In Figure 2.12, R_1 is plotted as a function of R_0 for typical values of J_0. These values, J_0=0.002, 0.004, 0.006, and 0.008, are all within a reasonable range of values calculated by equation (12) for typical bat shapes. It is clearly seen that for a constant J_0,

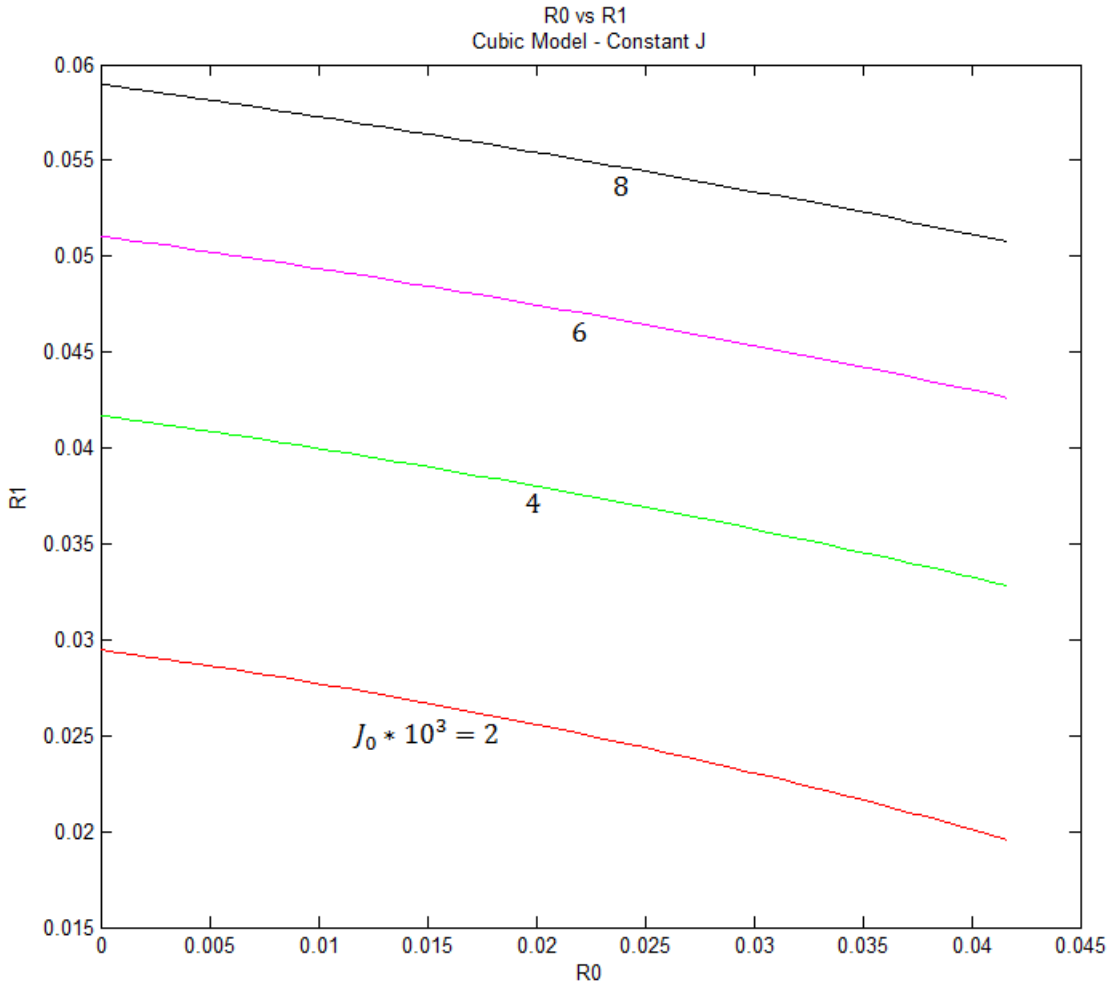

Figure 2.12: Barrel radius R_1 as a Function of Handle Radius R_0 with values of J_o=0.002, 0.004, 0.006 and 0.008 (MATLAB code 10, Appendix A)

as R_0 increases, the value of R_1 decreases. That is, in order to maintain constant moment of inertia of the bat, as the handle radius is increases, the barrel radius must be decreased. It is also clear that for fixed values of R_0, the value of R_1 increases with increasing J_0. That is, if the handle radius is held constant and the moment of inertia is increased, the barrel radius must increase as well. Unlike with constant mass, as in Figure 2.9, the graphs of R_1 versus R_0 are not symmetric. This is due to the non-symmetric effects of adding mass to either end. Mass added to the barrel has a bigger effect on J_0 than mass added to the handle end.

In Figure 2.13, the non-dimensional center of mass is then plotted against R_0 for same fixed values of J_0, which are J_0=0.002, 0.004, 0.006, and 0.008. Note that R_0 was taken from 0 to a maximum value of $\sqrt{\frac{10229J_0}{250}}$, since any calculation with R_0 greater than this maximum value will have an imaginary component. It is obvious that with increasing R_0 and constant J_0, the location of the center of mass decreases, that is, the location of the center of mass moves towards the knob. This is to be expected, as for a fixed moment of inertia, as the handle radius increases, the barrel radius must decrease, as seen in Figure 2.12. Therefore, the mass becomes more concentrated at the handle end, producing the expected effect. We also see that for a fixed value of R_0, as J_0 increases, the location of the center of mass will also increase. This is expected, as seenin Figure 2.12. With a fixed handle radius, any increase in moment of inertia must increase the barrel radius, therefore concentrating the mass closer to the barrel. Lastly, we see that for a handle radius of zero, the location of the center of mass will always be in the same place, independent of moment of inertia about the knob.

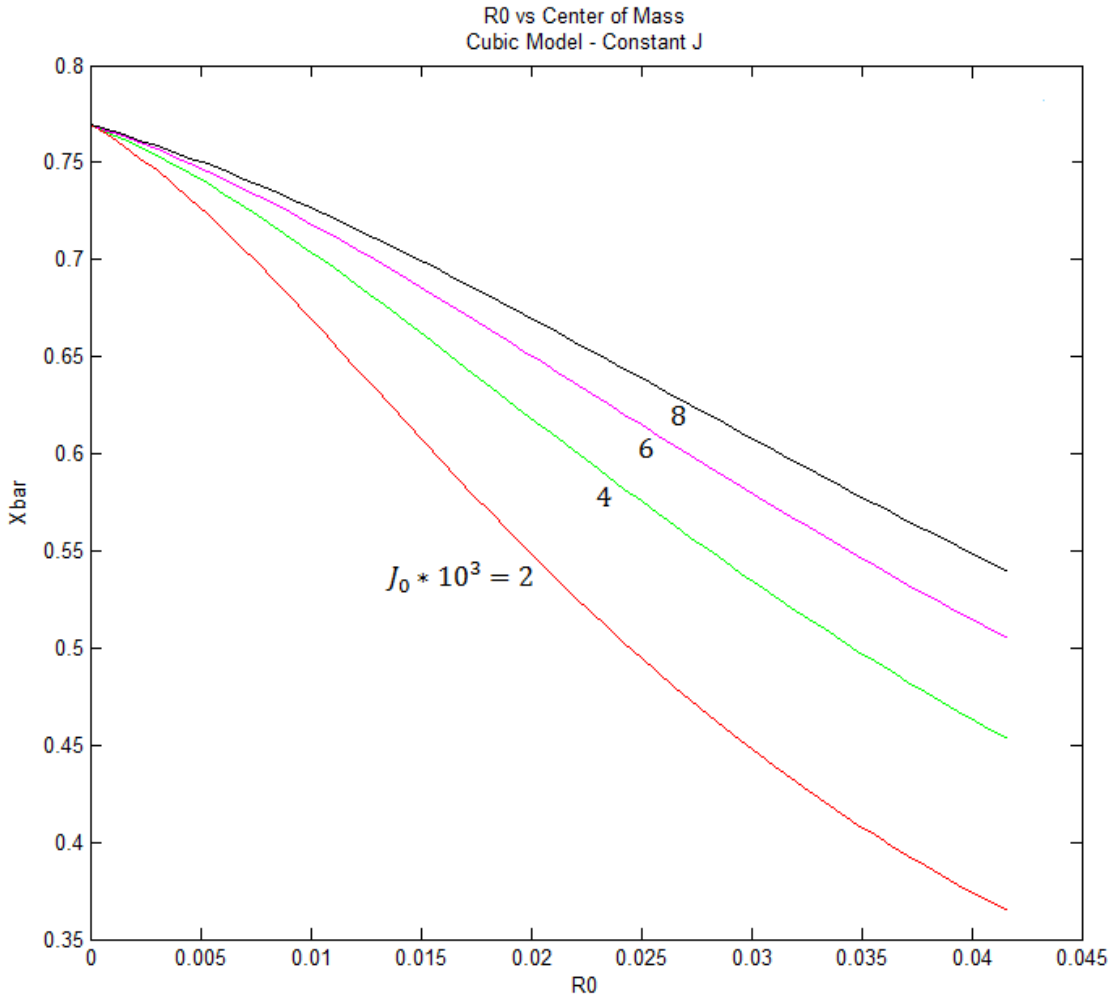

Figure 2.13: Location of center of mass $\bar{X}$ as a function of Handle Radius R_0 for values of J_0=0.0002, 0.0003, 0.0004, 0.0005, and 0.0006 (MATLAB code 11, Appendix A)

Figure 2.14 illustrates variations in the non-dimensional mass, M_1, versus R_0 for fixed values of J_0=0.002, 0.004, 0.006, and 0.008. As expected, with increasing handle radius, and constant moment of inertia about the knob, the mass of the bat increases. As seen in Figure 2.12, as handle radius increases with constant J_0, the barrel radius decreases much more slowly. The net effect is an increase in mass. Therefore, as handle radius increases, with constant moment of inertia about the knob, the mass of the bat increases. As expected, for a fixed value of R_0, the mass of the bat increases as moment of inertia about the knob increases.

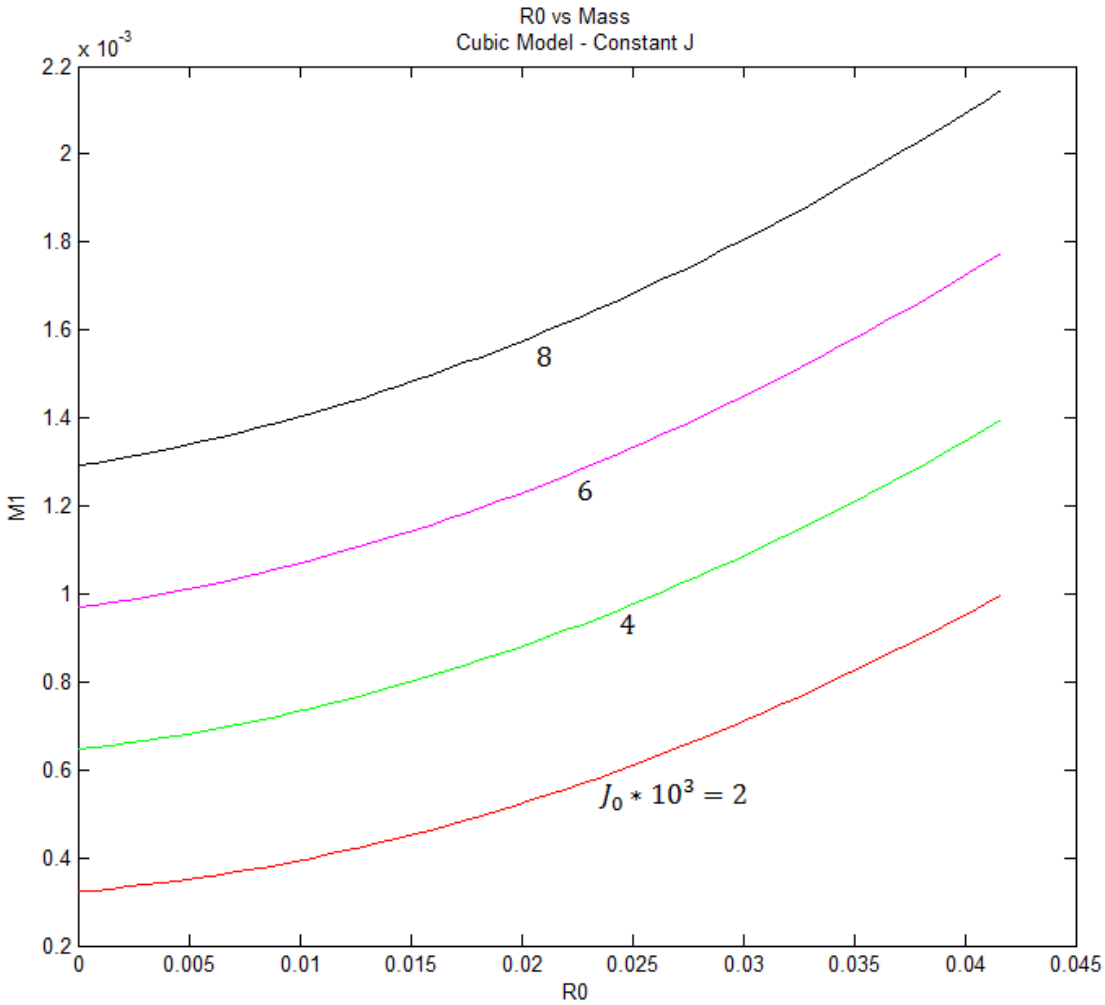

Figure 2.14: Mass M_1 as a Function of Handle Radius R_0 with values of J_o=0.0002, 0.0003, 0.0004, 0.0005 and 0.0006 (MATLAB code 12, Appendix A)

Chapter 3 Rigid Body Dynamics

We focus here on an instantaneous collision between a ball and a bat. At impact, both the ball and the bat move in the same plane, and the velocity of the ball just prior to impact is perpendicular to the longitudinal axis of the bat. The mass of the ball is m_2 and its velocity just prior to impact is v_2. The length of the bat is L, its mass is m_1, its moment of inertia about its center of mass is I_c, and its angular velocity just prior to impact is ω. The center of rotation of the bat just prior to impact is at a distance d off the bat along the longitudinal axis, the x-coordinate measures distance along the bat from the knob (so that $0 \le x \le L$), the x-coordinate of the center of mass of the bat is $\bar{x}$, and the y-coordinate measures distance along the bat from the center of mass (so that $-\bar{x} \le y \le L - \bar{x}$). Defined in this way, the x- and y-coordinates are related by

$$x = \bar{x} + y \quad , \tag{1}$$

and the velocity v_c of the center of mass of the bat just prior to impact is given by

$$v_c = (d + \bar{x})\omega \quad . \tag{2}$$

It is important to realize that the location of the center of rotation just after impact will not be the same as is just before impact.

In what follows, we focus on collisions in which the point of impact between the ball and the bat is at a location y from the center of mass. The velocity v_1 of the contact point on the bat just prior to impact is therefore,

$$v_1 = v_c + \omega y \quad , \tag{3}$$

where v_c itself depends on ω according to equation (2).

In a typical situation, the mass m_2 of the ball, as well as the bat mass m_1, the location $\bar{x}$ of the center of mass, and the moment of inertia I_c of the bat are all known. In addition, the incoming velocity v_2 of the ball, the location y of the contact point, the location d of the center of rotation of the bat before impact, and the angular velocity ω of the bat before impact are also known. The goal here is to use rigid body dynamics to predict the outgoing velocity v_2' of the ball, the velocity v_1' of the contact point just after impact, the velocity v_c' of the center of mass of the bat just after impact, the angular velocity ω' of the bat just after impact, and the distance d' (measured positive off the bat) from the end of the bat to the center of rotation of the bat just after impact.

Because the impulsive force between the bat and the ball is so much larger than the forces that can be exerted by a batter on the bat during impact, these latter forces may be neglected when analyzing the dynamics of the collision between the bat and the ball. In this case, the bat is essentially free of external forces when it contacts the ball, and the conservation of linear momentum dictates that

$$m_2 v_2 + m_1 v_c = m_2 v'_2 + m_1 v'_c \quad , \tag{4}$$

while the conservation of angular momentum about the center of mass of the bat requires that

$$m_2 v_2 y + I_c \omega = m_2 v'_2 y + I_c \omega' \quad . \tag{5}$$

The coefficient of restitution e characterizes the energy lost in the collision, and is defined as the ratio of outgoing relative velocity to the incoming relative velocity according to

$$e = \frac{-(v'_1 - v'_2)}{(v_1 - v_2)} \quad . \tag{6}$$

When $e=1$, the direction of the relative velocity is reversed, its magnitude remains unchanged, the collision is elastic and there is no energy dissipated.

Finally, the relation between the post-collisional velocity v_1' of the contact point on the bat and the post collisional velocity v_c' of the center of mass of the bat is fixed kinematically by

$$v'_1 = v'_c + \omega' y \quad , \tag{7}$$

in which v_c' is given in terms of d' and ω' by the post-collisional analog of equation (2),

$$v'_c = (d' + \bar{x})\omega' \quad . \tag{8}$$

Equations (4), (5), (6), (7), and (8) are five equations that determine $v_1', v_2', v_c', \omega'$ and d'. Equation (4) may be rearranged to find $(v_2' - v_2)$ in terms of the difference $(v_c' - v_c)$, which by subtracting equation (3) from equation (7) gives $(v_c' - v_c)$ in terms of the differences $v_1' - v_1$ and $(\omega' - \omega)$. Equations (6) and (7), in turn, may be used to write v_1' and ω' in terms of v_2'. The result is a single equation for v_2' that yields

$$v'_2 = v_2 + \frac{m(1+e)(v_c - v_2 + \omega y)}{\left[1 + m + (\frac{m_2}{I_c})y^2\right]} \quad , \tag{9}$$

where $m = m_2 / m_1$ and v_c is given by equation (2). With v_2' given by equation (9), equation (6) gives v_1':

$$v'_1 = v'_2 + (v_2 - v_1)e \quad ; \tag{10}$$

and equation (5) gives ω':

$$\omega' = \omega + \frac{m_2}{I_c}(v_2 - v'_2)y \quad . \tag{11}$$

Then with v_1' given by equation (10), equation (7) gives v_c':

$$v'_c = v'_1 - \omega' y \tag{12}$$

and with v_c' given by equation (12) and ω' given by equation (11), equation (8) gives d':

$$d' = -\bar{x} + \frac{v'_c}{\omega'} \quad . \tag{13}$$

After the development of these equations for the rigid body dynamics of the baseball bat collision, we analyze these equations using typical values of the constants for an average major league baseball (MLB) bat. These typical values were found both from average bat dimensions and through mathematical models of a common cubic profile. The typical profile used for the average bat is that with a handle radius of 0.5 inches and an end radius of 1.375 inches. The handle radius was chosen so as to be thin enough to grip but thick enough to not cause breakage during a bat-ball collision. The end radius was chosen as the maximum allowed by major league rules. The locations of zero slope are at x=0 and x=L. The length used was 36 inches. From these parameters the cubic profile was determined, and from that profile the mass, the axial location of the center of mass, and the moment of inertia about the knob and the center of mass can be determined from equations (2.1), (2.2), (2.3), and (2.4). The mass that is determined from this cubic profile and equation (2.1) is 34.5436 ounces; this mass is reasonable for an MLB baseball bat of that length. Through similar calculations the moment of inertia about the center of mass calculated is 158.43 lb in^3. The axial location of the center of mass given by equation (2.2) and this cubic profile is 0.672907 times the length of the bat, which is a reasonable value for an average bat shape. The standard mass of a MLB baseball is 5 ounces.

The values of the incoming ball velocity, v_2, the coefficient of restitution, *e*, the location of the center of rotation, *d*, and the initial angular velocity of the baseball bat, ω, are all treated as known constants. The average incoming ball velocity used is 90 mph

and the average angular velocity of the baseball bat before collision is 50 radians per second. The axial location of the center of rotation is 2.5 inches from the knob in the negative *x* direction. The average coefficient of restitution in the bat-ball collision is 0.5.

All of these values can be non-dimensionalized and used to calculate and plot the outgoing ball velocity, v'_2, versus the location of impact, *x*. This relationship is shown in Figure 3.1. Quantities have been non-dimensionalized such that velocity is given as a fraction of incoming ball velocity so that $V'_2 = \frac{v'_2}{-v_2}$ and X is given as a fraction of the total bat length so that $X = \frac{x}{L}$. We see that exit velocity is highly dependent upon the point of impact and is greatest a few inches in from the barrel end. This is the qualitative behavior we expect. Hitters try to make contact close to this point of maximum in order to obtain more distance. As shown in this figure, there is a location on the bat which provides a maximum outgoing ball velocity, v'_2. This location of maximum is of great interest, and is evaluated further. Interestingly, for values of X less than 0.14, batted ball speed is negative. This happens because collisions that occur close to the handle-end of the bat transfer less momentum to the ball than is required to change its direction (the pitched velocity is taken as negative). There are two reasons for this behavior. First, as the point of collision moves closer to the handle (and closer to the center of rotation), the linear velocity of the impact point is decreased. Also, the effective mass decreases as the impact point is moved from the bat center of mass.

Equation (9) gives the exit velocity of a batted ball as a function of y, which is defined as the distance from the center of mass of the bat to the impact location. From this equation we wish to derive an expression for the value of y at which the maximum velocity occurs for a given bat profile. By setting $\frac{dv'_2}{dy} = 0$, we can isolate the minimum

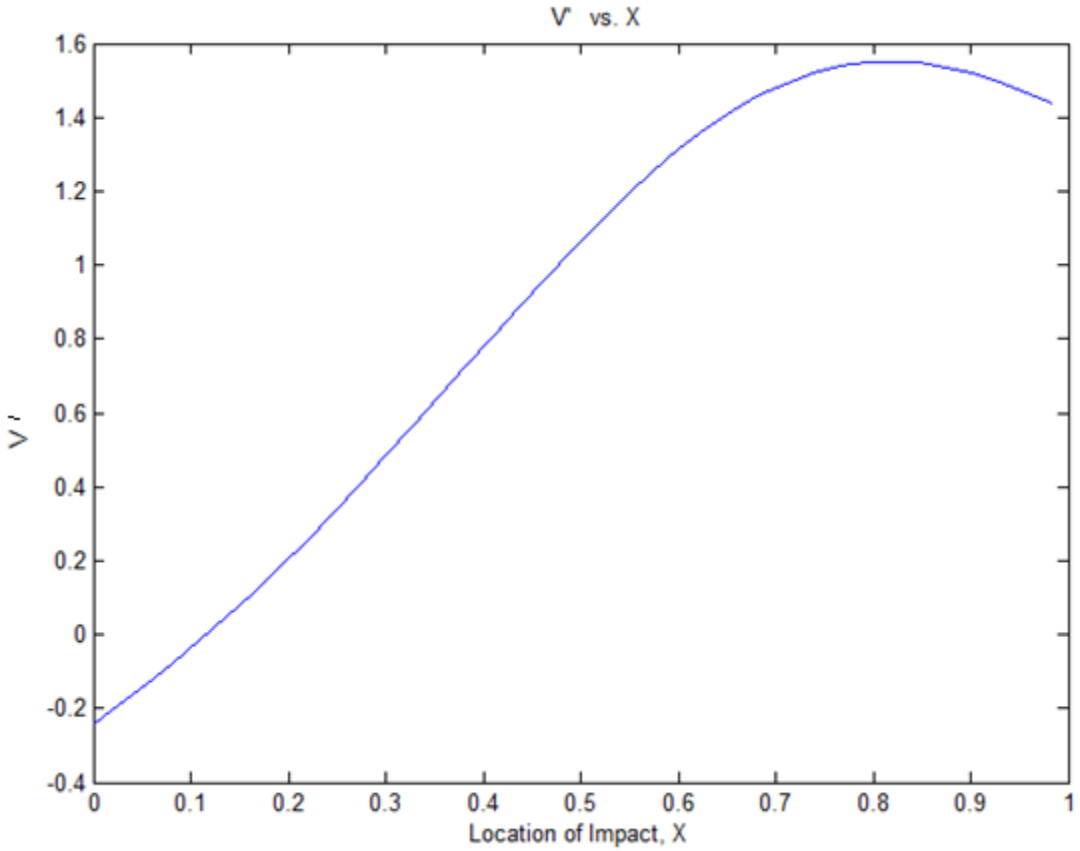

Figure 3.1: Outgoing Ball Velocity, V'_2, versus location of impact, X (MATLAB code 13, Appendix A)

and maximum values of the function. This results in two roots as follows:

$$y = \frac{1}{\omega}\left[-(v_c - v_2) \pm \sqrt{(v_c - v_2)^2 + \omega^2(1+m)\left(\frac{I_c}{m_1}\right)}\right] \tag{14}$$

By specifying that $\frac{d^2 v_2'}{dy^2} < 0$, we identify the point at which velocity is a maximum. We are left with a single value of y.

$$y_{max} = \frac{1}{\omega}\left[-(v_c - v_2) + \sqrt{(v_c - v_2)^2 + \omega^2(1+m)\left(\frac{I_c}{m_1}\right)}\right] \tag{15}$$

We then apply a simple transformation to establish the optimal impact location in terms of x, the distance along the bat from the handle-end.

$$x_{max} = \bar{x} + \frac{1}{\omega}\left[-(v_c - v_2) + \sqrt{(v_c - v_2)^2 + \omega^2(1+m)\left(\frac{I_c}{m_1}\right)}\right] \tag{16}$$

This value of x_{max} allows us to analyze a given bat shape in order to find the impact point which results in the highest ball output velocity. More importantly, by using expression (16) in equation (9), where $y = x - \bar{x}$, we are able to determine the maximum ball exit speed, v_{max}, as a function of the geometry of a bat for a given v_2, e, d, and ω. That is, $v_{max} = v_2'(x = x_{max})$, where $v_2'(x)$ is given by equation (9) and x_{max} is given by equation (16).

$$v_{max} = v_2 + \frac{m(1+e)\sqrt{(v_c - v_2)^2 + \omega^2(1+m)(\frac{I_c}{m_1})}}{1+m+\left(\frac{m_1}{I_c\omega^2}\right)\left[v_2 - v_c + \sqrt{(v_c - v_2)^2 + \omega^2(1+m)\left(\frac{I_c}{m_1}\right)}\right]^2} \tag{17}$$

This analysis tool is useful in comparing the performance of different bat geometries.

All comparisons are done using dimensionless terms, to facilitate finding and analyzing trends. All lengths were non-dimensionalized by dividing by the length of the bat, L. This is done because the initial ball velocity is taken to be negative. For

example, the distance on the bat from the center of mass to the impact point is non-dimensionalized by the following:

$$Y = \frac{y}{L} \text{ and } R = \frac{r}{L} \quad . \tag{18}$$

All velocities were non-dimensionalized by dividing by the negative value of the initial velocity of the ball. For example, the non-dimensional velocity of the center of mass of the bat and the impact point are given by

$$V_c = \frac{v_c}{-v_2} \text{ and } V_1 = \frac{v_1}{-v_2} \tag{19}$$

respectively. Angular velocity is non-dimensionalized by:

$$\Omega = \frac{\omega L}{-v_2} \quad . \tag{20}$$

To create a non-dimensional term M for mass, the mass of the bat, m_2, is divided by the mass of the ball, m_1 The last terms that needs to be non-dimensionalized are the moment of inertia about the center of mass and about the knob (x=0). This is done by:

$$J_c = \frac{I_c}{m_1 L^2} \text{ and} \tag{21}$$

$$J_o = \frac{I_o}{m_1 L^2} \quad . \tag{22}$$

Using each of these non-dimensional terms we can non-dimensionalize all equations that have been derived previously. These equations are then used in our later comparisons.

3.1 Cubic Profile, Fixed Mass, Zero End Slopes

Figure 3.2 shows the variation of the bat handle-end radius with the barrel-end radius for a constant non-dimensional mass, M = 6.73. As one radius changes, the other must vary in such a way that the total mass is held constant. The maximum radius does

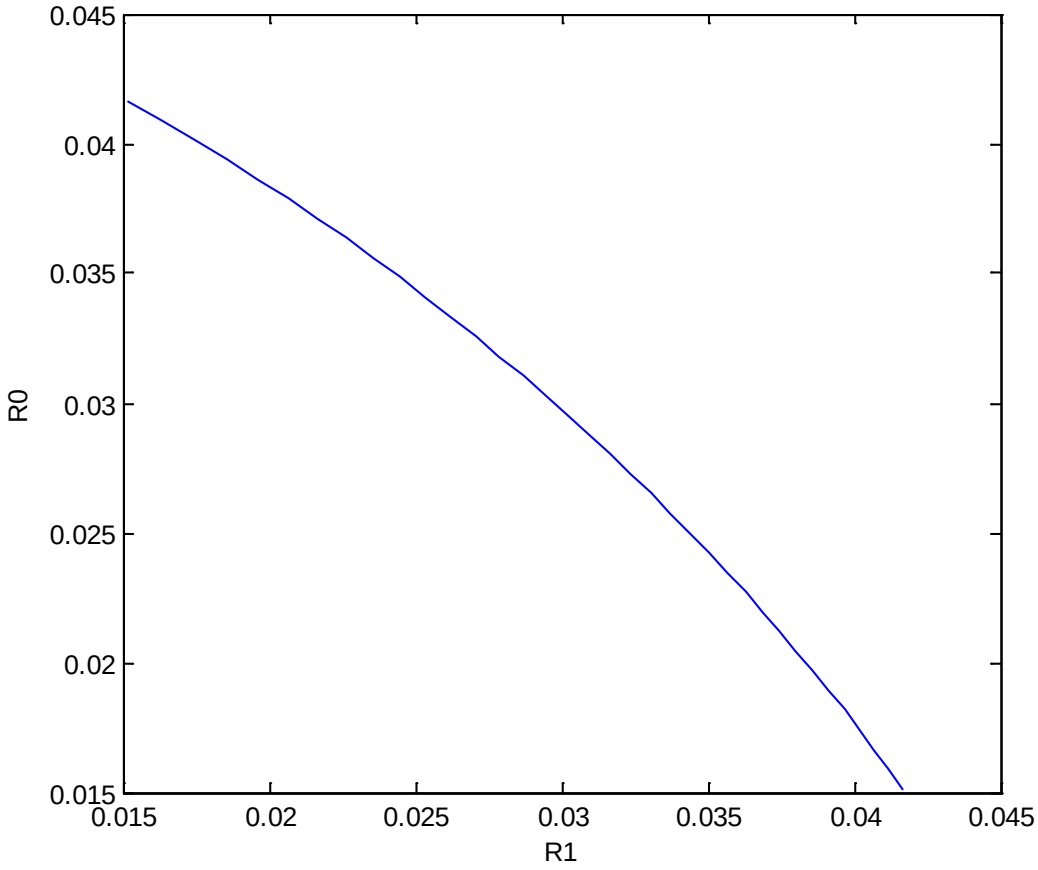

Figure 3.2: Variance of the bat handle-end radius versus the barrel-end radius for a constant mass scenario for *e*=0.5, ω =50 radians/second, and *d*=2.5 inches (MATLAB code 14, Appendix A)

not exceed a non-dimensionalized value of 0.0416, the MLB maximum for a 33 inch bat. It is interesting to note that this plot is symmetrical about the line $R_0=R_1$. This means that if a given value of $R_0=A$ has a corresponding $R_1=B$, then a given value of $R_1=A$ will have a corresponding $R_0=B$. In other words, any valid bat profile mirrored about the mid-point of the bat is also a valid profile.

Figure 3.3 displays the movement of the optimal impact point along the bat as the barrel-end radius changes. As the barrel-end radius increases from a minimum value of 0.015 to a maximum value of 0.0416, the optimal impact point moves toward the barrel-end of the bat, from a point 33% of the length from the handle-end to a point 66% of the length from the handle-end. This result is intuitive, as the optimal impact point is expected to shift as the mass distribution shifts.

Figure 3.4 shows the corresponding maximum ball exit velocity as a function of the barrel-end radius. As the barrel-end radius increases from a minimum value of 0.015 to a maximum value of 0.0416, the ball exit velocity increases from a magnitude of 87.5% of incoming ball velocity to a magnitude of 135% of incoming ball velocity. Again, this result is intuitive. As the mass is shifted further to the barrel-end, the profile begins to take the obvious form of a typical baseball bat. We expect this shape to perform better than a bat with more mass concentrated on the handle-end. If we imagine the extreme case, we would expect a batter holding the barrel-end of the bat and striking the ball with the handle-end to experience sub-optimal performance. According to these particular constraints (zero end slopes with minimum and maximum radii occurring at the bat ends), it is most beneficial to utilize the maximum allowable radius at the extreme

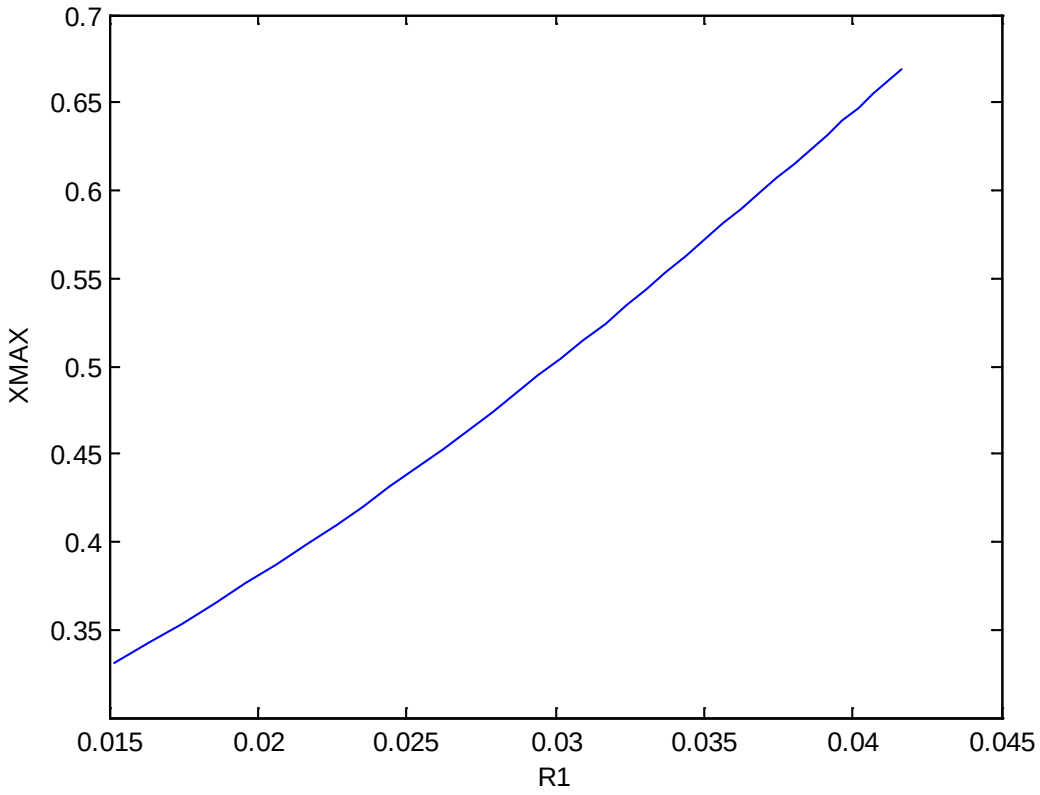

Figure 3.3: Location of the optimal impact point along the bat as the barrel-end radius changes for *e*=0.5, ω =50 radians/second, and *d*=2.5 inches (MATLAB code 15, Appendix A)

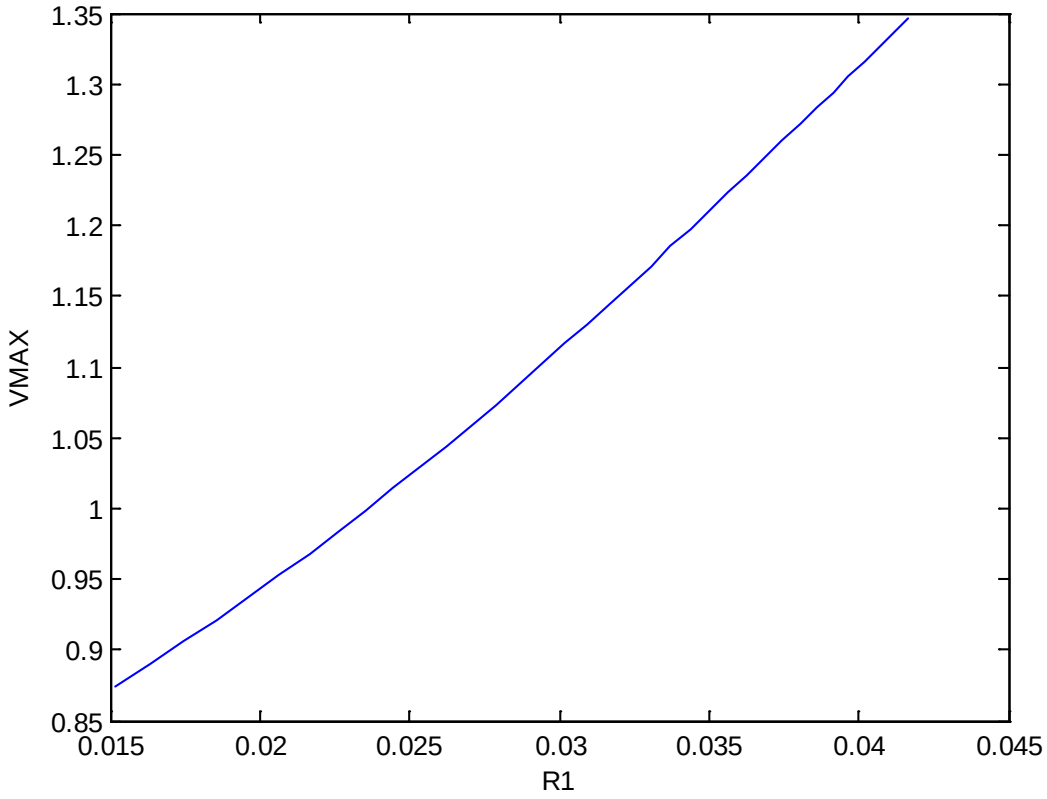

Figure 3.4: Maximum ball exit velocity as a function of the barrel-end radius for *e*=0.5, ω =50 radians/second, and *d*=2.5 inches (MATLAB code 16, Appendix A)

barrel-end and the minimum selected radius at the extreme handle-end. In the following sections, we will observe the effects of moving the locations of minimum and maximum radii from the extreme ends toward the center of the bat.

3.2 Cubic Profile, Fixed Minimum and Maximum Radii, Zero Handle Slope

In order to better understand how modifying the cubic profile affects the maximum outgoing ball velocity, the location of the maximum radius is varied along the axis of the bat while the location of the minimum radius is fixed at the handle. For this case, the maximum radius is moved from x=23" to x=33", which corresponds to X=0.70 and X=1 in non-dimensional terms. The maximum radius is set to 1.375 inches, and the minimum radius is set to 0.5 inches. The minimum radius is located at the handle end of the bat, or X=0. Non-dimensional values of bat mass, $M = \frac{m_1}{m_2}$, moment about the handle end, $J_0 = \frac{I_0}{m_1 L^2}$, and moment of inertia about the center of mass, $J_c = \frac{I_c}{m_1 L^2}$, the maximum outgoing ball velocity, V_{MAX}, and the location on the bat that gives maximum outgoing ball velocity, X_{MAX}, are each calculated as functions of the location of the maximum radius. These values are plotted for comparison.

When the cubic radial profile is changed and the density is held constant, it is expected that the overall bat mass will change. As seen in Figure 3.5, the non-dimensional mass of the bat is at a maximum value of approximately 10.4e-4, which corresponds to 40.5 ounces, when the maximum radius is located at about X=0.76. M at X=1 is significantly lower, at only about 8.9e-4. Therefore, when constrained by a maximum radius of 1.375 inches and a minimum radius of 0.5 inches, located at X=0, the

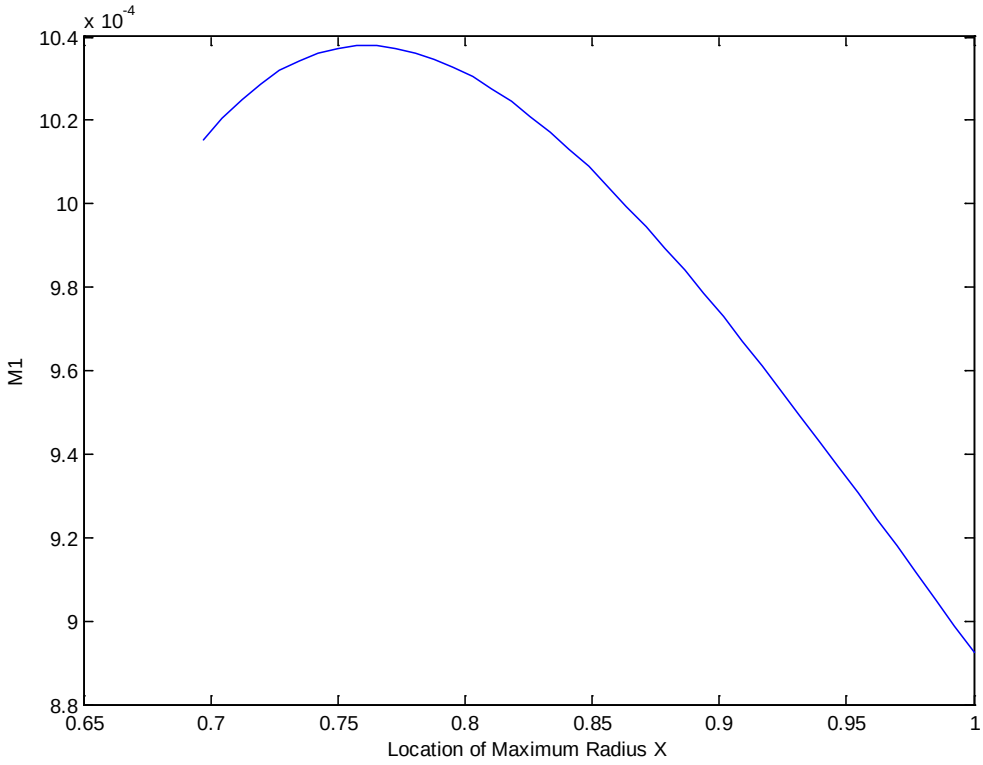

Figure 3.5: Non-dimensional bat mass vs. location of max radius for e=0.5, ω=50 radians/second, and d=2.5 inches (MATLAB code 17, Appendix A)

heaviest bat occurs when the maximum radius is set to occur not at the end, but approximately 8 inches from the barrel end.

The moments of inertia about the handle end ($X=0$) and about the center of mass both vary with the movement of the location of the maximum radius. Similar to the mass, the maximum value of moment of inertia occurs when the maximum radius is away from the end of the bat. When taken about the handle end (X=0), the moment is maximum at approximately X=0.84, as seen in Figure 3.6. When taken about the center of mass, the maximum moment occurs even farther from the end, at about X=0.82, as seen in Figure 3.7. Because both these values and the overall bat mass contribute to the outgoing ball velocity, it is expected that the maximum outgoing ball velocity will be dependent on the location of maximum radius.

Finally, the maximum outgoing ball velocity and the location at which it is achieved are considered. The non-dimensional V_{MAX} is plotted as a function of the location of the maximum radius for three typical values of the angular velocity: ω=40, 50 and 60 rad/s. It is clear from Figure 3.8 that the maximum outgoing ball velocity is largest at approximately X=0.855, 0.86 and 0.865 for angular velocities ω=40, 50 and 60 rad/s, respectively. As the optimum location of the maximum radius purely in terms of maximum batted ball speed is further along the bat than the location that provides maximum values of mass and moment, but not at the end. As seen above, the greatest masses and moments occur to the left of $X\approx0.86$, but the value of $X\approx0.86$ is still significantly removed from the end of the bat. The competing effects that give this optimal location are the mass and moment, as mentioned previously, as well as the

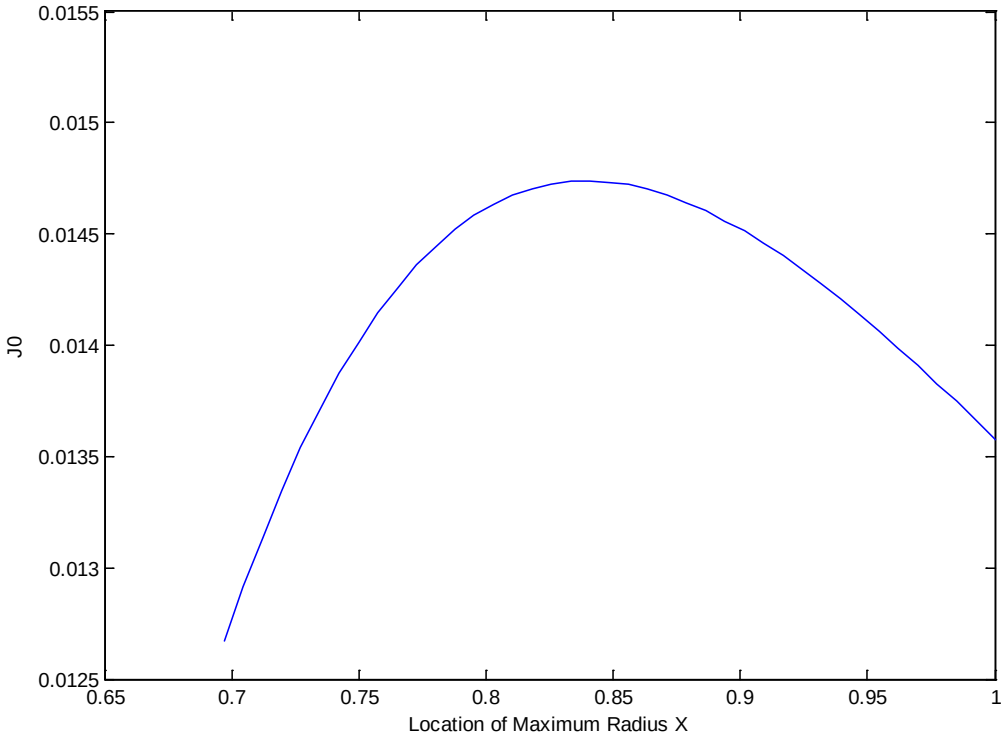

Figure 3.6: Moment of inertia about x=0 vs. location of max radius for e=0.5, ω=50 radians/second, and d=2.5 inches (MATLAB code 18, Appendix A)

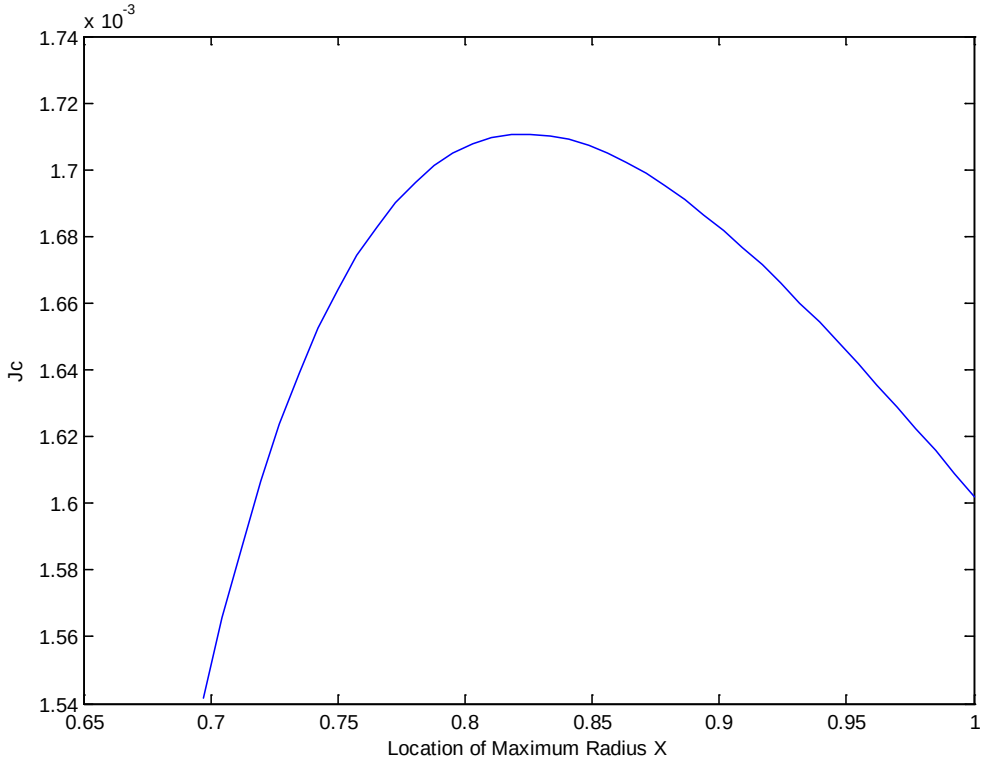

Figure 3.7: Moment of inertia about the center of mass vs. location of maximum radius for e=0.5, ω=50 radians/second, and d=2.5 inches (MATLAB code 19, Appendix A)

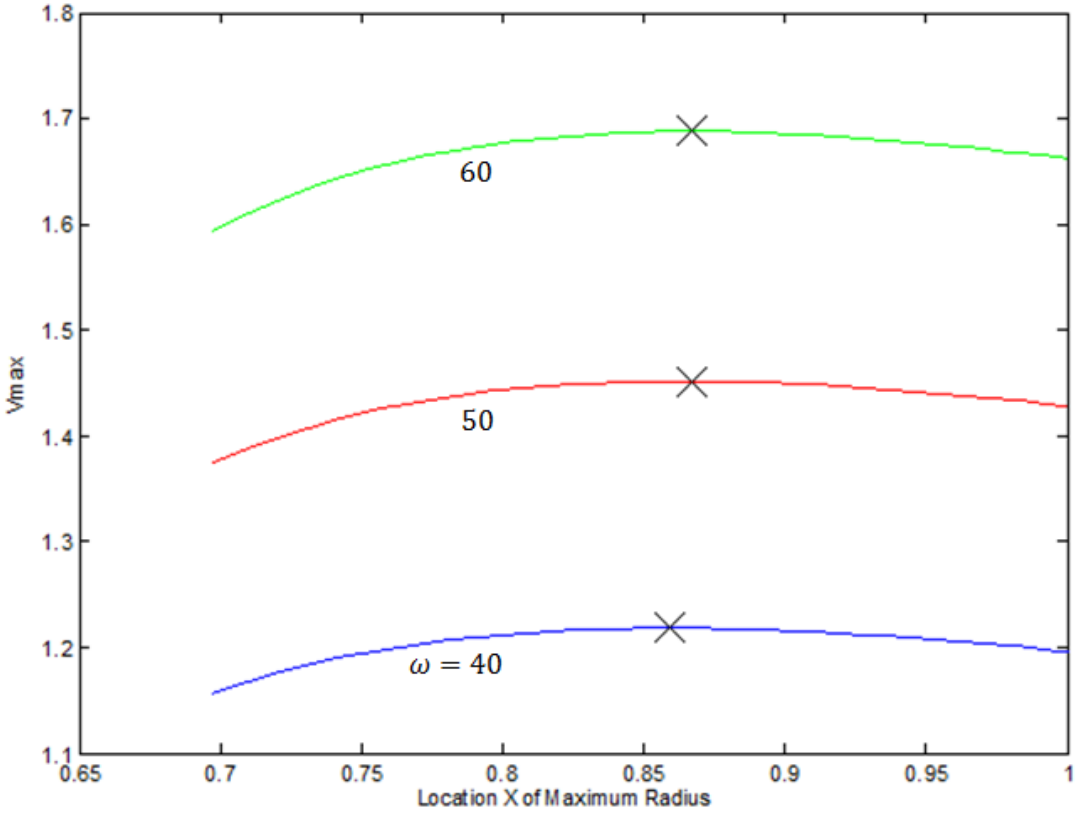

Figure 3.8: Non-dimensional V_{MAX} vs. location of maximum radius (MATLAB code 20, Appendix A)

rotation of the bat, which increases the local bat velocity linearly along the bat, with a maximum linear velocity occurring at the barrel end. This effect is best illustrated in Figure 3.9, as the location of impact that provides the maximum batted ball speed remains almost constant for values of X>0.90. Even with the maximum radius moving away from the end of the bat, the combination of overall mass, moment and angular velocity produce insignificant change in the optimal location of impact.

It should be noted that if the angular velocity of the bat is increased, the location of the maximum radius that provides maximum batted ball speed would move closer to the barrel end, as this effect would become more dominant. This is illustrated in Figure 3.9. The batted ball speed itself will also increase with increases in angular velocity, as seen in Figure 3.8. It should also be noted that the net increase in batted ball speed achieved by moving the location of maximum radius away from the barrel end is approximately 2% of the incoming ball velocity. In dimensional terms, this translates into about 2 mph. Although this value is not large, it is an improvement over the bat with maximum radius occurring at the barrel end.

3.3 Cubic Profile, Fixed Mass and Maximum Radius, Zero Handle Slope

Here we consider a special case of the cubic profile in which the maximum radius, the location of the minimum radius and the mass are held constant. The location of the maximum radius is moved along the barrel end of the bat from x-coordinates x=23" to x=33" (which corresponds to the end of the bat. Due to the restriction of constant mass, the value of the minimum radius will change with varying location of maximum radius.

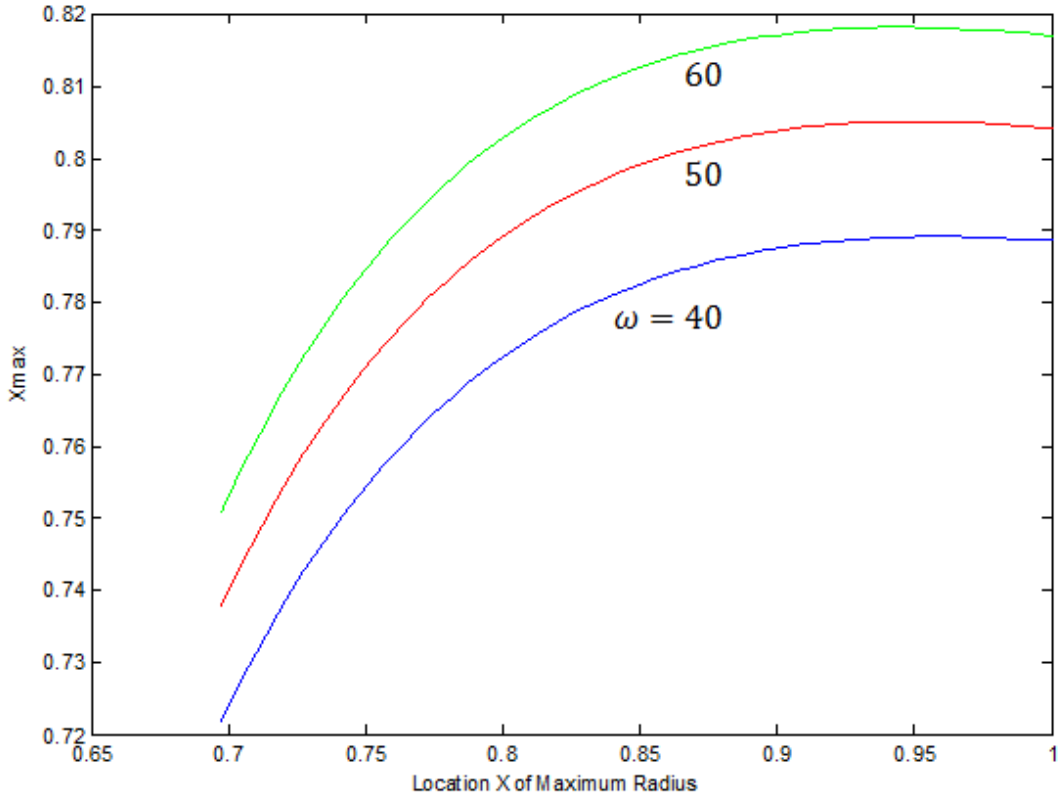

Figure 3.9: Location at which maximum outgoing velocity occurs (X_{MAX}) vs. location of Max radius (MATLAB code 21, Appendix A)

We see in Figure 3.10 that minimum radius reaches a minimum value when the location of the maximum radius is placed about three fourths of the way along the bat, or at X=0.76. Since the mass of the bat is held constant, when the location of the maximum radius being placed at approximately X=0.76, the least amount of the mass is concentrated in the handle end, and therefore the greatest amount of mass is concentrated at the barrel end.

Figure 3.11 plots the moment of inertia about the handle end of the bat (X=0) as a function of the location of the maximum radius. The moment about the handle end reaches a maximum when the location of the maximum radius is placed at approximately X=0.85. This is due to the effect seen in Figure 3.10, where with the maximum radius placed away from the end of the bat, the minimum radius decreases, and more mass is concentrated in the barrel. The moment of inertia is also increased. If the maximum radius is moved too far, i.e. X<0.85, the concentration of mass begins to move away from the barrel end, reducing the moment.

In Figure 3.12, the moment of inertia about the center of mass is plotted as a function of the location of maximum radius. In contrast to the moment about the end, the moment about the center of mass decreases as the maximum radius is moved away from the barrel end. This is due to the concentration of mass moving closer to the center of mass. This effect is more powerful than the concentrating of mass in the barrel, which is why we see a decrease in the moment.

Now that all relevant geometric properties have been described, the dynamic effects of the variation in the location of maximum radius are considered. First we consider the optimal impact location, X_{MAX}, as a function of the variable location of

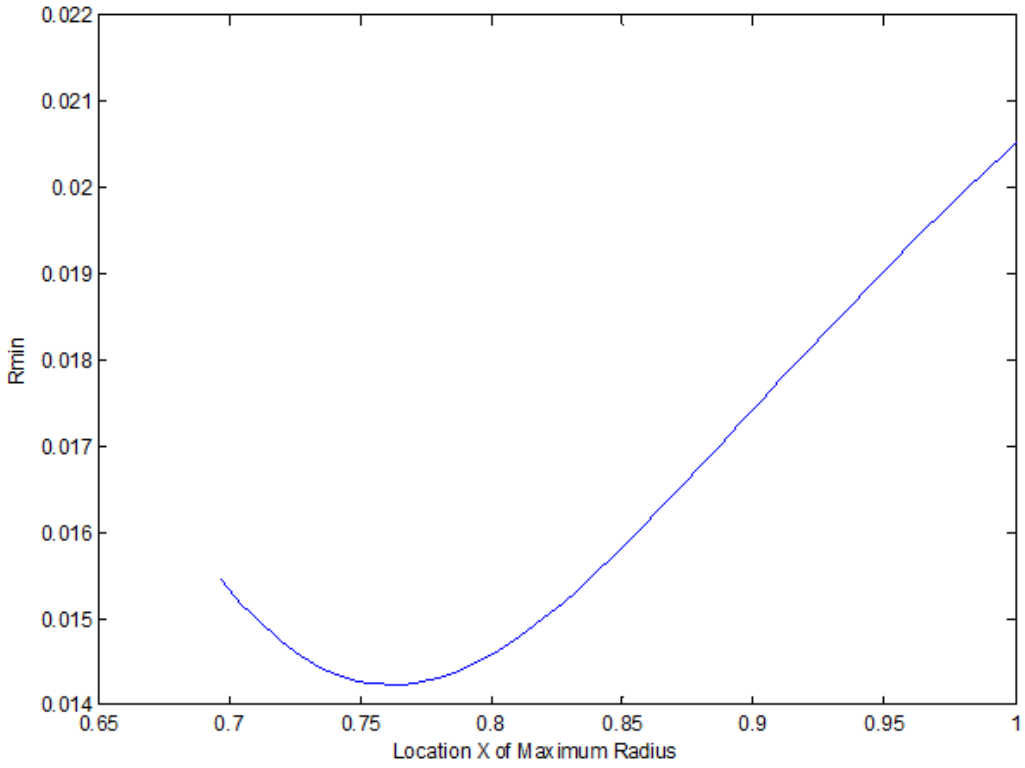

Figure 3.10: R_{min} versus the Location of the Maximum Radius X with m_1=40 oz, l=33" and r_{max}=1.375" (MATLAB code 22, Appendix A)

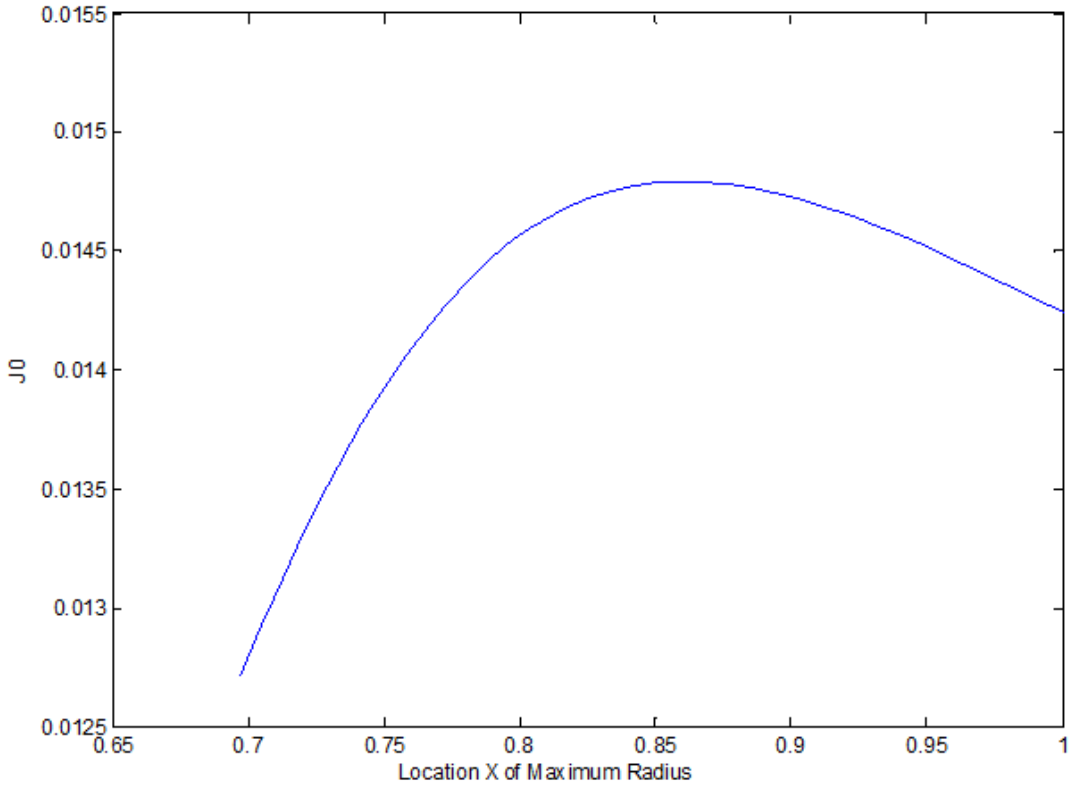

Figure 3.11: Non-dimensional J_0 versus the Location of the Maximum Radius X with m_1=40 oz, l=33" and r_{max}=1.375" (MATLAB code 23, Appendix A)

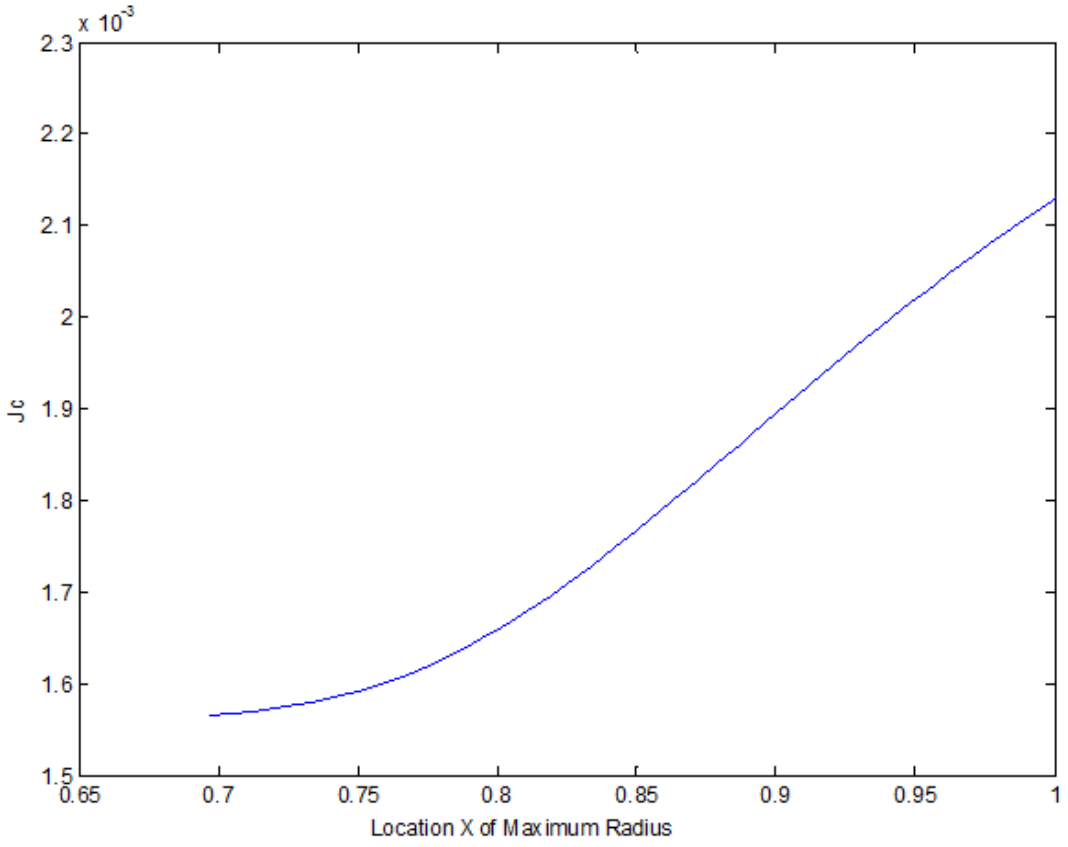

Figure 3.12: Non-dimensional J_c versus the Location of the Maximum Radius X with m_1=40 oz, l=33" and r_{MAX}=1.375" (MATLAB code 24, Appendix A)

maximum radius, which is plotted in Figure 3.13 for three typical values of angular velocity, ω=40, 50 and 60 rad/s. For locations of the maximum radius falling in the range $0.90<X<1.0$, the optimal impact location changes very little. This is because movement of the maximum radius has a very small effect on mass and moment until it reaches approximately $X = 0.90$. Once the location of the maximum radius is moved away from the barrel end beyond $X < 0.90$, the optimal impact location begins to move more dramatically. As expected, with increased angular velocity, the optimal impact location is moved closer to the end of the bat, again due to linear velocity effects.

Finally we consider the maximum outgoing ball velocity, V_{MAX}. Although there are not large variations in maximum ball exit velocity with variations in the location of maximum radius, there are some interesting effects. In Figure 3.14, the outgoing ball velocity is increased with increasing angular velocity. However, for all three values of omega, there is an optimal location of the maximum radius. For ω =40, 50 and 60 rad/s, this location is approximately X=0.87, 0.88, and 0.89. This means that by moving the location of the maximum radius away from the end of the bat, effectively concentrating more mass at the barrel end, the outgoing ball velocity can be increased.

3.4 Effects of Coefficient of Restitution and Angular Velocity

Here we investigate how varying the coefficient of restitution and angular velocity affects swing dynamics.

To analyze the influence that the coefficient of restitution, e, has on the angular velocity of the bat after impact, Figure 3.15 plots $\frac{\Omega'}{\Omega}$versus Y for a range values of e: 0.3,

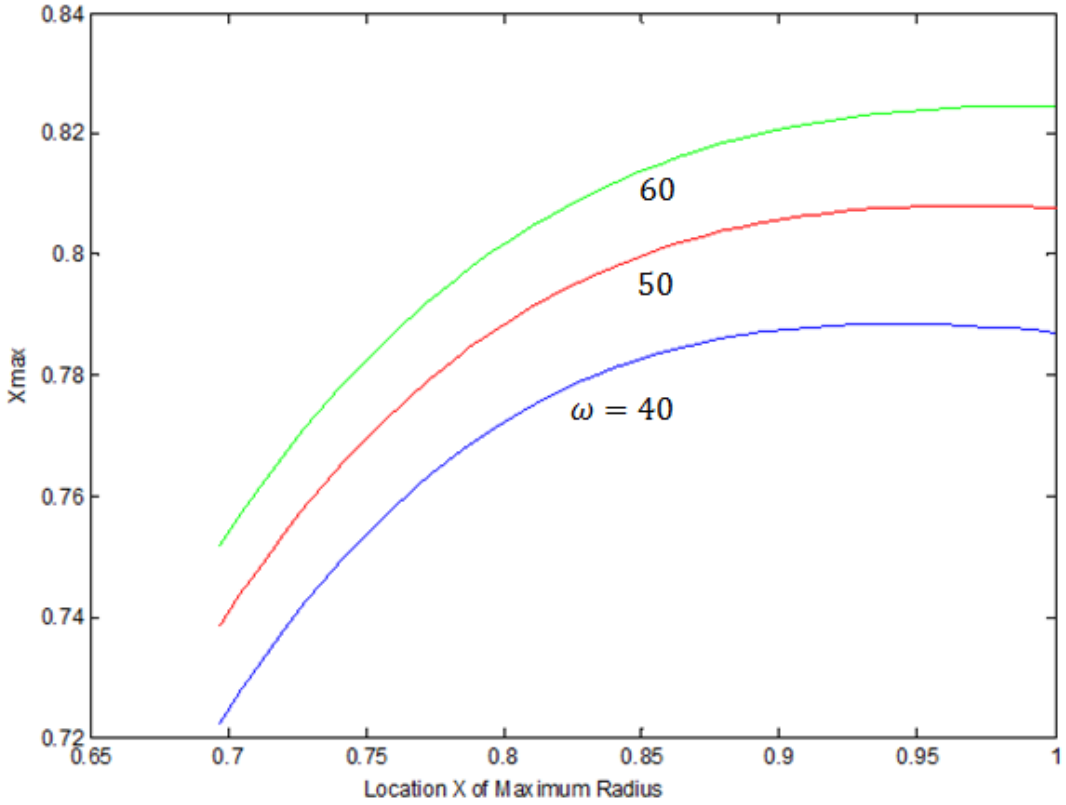

Figure 3.13: Optimal impact location X_{MAX} versus the Location of the Maximum Radius X with m_1=40 oz, l=33", r_{MAX}=1.375", and ω=40, 50 and 60 rad/s (MATLAB code 25, Appendix A)

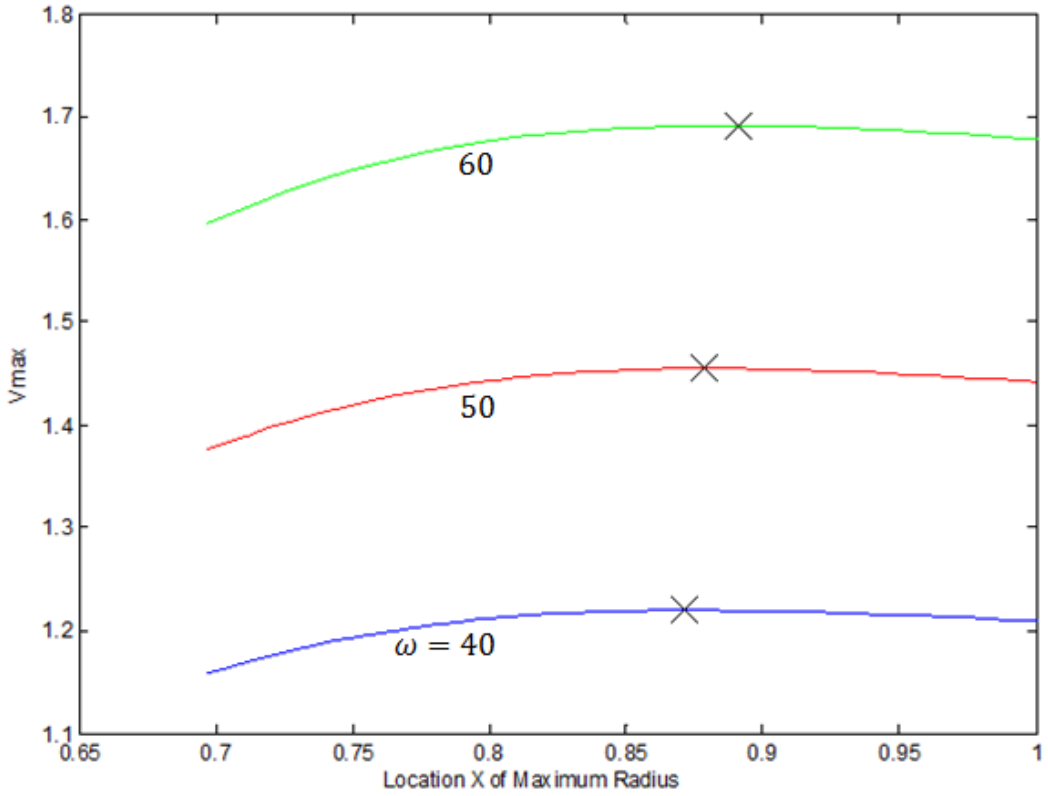

Figure 3.14: Maximum ball exit velocity V_{MAX} versus the Location of the Maximum Radius X with m_1=40 oz, l=33", r_{MAX}=1.375", and ω=40, 50 and 60 rad/s (MATLAB code 26, Appendix A)

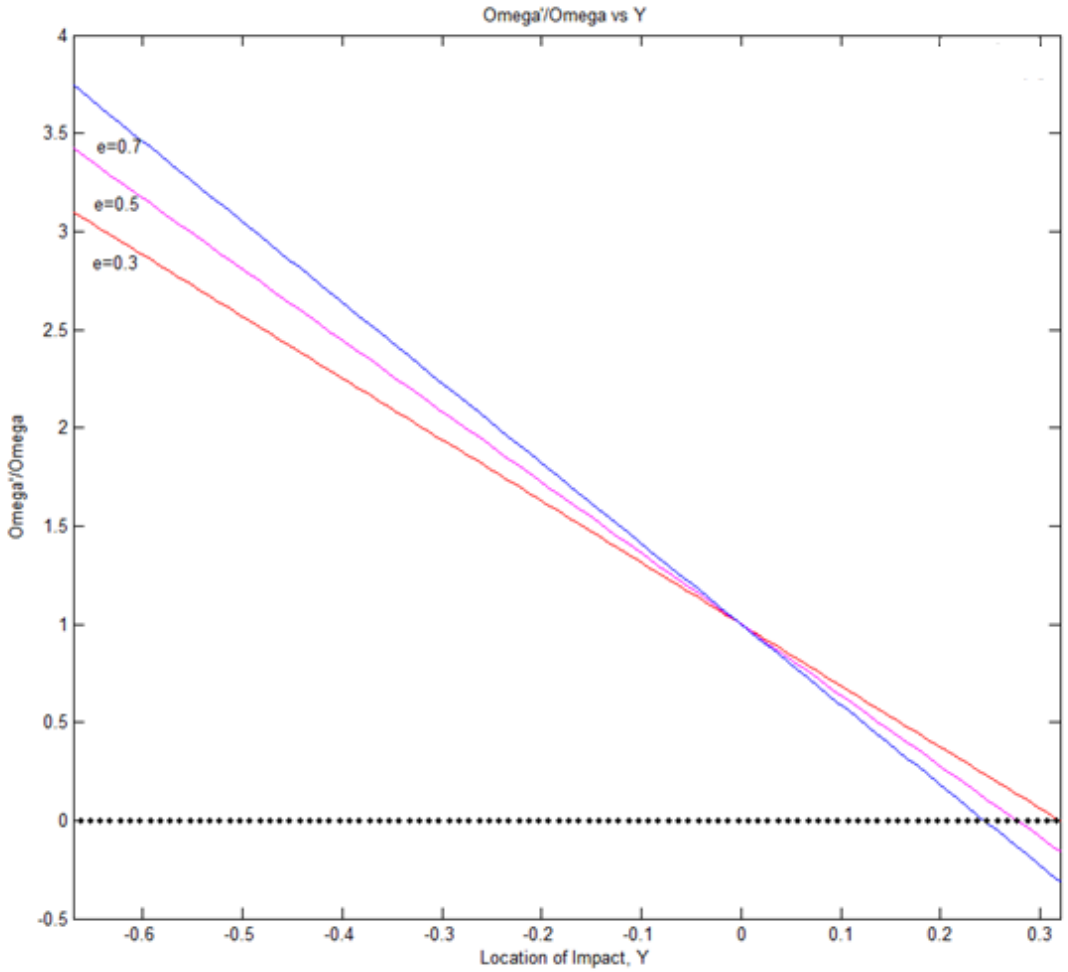

Figure 3.15: Ω'/ Ω vs. Location of impact, Y, with e = 0.3, 0.5, 0.7 (MATLAB code 27, Appendix A)

0.5, and 0.7. $\frac{\Omega'}{\Omega}$ represents the ratio of the post-impact angular velocity to the pre-impact angular velocity. In each case the relationship is linear, and as the impact location moves away from the knob, the value of $\frac{\Omega'}{\Omega}$ decreases. For a constant value of *Y* which is closer to the knob than the axial location of the center of mass, $\frac{\Omega'}{\Omega}$ increases as *e* increases. For a constant value of *Y* which is farther from the knob than the axial location of the center of mass, $\frac{\Omega'}{\Omega}$ decreases as *e* increases. Each line intersects at *Y*=0 (the location of the center of mass), and the value of $\frac{\Omega'}{\Omega}$ at this point is 1, indicating that an impact at this location will not change the angular velocity of the bat. An important note is that each line crosses $\frac{\Omega'}{\Omega} = 0$. This indicates that for each of these values of *e* there is an impact location which will result in an angular velocity after impact of zero.

The next value to be considered versus *e* is that of the post-collision location of the center of rotation of the bat, *D'*. This parameter is highly dependent upon the location of the impact. The initial location of the center of rotation, *D*, is assumed to be 2.5" off the knob and is extracted from experimental data from outside sources. The location after impact, *D*', is given by equation (13). This equation is where the note from the previous analysis comes into play: when *Ω'* is equal to zero, the equation is undefined. As the value of *Ω'* approaches zero, the value of *D'* becomes larger. The limit of *D'* as *Ω'* approaches zero from the negative side is ∞. However, the limit of *D'* as *Ω'* approaches zero from the positive side is $-\infty$. Infinite values of *D'* imply that the bat is moving with pure linear motion and does not rotate after collision. This effect is reflected in Figure 3.16 where $\frac{D'}{D}$ is taken to be the ratio of the post-collision distance to the center

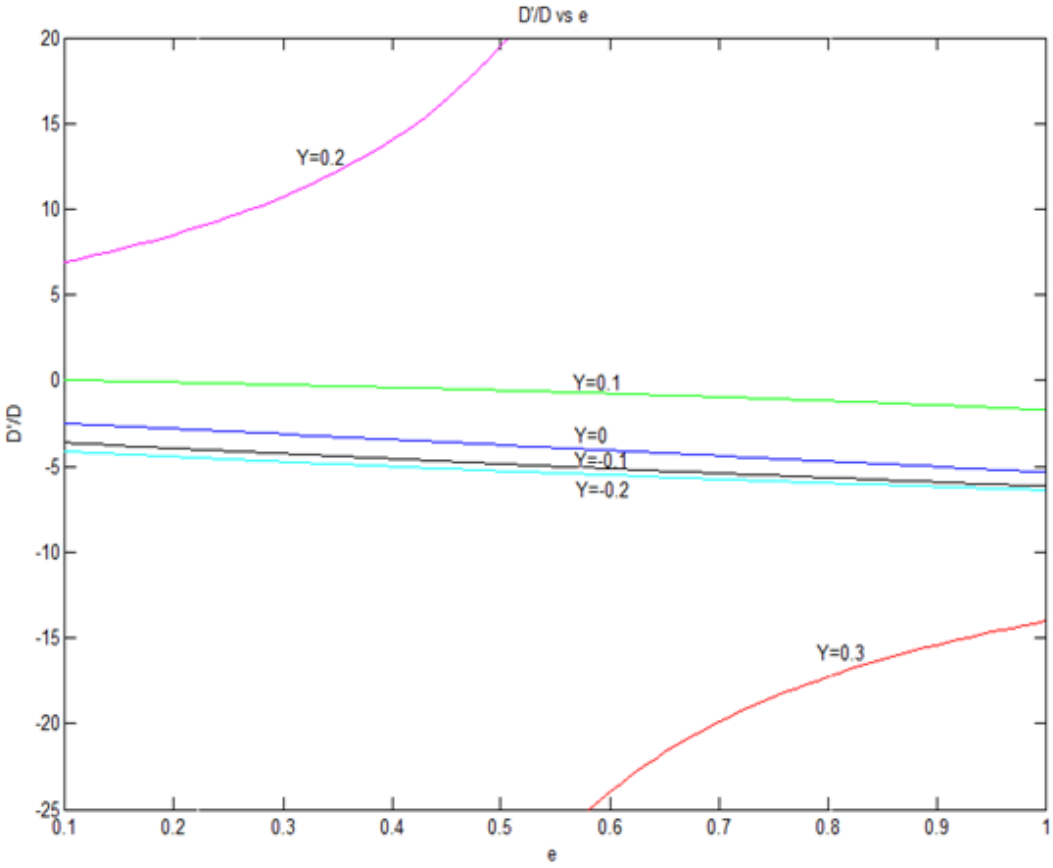

Figure 3.16: D'/D vs. coefficient of restitution, *e*, with *Y*= -0.2, -0.1, 0, 0.1, 0.2, and 0.3 (MATLAB code 28, Appendix A)

of rotation over the pre-collision distance. For the values of *Y*=0.1, 0, -0.1, and -0.2, the value of $\frac{\Omega'}{\Omega}$ does not reach zero for the applicable range. For these values of *Y*, the value of $\frac{D'}{D}$ becomes more negative as *e* increases. Both the values of *Y*=0.2 and 0.3 contain a value of $\frac{\Omega'}{\Omega} = 0$, which causes the dramatic curve in those graphs.

The final parameter that is analyzed versus the coefficient of restitution is the magnitude of V_{MAX}, shown in Figure 3.17. As expected, the value of V_{MAX} increases linearly with the value of the coefficient of restitution, *e*. The location of the maximum velocity, X_{MAX}, is not dependent upon the coefficient of restitution.

Several parameters are plotted versus Ω to examine its affect on the dynamic properties of the bat-ball impact, the first of which is $\frac{D'}{D}$ shown in Figure 3.18. This relationship is similar to that of $\frac{D'}{D}$ versus *e*, as the locations of impact which produce $\frac{\Omega'}{\Omega} = 0$ affect the behavior. For the values of *Y*=0.1, 0, -0.1, and -0.2, the value of $\frac{\Omega'}{\Omega}$ does not reach zero for the applicable range. For these values $\frac{D'}{D}$ increases as Ω increases, and for a fixed value of Ω, $\frac{D'}{D}$ increases as *Y* increases. For the values of *Y* = 0.2 and 0.3, there is a location of impact which results in $\frac{\Omega'}{\Omega} = 0$.

Other parameters that are plotted versus Ω are V_{MAX} and X_{MAX}, shown in Figures 3.19 and 3.20 respectively. As the value of Ω increases, the value of V_{MAX} increases. Also, at a fixed value of Ω the value of V_{MAX} increases as the mass of the bat increases. X_{MAX} moves away from the knob of the bat as the angular velocity, Ω, increases.

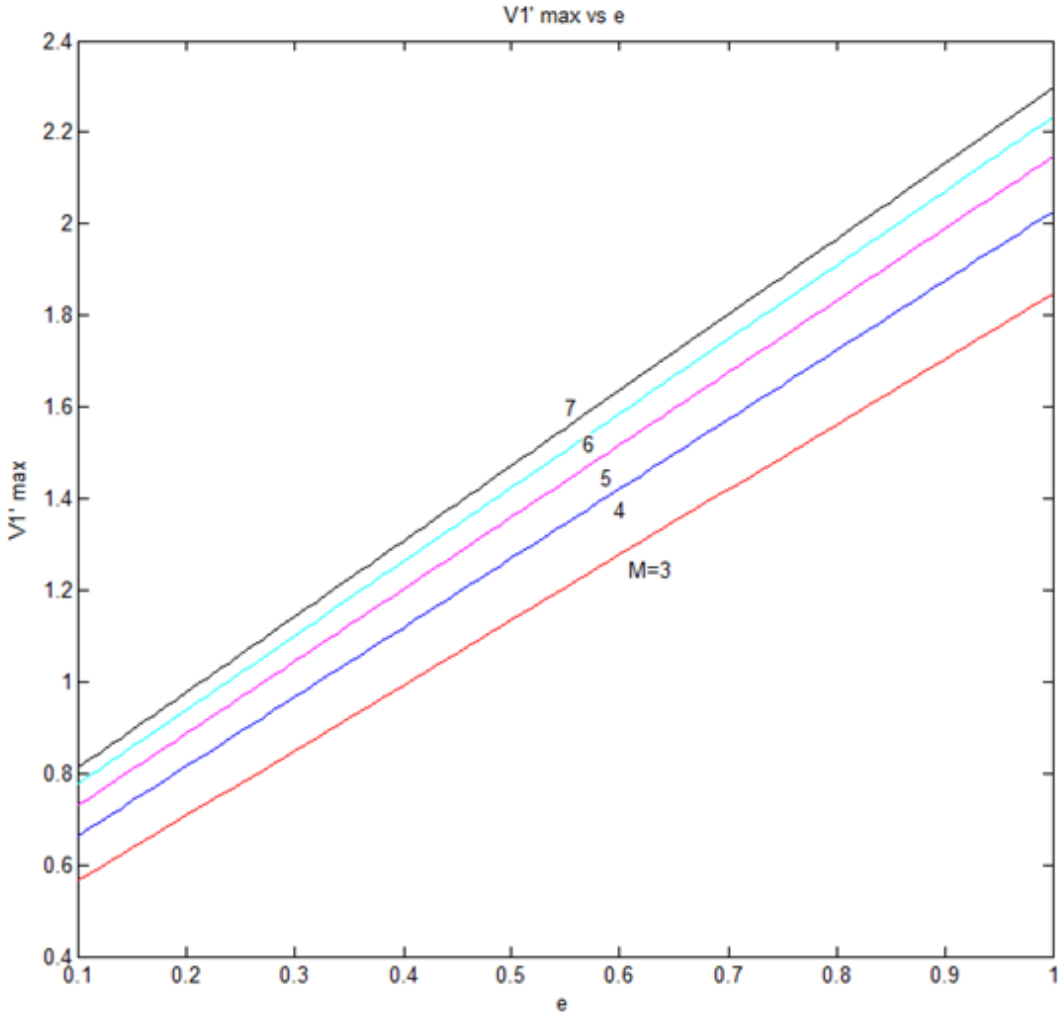

Figure 3.17: V_{max} versus coefficient of restitution, *e*, with *M*=3, 4, 5, 6, and 7 (MATLAB code 29, Appendix A)

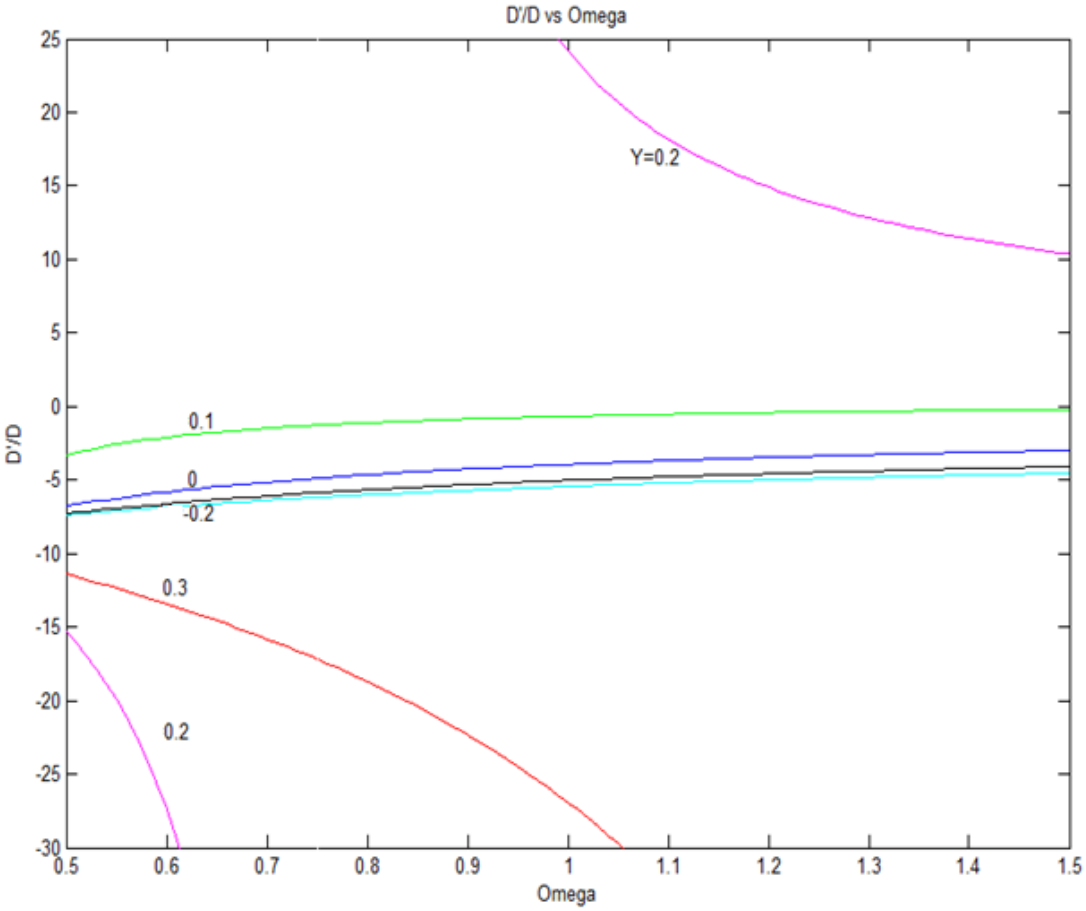

Figure 3.18: *D'/D* vs. Ω, with *Y*= -0.2, -0.1, 0, 0.1, 0.2, and 0.3 (MATLAB code 30, Appendix A)

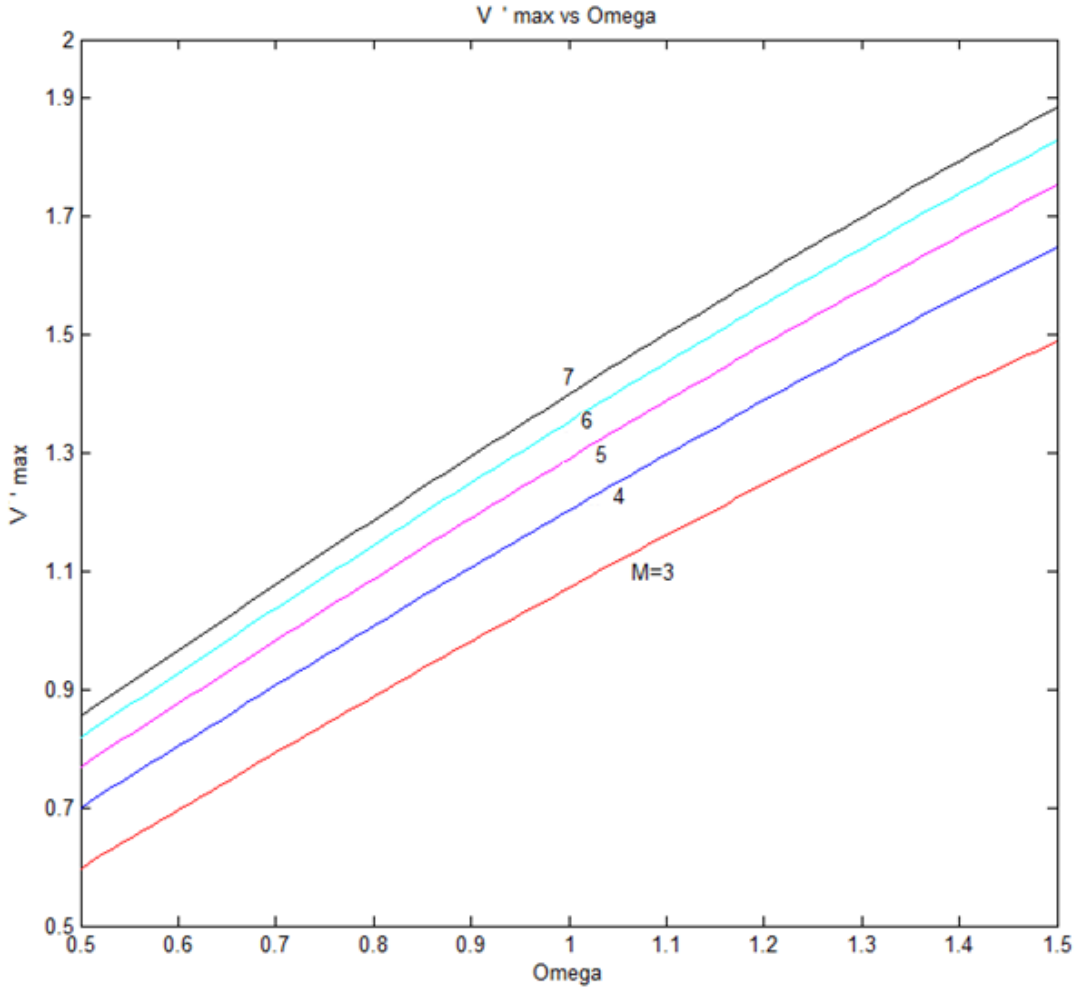

Figure 3.19: V_{MAX} versus Ω, with M= 3, 4, 5, 6, and 7 (MATLAB code 31, Appendix A)

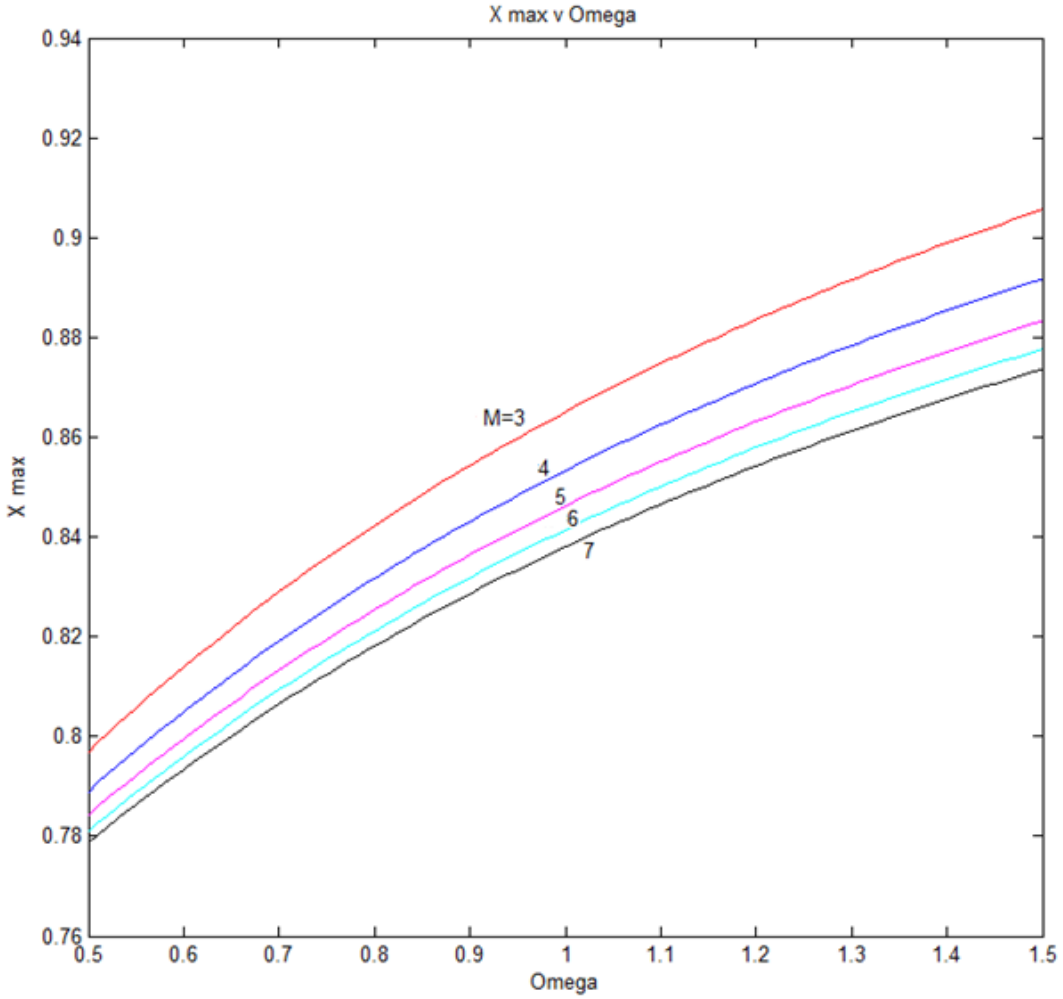

Figure 3.20: X_{MAX} versus Ω, with M = 3, 4 , 5, 6, and 7 (MATLAB code 32, Appendix A)

Chapter 4 Dynamics of the Swing

In this section, we further refine our model. First, we determine, for a fixed applied torque, the dependence of the angular velocity of the bat on its moment of inertia. In our previous analysis we assumed a constant rotational velocity independent of bat profile. Now we consider the influence of moment of inertia on the swing speed as the radial profile changes. We will quantify the competing effects of increased moment of inertia and decreased swing speed as they affect hitting performance. Secondly, we will conduct an analysis of "cupping," a practice in which a small, round cup is bored from the end of the bat to decrease moment of inertia and increase swing speed. Again this produces competing effects, as increased swing speed decreases the time of the swing, but lower mass diminishes the inertial effects imparted to the ball. In an anecdotal sense, the practice of cupping is widely considered among players to be beneficial to hitting performance. We will quantify the competing effects in order to comment more decisively on the net effect.

4.1 Ω, as Dependent on Moment of Inertia about the Center of Rotation

An aspect of the dynamics of the ball-bat collision that was omitted from the previous analysis to simplify the model was the dependence of the angular velocity, ω, on the moment of inertia about the center of rotation. In the previous analysis, ω was considered a known variable, obtained from experimental data, which was held constant, even as the mass distribution of the bat varied. In reality, changes in the distribution of the mass of the bat affect a batter's ability to swing the bat up to maximum speed. This effect is reflected in the torque required to swing the bat,

$$T = I_R \alpha \tag{1}$$

where I_R is the moment of inertia about the center of rotation (located a distance *d* off the handle) and α is the angular acceleration of the bat. The moment of inertia about the center of rotation is given by:

$$I_R = I_c + m_1(\bar{x} + d)^2 \quad . \tag{2}$$

This angular acceleration is related to the angular velocity, ω, by equation (3):

$$\frac{d\omega}{dt} = \alpha \quad . \tag{3}$$

After integration with respect to t this equation becomes

$$\omega = \alpha t \tag{4}$$

in which t is the time duration of the swing. Similarly, the angular velocity of the bat can be equated to the angular displacement of the bat, θ, by

$$\frac{d\theta}{dt} = \omega = \alpha t \tag{5}$$

which, after integration can be defined as

$$\theta = \frac{1}{2}\alpha t^2 \quad . \tag{6}$$

To obtain an expression of ω in terms of I_R, equation (6) must be solved for t

$$t = \sqrt{\frac{2\theta}{\alpha}} \tag{7}$$

and equation (1), solved for α, can be substituted into equation (7).

$$t = \sqrt{\frac{2\theta I_R}{T}} \tag{8}$$

This expression for time in equation (8) and equation (1), solved for α, are substituted into equation (4) to find an equation for ω in terms of I_R:

$$\omega = \sqrt{\frac{2T\theta}{I_R}} \quad . \tag{9}$$

However, due to the complex geometry of the swing, the bat is not accelerated purely by the torque. There is a linear component to the acceleration, which is due to the movement of the center of rotation during the swing. This relationship is largely dependent on the mass of the bat, which for the following analyses remains nearly constant. For this reason, we introduce a constant angular velocity term, ω_0, which represents the angular velocity resultant from the linear acceleration effects, which is then added to the previously calculated variable angular velocity, that is purely dependent on torque.

$$\omega = \sqrt{\frac{2T\theta}{I_R}} + \omega_0. \tag{10}$$

Three constants are required for this equation, the angular displacement of the bat through the swing, θ, the torque required for the swing, T, and the constant angular velocity, ω_0, which is due to other effects. Through experimental data from several sources, the value for θ used in our analysis is 180 degrees, or π radians. A value for the torque, T, can also be found in experimental sources and was determined to be approximately 61Nm. By substituting these values into equation (10), along with our typical value of $\omega = 50$ rad/s, we obtain a reasonable value for the angular velocity due to other effects, $\omega_0 = 20$ rad/s.

For the purpose of non-dimensional analysis, the moment of inertia about the center of rotation must be non-dimensionalized. The non-dimensional form of equation (2) is

$$J_R = J_c + (\bar{X} + D)^2 \quad . \tag{11}$$

The torque equation need not be non-dimensionalized because the dimensional value of torque can be substituted into the dimensional equation for ω, which then can be non-dimensionalized.

4.2 Cubic Profile, Fixed Mass, Zero End Slopes, Omega-Moment Dependence

Here we perform the same analyses as in Chapter 3, but now account for the effect of moment of inertia on rotational velocity**.** First, we revisit the case in which we fix mass and zero slopes at each end of the bat and then vary the end radii. In this scenario, we begin with a standard-bat like profile at one extreme and a "reversed" profile at the other extreme. The effect of this variation on swing speed is quite pronounced and is shown in Figure 4.1. When the barrel radius is minimized, omega is approximately 64, 69 and 74 rad/s for applied torques of 49, 61 and 73 Nm, respectively. As we enlarge the barrel radius, this value drops by nearly 30 percent to 47, 50 and 53 rad/s for applied torques of 49, 61 and 73 Nm, respectively. Our results from section 3.1 (which do not take moment of inertia effects into account) indicated that outgoing velocity was at a maximum when the barrel radius was at a maximum. The results shown in Figure 4.1 show that there is a competing effect wherein increasing the barrel radius decreases swing speed and tends to lessen the outgoing ball velocity.

The net effect of varying barrel-radius on maximum outgoing ball velocity in this scenario is shown in Figure 4.2. The increased angular velocity that results from the barrel radius being small helps to balance the negative effect of having a small effective mass. As a result, the outgoing ball velocity does not decrease as sharply when the barrel radius is minimized. In the case where the barrel radius is maximized, that is when the

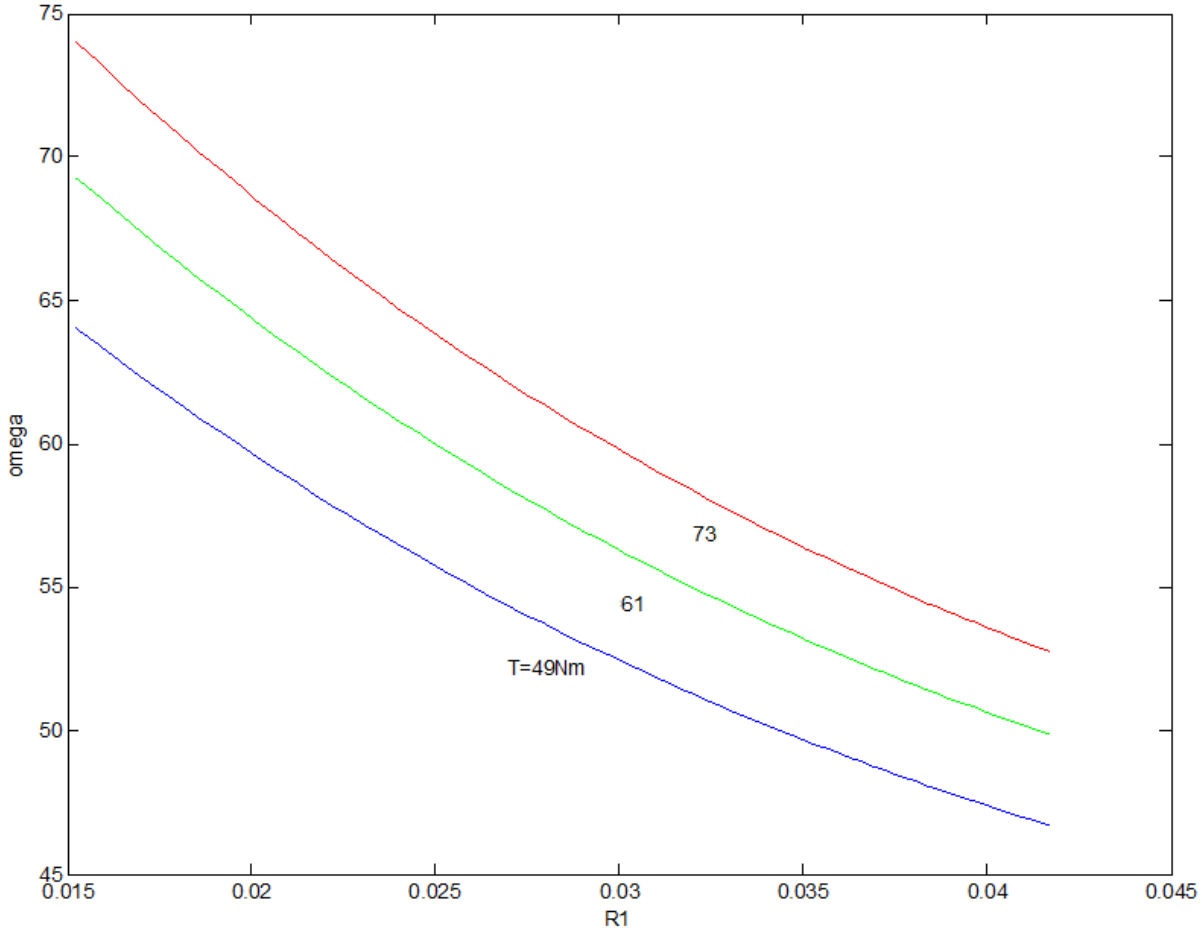

Figure 4.1: Angular velocity ω versus non-dimensional barrel radius R_1 for applied torques of T=49, 61 and 73 Nm and with ω_0 = 20 rad/s (MATLAB code 33, Appendix A)

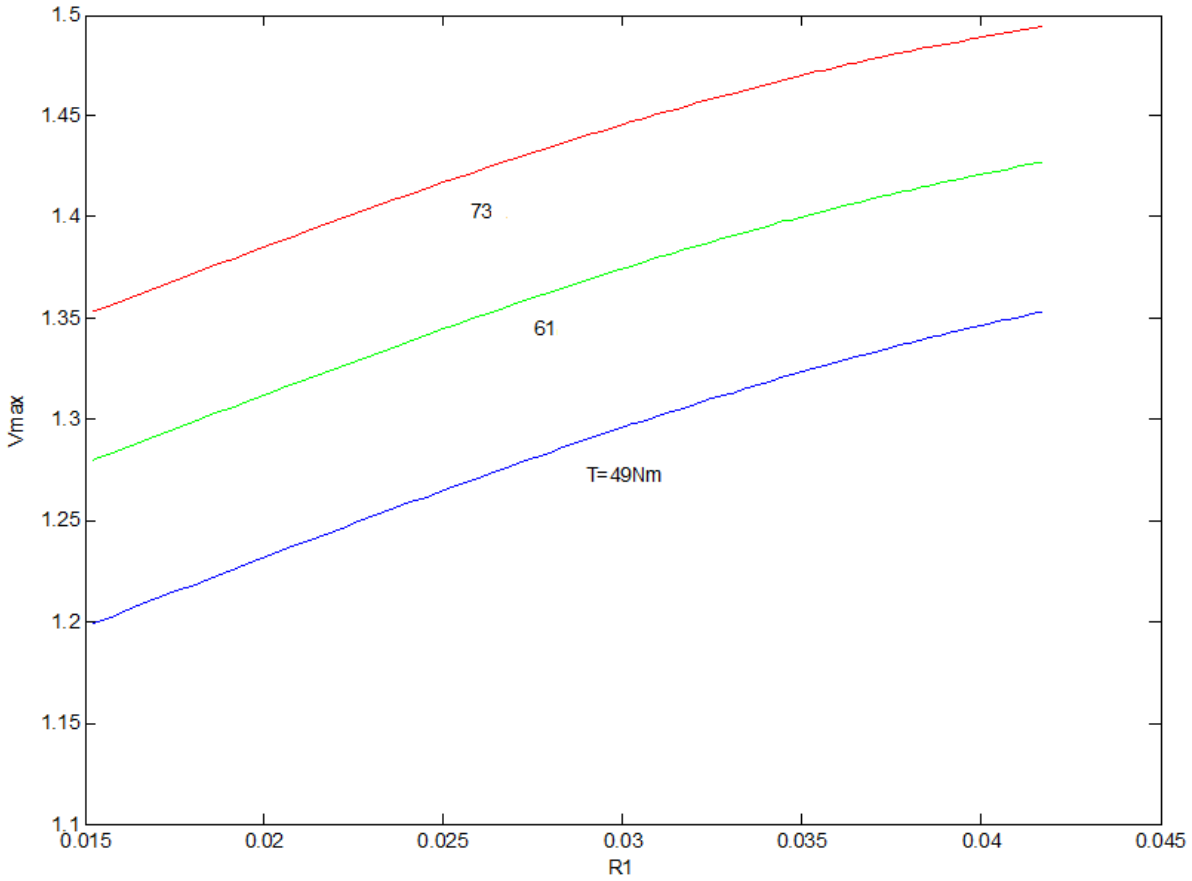

Figure 4.2: Maximum non-dimensional outgoing velocity V_{MAX} versus non-dimnesional barrel radius R_1 for applied torques of T=49, 61 and 73 Nm and with ω_0 = 20 rad/s (MATLAB code 34, Appendix A)

bat profile matches our typical profile, and when the typical value of torque is utilized, the outgoing ball velocity and the swing speed exactly match those values calculated in previous sections, as expected.

A final behavior noted here is the movement of the optimal impact location as we vary the end radii. Figure 4.3 shows that when the barrel radius is minimized, the optimal impact location occurs approximately at $X = 0.53$. When the barrel radius is maximized, this point moves to just over $X = 0.80$. This behavior is expected as the optimal impact point follows the variance in mass distribution.

4.3 Fixed Minimum and Maximum Radii, Zero Handle Slope, Omega-Moment Dependence

In this section, as in Section 3.2, we set the minimum and maximum radii, and then vary the location of the maximum radius from the extreme barrel-end toward the handle. As the shape changes, we allow the mass and moment of inertia to vary accordingly. We again consider the effect of moment of inertia on the swing speed.

Figure 4.4 plots the maximum outgoing ball velocity as a function of the location of the maximum radius. The leftmost point represents the maximum radius located distance 70 percent of the total length from the handle end. The rightmost point represents the maximum radius located at the extreme barrel-end. We see here that the optimal bat profile in this scenario is that which has the maximum radius located at the extreme barrel-end for torques of T= 61 and 73 Nm. However, for a lower applied torque, such as T= 49 Nm, there is an optimal location of R_{max}, in this case 96 percent of the way along the bat from the handle end. This is due to competing effects between both the actual and effective masses of the bat and the resultant swing speed, which is a

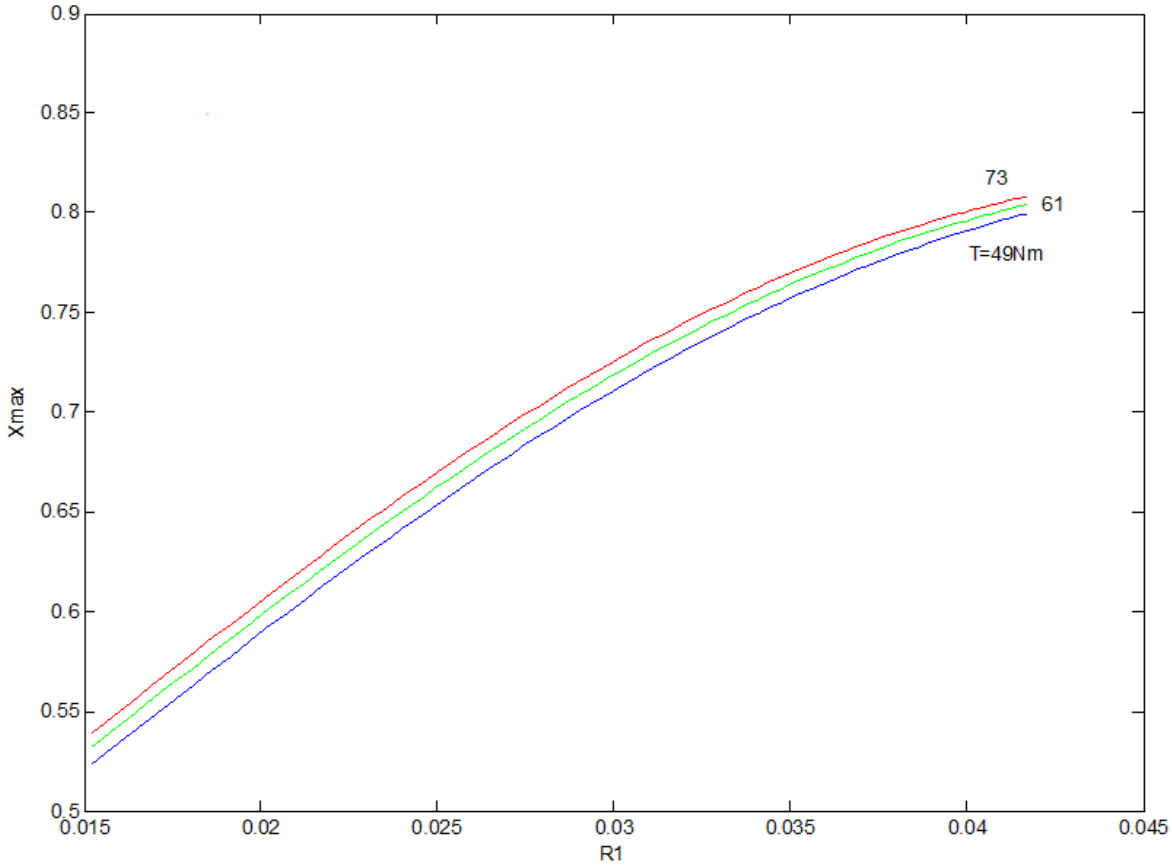

Figure 4.3: Non-dimensional location X_{MAX} that give maximum outgoing velocity versus non-dimensional barrel radius R_1 for applied torques of T=49, 61and 72 Nm and with ω_0 = 20 rad/s (MATLAB code 35, Appendix A)

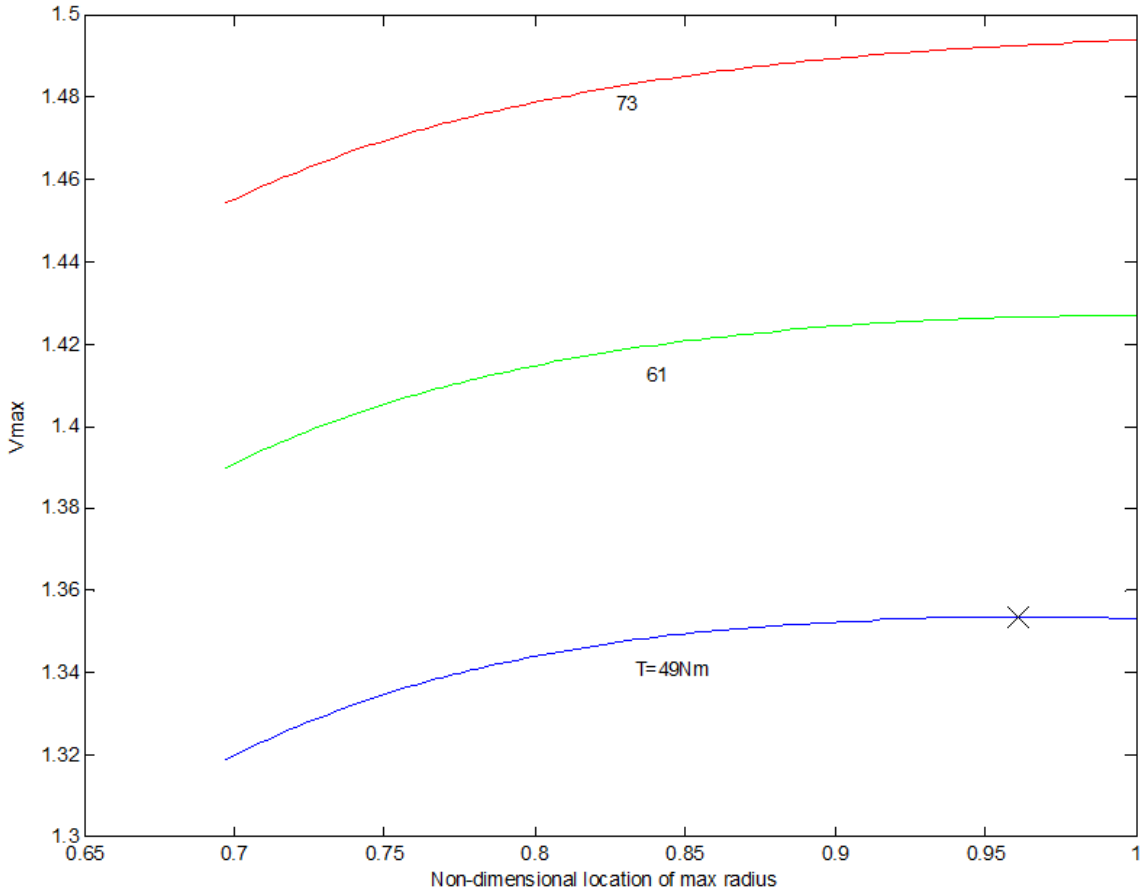

Figure 4.4: Non-dimensional maximum outgoing velocity V_{MAX} versus non-dimensional location of R_{max} with torques T = 49, 61 and 73 Nm and with ω_0 = 20 rad/s (MATLAB code 36, Appendix A)

function of the moment of inertia. The bat mass as a function of the location of maximum radius is plotted in Figure 3.5 and the resultant swing speed is plotted in Figure 4.5.

4.4 Fixed Mass and Maximum Radius, Zero Handle Slope, Omega-Moment Dependence

In this section, we vary the location of maximum radius as in Section 3.3 but let the extreme handle-end radius "adjust" in order to keep mass constant. Figure 4.6 shows the maximum outgoing ball velocity as a function of the maximum radius location. The behavior is similar to that in Figure 4.4. However, the greatest V_{MAX} occurs when the maximum radius is located away for the barrel end for all cases, unlike in Figure 4.4 where it was only for the low torque case that the optimal location was not at the extreme barrel end. Optimal locations for the maximum radius are approximately 92, 94 and 96 percent of the way along the bat from the handle end for torques of 49, 61 and 73 Nm, respectively. This plot again illustrates the competing effects of effective mass and angular velocity as a function of moment of inertia. Since the mass of the bat is held constant, it is only the distribution of that mass that effects the dynamics. The changing values of the angular velocities are plotted in Figure 4.7.

4.5 Analysis of Cupping

Here we consider a case where a small amount of material is removed from the interior of the end of the bat. This process is commonly referred to as cupping, and is believed to have a positive effect on overall bat performance. A mathematical approximation of this will be added to our model to investigate any effects this may have on performance. A diagram of the cupping is shown in Figure 4.8.

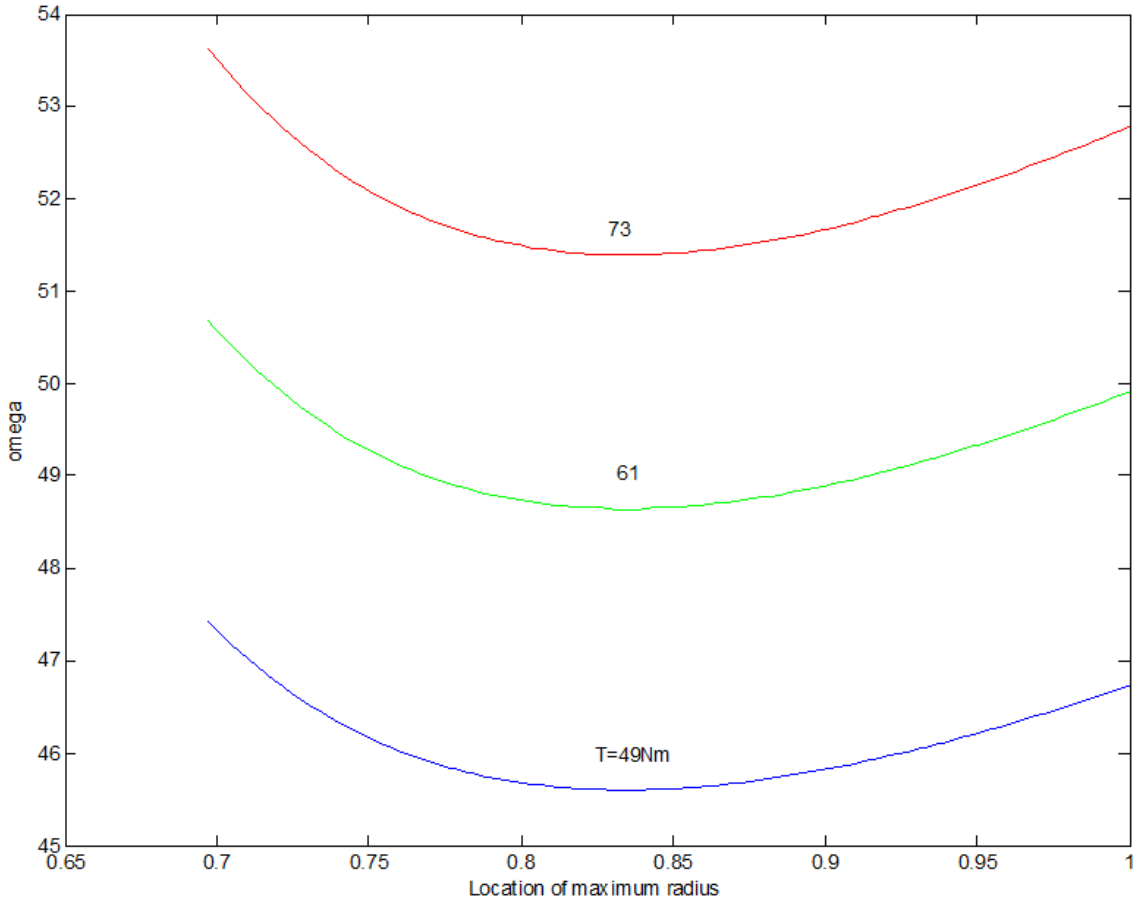

Figure 4.5: Angular velocity ω versus non-dimensional locations of R_{MAX} with torques T = 49, 61 and 73 Nm and with ω_0 = 20 rad/s (MATLAB code 37, Appendix A)

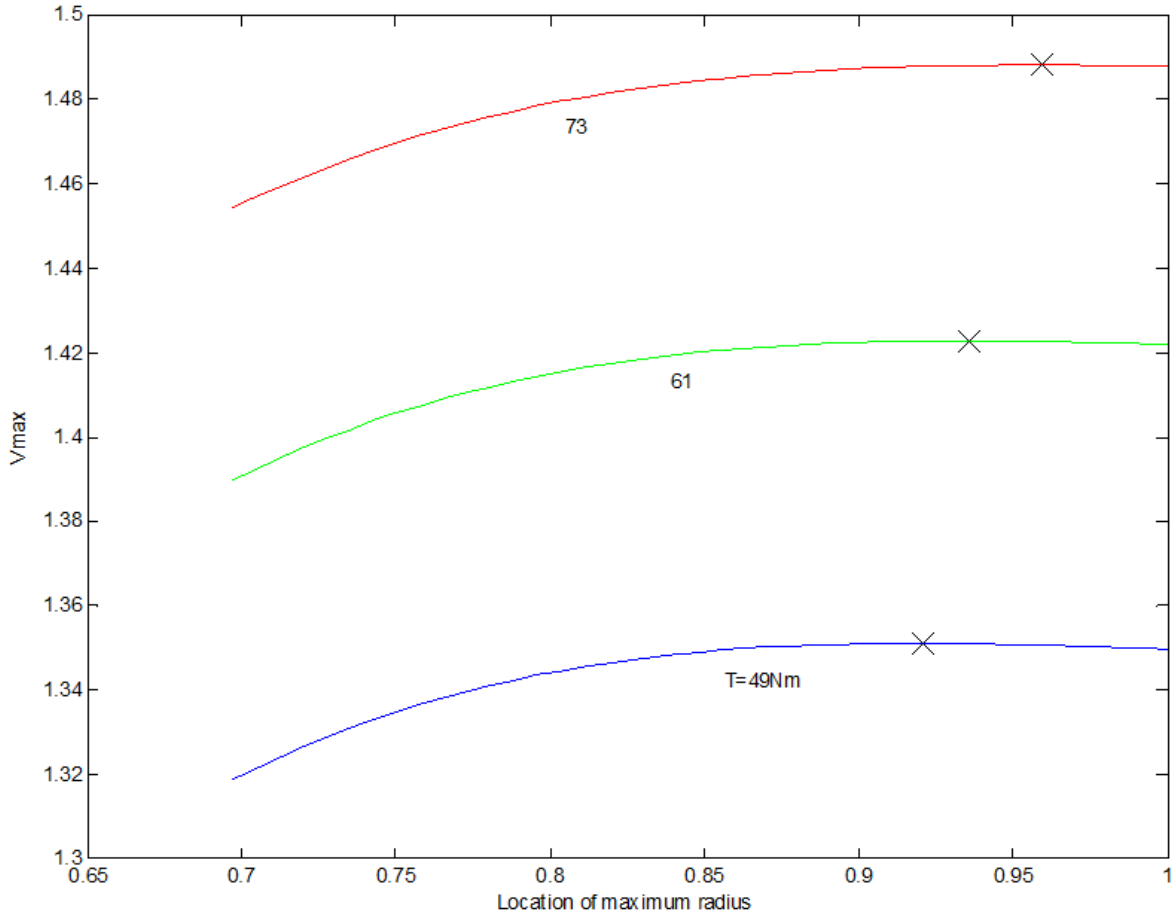

Figure 4.6: Non-dimensional maximum outgoing velocity V_{MAX} versus non-dimensional location of R_{MAX} with constant mass, torques T = 49, 61 and 73 NM and with ω_0 = 20 rad/s (MATLAB code 38, Appendix A)

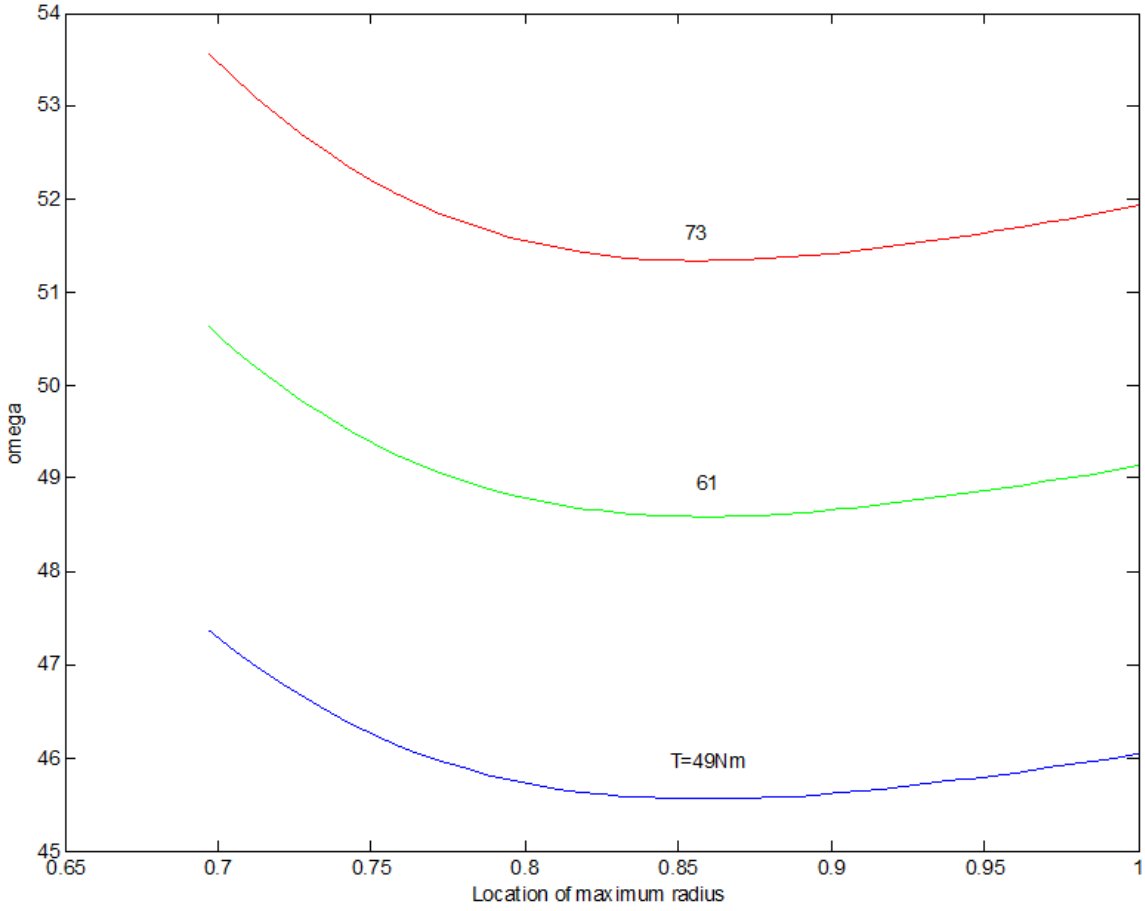

Figure 4.7: Angular velocity ω versus non-dimensional location of R_{MAX} with constant mass, torques T = 49, 61 and 73 and with ω_0 = 20 rad/s (MATLAB code 39, Appendix A)

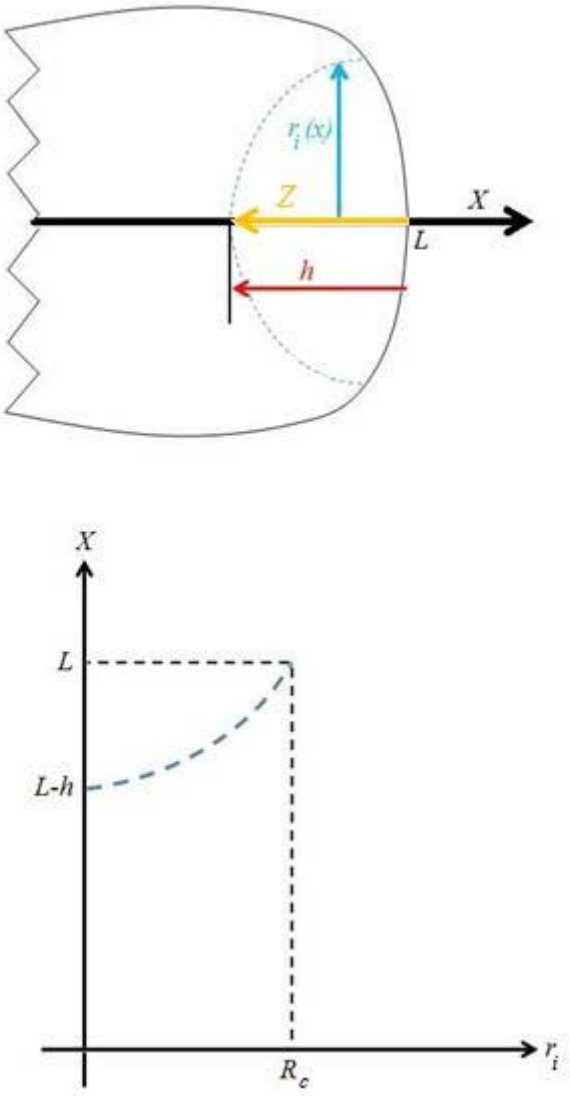

Figure 4.8: Diagram of cupping analysis

We will focus on a cup with a constant radius, R_c, at the extreme barrel end of the bat. The radius of the cup will taper down to zero in a parabolic arc, at a variable depth into the bat, *h*. We will consider here cup depths between 0 and 1 inch, as limited by MLB rules.

A temporary variable *z* is assigned to represent the depth into the bat from the barrel end, such that:

$$z = L - x \tag{12}$$

Since we want the bottom of the cup to be smooth, we take *z* to be a function of the radius, r_i, for calculation purposes, enabling us to set the slope of $z(r_i)$ equal to zero. The parabola therefore takes the form:

$$z = f + gr_i + kr_i^2 \tag{13}$$

where *f*, *g* and *k* are constants determined by the boundary conditions. The boundary conditions as defined by the limits on cup shape and size are as follows.

$$z(0) = h \tag{14}$$

$$z'(0) = 0 \tag{15}$$

$$z(R_c) = 0 \tag{16}$$

These are substituted into the parabolic equation and the constants *f*, *g* and *k* are solved for.

$$f = h \tag{17}$$

$$g = 0 \tag{18}$$

$$k = \frac{-h}{R_c^2} \tag{19}$$

Finally, these values are substituted into equation (13), the equation is solved for $r_i(z)$, and the relation for *z* (equation (12)) is substituted:

$$r_i = \sqrt{\frac{(h-L+x)R_c^2}{h}} \tag{20}$$

This equation for the radius of the cup as a function of *x* can be used to calculate the mass, first moment and moment of inertia of the cup by equations (2.1), (2.2) and (2.3). These values can be subtracted from the calculated values for the uncapped bat, resulting in new values of mass, first moment and moment of inertia. These combined values are then used in the dynamics equations.

Figure 4.9 plots the variation of the moment of inertia about the point of rotation versus h. Without any cupping ($h = 0$), the moment of inertia is equal to approximately 2340 oz-in^2. As we increase the cup depth, the moment of inertia decreases in a linear fashion to a value of about 2270 oz-in^2. This represents a decrease of 3 percent.

Figure 4.10 shows how mass varies with h. At $h = 0$, the bat mass is equal to about 34.95 oz. As h is increased, mass decreases in a linear fashion to about 34.4 oz, a difference of 1.6 percent.

Figure 4.11 plots omega versus h. We know that as h increases, the moment of inertia decreases. This contributes to an increase in omega. As cup depth goes from 0 to 1 inch, omega increases from 50 rad/s to 50.8 rad/s. This is an increase of 1.6 percent.

In Figure 4.12, we plot the effect of h on V_{MAX}. It is apparent that the more a bat is cupped, the lesser V_{MAX} will be. In this case, V_{MAX} varies from about 1.427 times the pitched ball speed to about 1.4245 the pitched ball speed, a difference of about 0.3 percent. Ultimately, while the cupping of a bat does not have a positive contribution to V_{MAX}, the effect is quite small.

Finally, in Figure 4.13, we plot the movement of the optimal impact point with varying h. Although this point moves in toward the handle-end as h is increased, it only

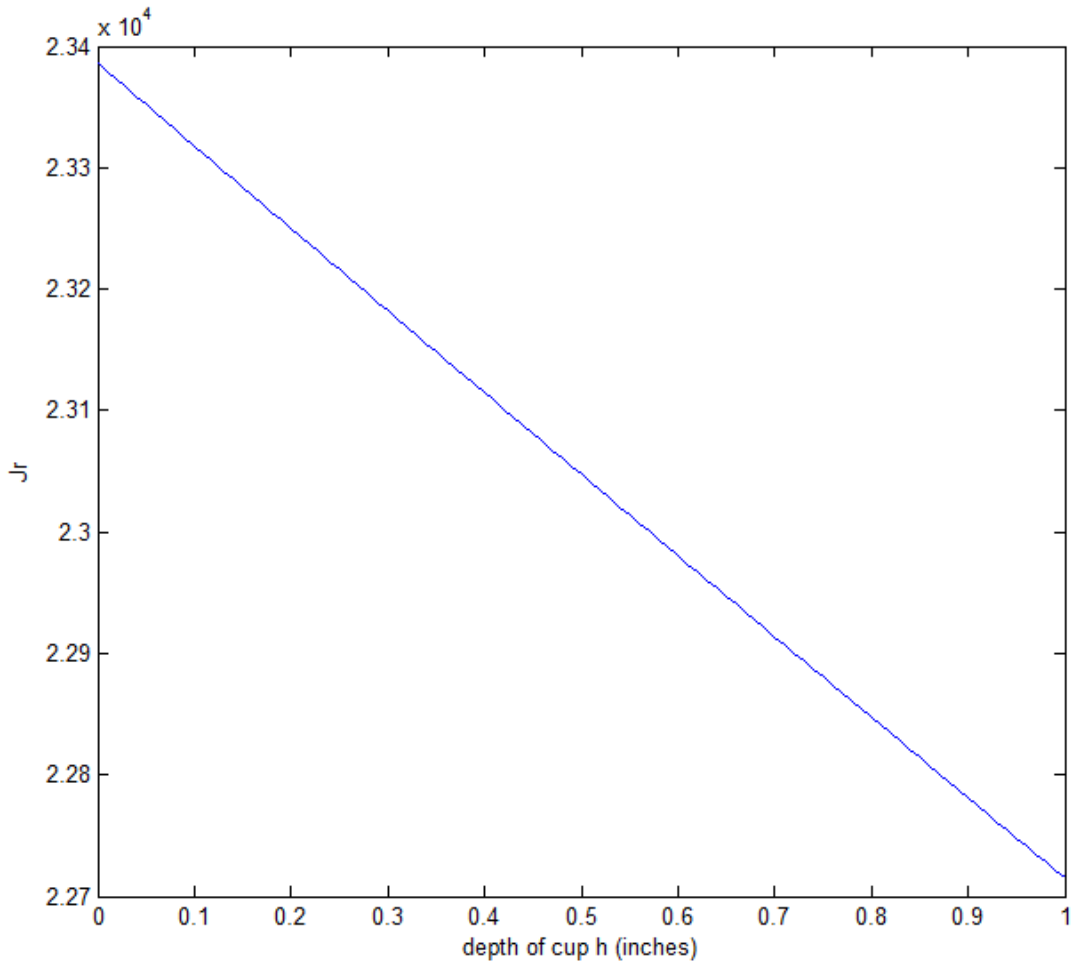

Figure 4.9: Depth of cup versus the moment of inertia about the center of rotation (MATLAB code 40, Appendix A)

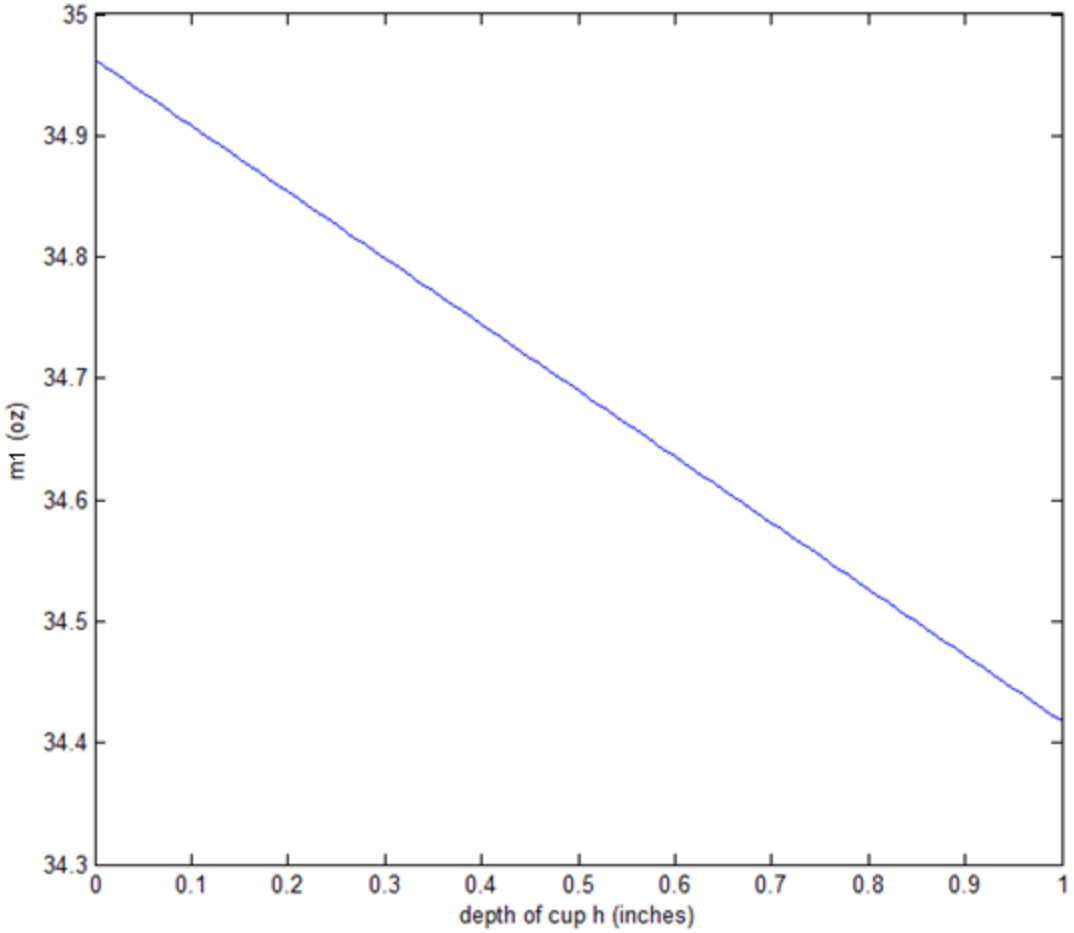

Figure 4.10: Depth of cup, *h*, versus the mass of the bat (MATLAB code 41, Appendix A)

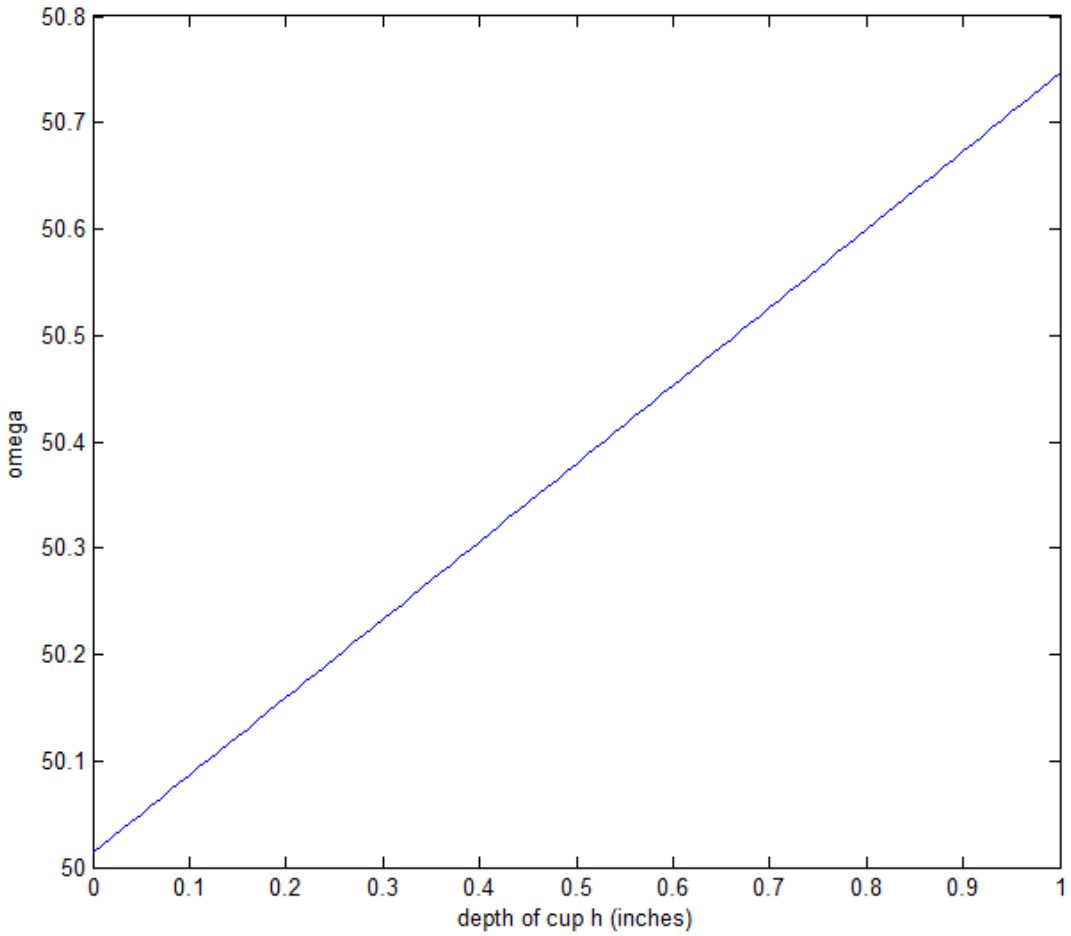

Figure 4.11: Angular velocity versus cup depth h for r_{MAX} = 1.375", r_{MIN} = 0.5", torque t = 61 Nm and ω_0 = 20 rad/s (MATLAB code 42, Appendix A)

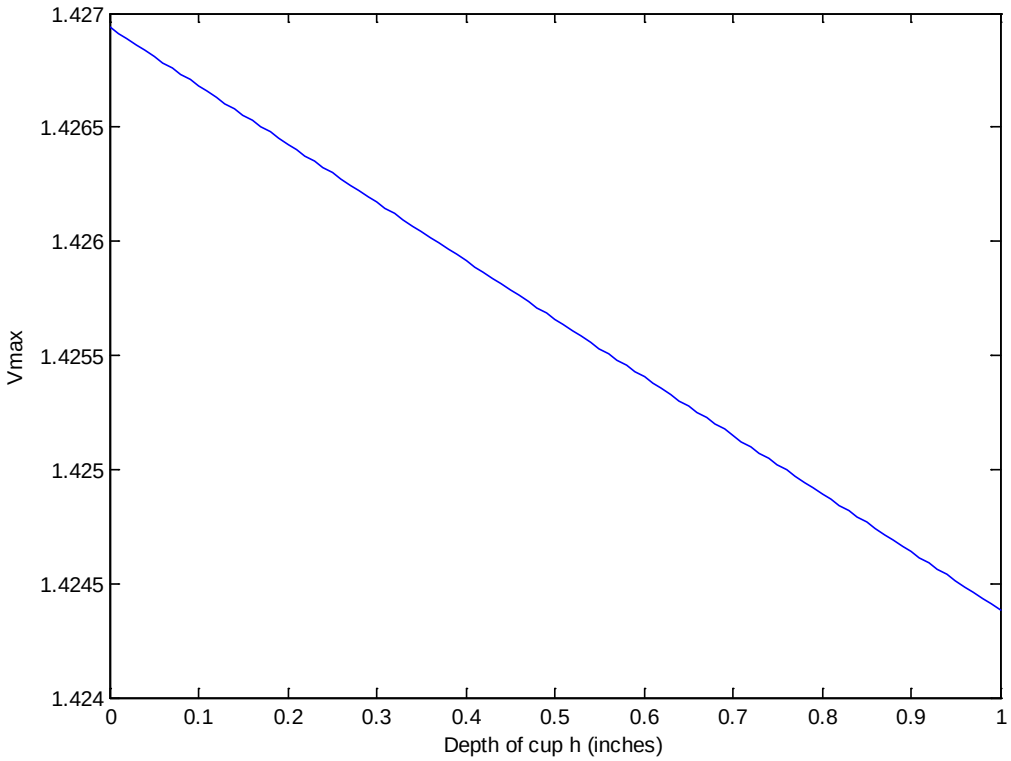

Figure 4.12: Non-dimensional maximum outgoing velocity versus cup depth for r_{MAX} = 1.375", r_{MIN} = 0.5", torque T = 61 Nm and ω_0 = 20 rad/s (MATLAB code 43, Appendix A)

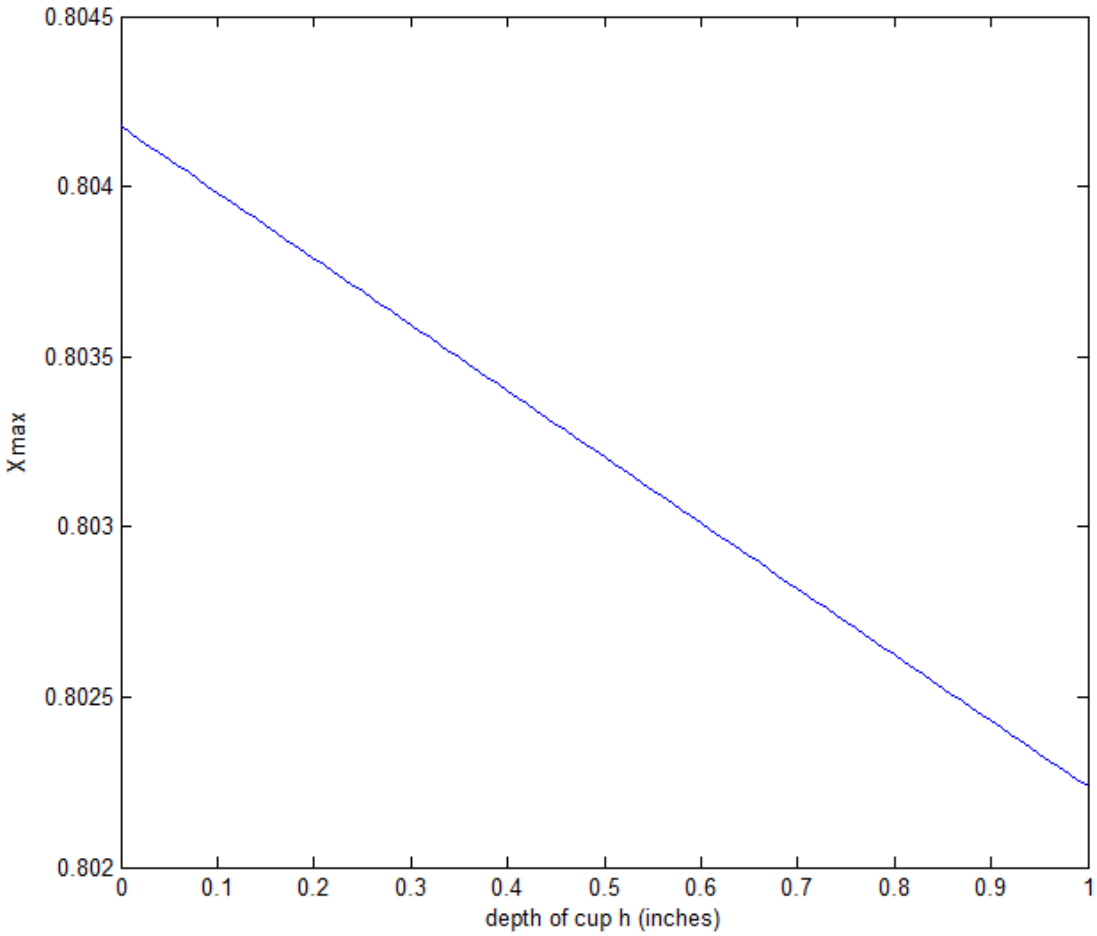

Figure 4.13: Non-dimensional X_{MAX} versus cup depth h for r_{MAX} = 1.375", r_{MIN} = 0.5", torque T = 61 Nm and ω_0 = 20 rad/s (MATLAB code 44, Appendix A)

moves by an amount equal to 0.002 times the length of the bat (0.8042 to 0.8022). This is an overall difference of 0.2 percent, a negligible effect.

Conclusion

We have developed a mathematical model that predicts the outgoing ball velocity as a function of impact point along the bat, coefficient of restitution, bat density, angular swing velocity, swing geometry and bat geometry. This model can be utilized to predict at what point along the bat the outgoing ball velocity is maximized, and the resultant velocity from an impact at this location is used as a metric for overall bat performance. A cubic function was utilized to represent the radial profile of the bat, and the bat geometry was varied by substituting different boundary conditions. A relation was also developed that predicted bat angular velocity at the moment of impact as a function of the torque applied and the moment of inertia about the center of rotation. These relations were combined to study the effects of variable bat geometry on the overall bat performance. We noted that the optimal bat in our analysis had a maximum radius near the barrel-end and a minimum radius at the handle-end. Using the maximum allowable bat radius yielded the highest outgoing ball speed. We also noted that the optimal location for the maximum radius is a few inches in from the extreme barrel-end. Our model was then utilized to analyze the effects of "cupping." It was determined that cupping the bat decreased the outgoing ball velocity for a constant torque swing, but the swing speed was simultaneously increased. Therefore, the choice of whether or not to cup the bat is a matter of individual batter preference. If optimal swing speed is of the utmost concern, then cupping provides an advantage. However, if maximizing outgoing ball speed is the dominant consideration, cupping the bat will yield negative effects.

References

Adair, Robert K., (1998). Comment on "The sweet spot of a baseball bat," by Rod Cross." American Journal of Physics, Volume 69, Number 2, pp 229-230.

Bahill, A. Terry, (2004). The ideal moment of inertia for a baseball or softball bat. IEEE Transactions on Systems, Man and Cybernetics – Part A: Systems and Humans, Volume 34, Number 2.

Cross, Rod. (1998a). The sweet spot of a baseball bat. American Journal of Physics, Volume 68, Number 9, pp 772-779.

Cross, Rod, (1998b). Response to "Comment on 'The sweet spot of a baseball bat,' by Rod Cross." American Journal of Physics, Volume 69, Number 2, pp 231-232.

Cross, Rod, (1999). Impact of a ball with a bat or racket. American Journal of Physics, Volume 67, Number 8, pp 692-702.

Cross, Rod., (2008a). Physics of baseball. University of Sydney Physics Department. http://physics.usyd.edu.au/~cross/baseball.html

Cross, Rod., (2008b). "Simple" Collisions. University of Sydney Physics Department. http://physics.usyd.edu.au/~cross/Collisions.html

Fleisig, G. S., Zheng, N., Stodden, D. F., Andrews, J. R., (2002). Relationship between bat mass properties and bat velocity. Sports Engineering, Volume 5, pp 1-8.

Nathan, Alan M., (2000). Dynamics of the baseball-bat collision. American Journal of Physics, Volume 68, Number 11, pp 979-990.

Nathan, Alan M., (2002). Characterizing the performance of baseball bats. American Journal of Physics, Volume 71, Number 2, pp 134-143.

Russell, Daniel A., (2003). Forces between bat and ball. Science and Mathematics Department, Kettering University. http://kettering.edu/~drussell/bats-new/impulse.html

Russell, Daniel A., (2004a). The sweet spot of a hollow baseball or softball bat. Science and Mathematics Department, Kettering University. http://kettering.edu/~drussell/bats-new/sweetspot.html

Russell, Daniel A., (2004b). What about corked bats? Science and Mathematics Department, Kettering University. http://kettering.edu/~drussell/bats-new/corkedbat.html

Russell, Daniel A., (2005a). How are baseball and softball bats different? Science and Mathematics Department, Kettering University. http://kettering.edu/~drussell/bats-new/baseball-ssoftball.html

Russell, Daniel A., (2005b). Does it matter how tightly you grip the bat? Science and Mathematics Department, Kettering University. http://kettering.edu/~drussell/bats-new/grip.html

Russell, Daniel A., (2005c). What is the COP (Center of Percussion) and does it matter? Science and Mathematics Department, Kettering University. http://kettering.edu/~drussell/bats-new/cop.html

Russell, Daniel A., (2008a). Swing weight of a bat (Why moment of inertia matters more than weight). Science and Mathematics Department, Kettering University. http://kettering.edu/~drussell/bats-new/bat-moi.html

Russell, Daniel A., (2008b). Bat weight, swing speed and ball velocity. Science and Mathematics Department, Kettering University. http://kettering.edu/~drussell/bats-new/batw8.html

Sawicki, Gregory S., Hubbard, Mont, Stronge, William J., (2003). How to hit home runs: Optimum baseball bat swing parameters for maximum range trajectories. American Journal of Physics, Volume 71, Number 11, pp 1152-1162.

Shenoy, Mahesh M., Smith, Lloyd V., Axtell, John T., (2001). Performance assessment of wood, metal, and composite baseball bats. Elsevier Science Ltd. Composite Structures 52, pp 397-404.

Appendix A: MatLab Code

MatLab File 1

R_o vs. R_1
Linear Model – Constant Mass (Figure 2.3)

```
M= 0.0006;
R0= 0:0.001:sqrt(3*M);
R1= (-R0+sqrt(12*M-3*R0.*R0))/2;
plot(R0,R1, 'r');
hold on;
M= 0.0008;
R0= 0:0.001:sqrt(3*M);
R1= (-R0+sqrt(12*M-3*R0.*R0))/2;
plot(R0,R1, 'g');
hold on;
M= 0.001;
R0= 0:0.001:sqrt(3*M);
R1= (-R0+sqrt(12*M-3*R0.*R0))/2;
plot(R0,R1, 'm');
hold on;
M= 0.0012;
R0= 0:0.001:sqrt(3*M);
R1= (-R0+sqrt(12*M-3*R0.*R0))/2;
plot(R0,R1, 'c');
hold on;
M= 0.0014;
R0= 0:0.001:sqrt(3*M);
R1= (-R0+sqrt(12*M-3*R0.*R0))/2;
plot(R0,R1, 'k');
hold on;
```

MatLab File 2

R_o vs. Center of Mass
Linear Model – Constant Mass (Figure 2.4)

```
M=0.0006;
R0=0:0.001:sqrt(3*M);
R1=(-R0+sqrt(12*M-3*R0.*R0))/2;
X=(R0.*R0+2*R0.*R1+3*R1.*R1)/(12*M);
plot(R0,X, 'r')
hold on
M=0.0008;
R0=0:0.001:sqrt(3*M);
R1=(-R0+sqrt(12*M-3*R0.*R0))/2;
X=(R0.*R0+2*R0.*R1+3*R1.*R1)/(12*M);
plot(R0,X, 'g')
hold on
M=0.001;
R0=0:0.001:sqrt(3*M);
R1=(-R0+sqrt(12*M-3*R0.*R0))/2;
X=(R0.*R0+2*R0.*R1+3*R1.*R1)/(12*M);
plot(R0,X, 'm')
hold on
M=0.0012;
R0=0:0.001:sqrt(3*M);
R1=(-R0+sqrt(12*M-3*R0.*R0))/2;
X=(R0.*R0+2*R0.*R1+3*R1.*R1)/(12*M);
plot(R0,X, 'c')
hold on
M=0.0014;
R0=0:0.001:sqrt(3*M);
R1=(-R0+sqrt(12*M-3*R0.*R0))/2;
X=(R0.*R0+2*R0.*R1+3*R1.*R1)/(12*M);
plot(R0,X, 'k')
hold on
```

MatLab File 3

R_o vs. Moment of Inertia about X=0
Linear Model – Constant Mass (Figure 2.5)

```
M= 0.0006;
R0= 0:0.001:sqrt(3*M);
R1= (-R0+sqrt(12*M-3*R0.*R0))/2;
I=R0.*R0+3*R0.*R1+6*R1.*R1;
plot(R0,I, 'r');
hold on
M= 0.0008;
R0= 0:0.001:sqrt(3*M);
R1= (-R0+sqrt(12*M-3*R0.*R0))/2;
I=R0.*R0+3*R0.*R1+6*R1.*R1;
plot(R0,I, 'g');
hold on
M= 0.001;
R0= 0:0.001:sqrt(3*M);
R1= (-R0+sqrt(12*M-3*R0.*R0))/2;
I=R0.*R0+3*R0.*R1+6*R1.*R1;
plot(R0,I, 'm');
hold on
M= 0.0012;
R0= 0:0.001:sqrt(3*M);
R1= (-R0+sqrt(12*M-3*R0.*R0))/2;
I=R0.*R0+3*R0.*R1+6*R1.*R1;
plot(R0,I, 'c');
hold on
M= 0.0014;
R0= 0:0.001:sqrt(3*M);
R1= (-R0+sqrt(12*M-3*R0.*R0))/2;
I=R0.*R0+3*R0.*R1+6*R1.*R1;
plot(R0,I, 'k');
hold on
legend('M=0.0006', 'M=0.0008', 'M=0.001', 'M=0.0012', 'M=0.0014')
```

MatLab File 4

R_o vs. R_1
Linear Model – Constant Moment of Inertia about X=0 (Figure 2.6)

```
I=0.2;
R1=0:0.01:sqrt(6*I);
R0=(-3*R1+sqrt(9*R1.*R1-4*(6*R1.*R1-I)))/2;
plot(R0,R1, 'r');
hold on
I=0.4;
R1=0:0.01:sqrt(6*I);
R0=(-3*R1+sqrt(9*R1.*R1-4*(6*R1.*R1-I)))/2;
plot(R0,R1, 'g');
hold on
I=0.6;
R1=0:0.01:sqrt(6*I);
R0=(-3*R1+sqrt(9*R1.*R1-4*(6*R1.*R1-I)))/2;
plot(R0,R1, 'm');
hold on
I=0.8;
R1=0:0.01:sqrt(6*I);
R0=(-3*R1+sqrt(9*R1.*R1-4*(6*R1.*R1-I)))/2;
plot(R0,R1, 'k');
hold on
```

MatLab File 5

R_o vs. Center of Mass
Linear Model – Constant Moment of Inertia about X=0 (Figure 2.7)

```
I=0.2;
R0=0:0.001:sqrt(6*I);
R1=(-3*R0+sqrt(9*R0.*R0-4*(6*R0.*R0-I)))/2;
X=(3/4)*(R0.*R0+R0.*R1+I)/(5*R0.*R0+3*R0.*R1+I);
plot(R0,X, 'r');
hold on
I=0.4;
R0=0:0.001:sqrt(6*I);
R1=(-3*R0+sqrt(9*R0.*R0-4*(6*R0.*R0-I)))/2;
X=(3/4)*(R0.*R0+R0.*R1+I)/(5*R0.*R0+3*R0.*R1+I);
plot(R0,X, 'g');
hold on
I=0.6;
R0=0:0.001:sqrt(6*I);
R1=(-3*R0+sqrt(9*R0.*R0-4*(6*R0.*R0-I)))/2;
X=(3/4)*(R0.*R0+R0.*R1+I)/(5*R0.*R0+3*R0.*R1+I);
plot(R0,X, 'm');
hold on
I=0.8;
R0=0:0.001:sqrt(6*I);
R1=(-3*R0+sqrt(9*R0.*R0-4*(6*R0.*R0-I)))/2;
X=(3/4)*(R0.*R0+R0.*R1+I)/(5*R0.*R0+3*R0.*R1+I);
plot(R0,X, 'k');
hold on
```

MatLab File 6

R_o vs. Mass
Linear Model – Constant Moment of Inertia about X=0 (Figure 2.8)

```
I=0.2;
R1=0:0.01:sqrt(6*I);
R0=(-3*R1+sqrt(9*R1.*R1-4*(6*R1.*R1-I)))/2;
M=(I-2*R0.*R1)/3;
plot(R0,M, 'r');
hold on
I=0.4;
R1=0:0.01:sqrt(6*I);
R0=(-3*R1+sqrt(9*R1.*R1-4*(6*R1.*R1-I)))/2;
M=(I-2*R0.*R1)/3;
plot(R0,M, 'g');
hold on
I=0.6;
R1=0:0.01:sqrt(6*I);
R0=(-3*R1+sqrt(9*R1.*R1-4*(6*R1.*R1-I)))/2;
M=(I-2*R0.*R1)/3;
plot(R0,M, 'm');
hold on
I=0.8;
R1=0:0.01:sqrt(6*I);
R0=(-3*R1+sqrt(9*R1.*R1-4*(6*R1.*R1-I)))/2;
M=(I-2*R0.*R1)/3;
plot(R0,M, 'k');
hold on
legend('I=0.2', 'I=0.4', 'I=0.6', 'I=0.8')
```

MatLab File 7

R_o vs. R_1
Cubic Model – Constant Mass (Figure 2.9)

```
clear
clc

M2=0.0014;
rho=0.347;
l=33; d=2.5;
rmin=0.5;
D=d/l;

A=rmin./l;
C=((-1/3)*A+sqrt((A.^2)/9-4*13/315*(A.^2-M2)))/(26/315);

R1=A+C/3;
R0=A;

MOM=(A.^2)/2+(7/30)*A.*C+(2/63)*C.^2;
Xbar=MOM/M2;
J0=(A.^2)/3+(8/45)*A.*C+(29/1134)*C.^2;
Jc=J0-M2.*Xbar.^2;
Jr=Jc+M2.*(Xbar+D).^2;

hold on
plot(R0,R1,'k')
```

MatLab File 8

R_o vs. Center of Mass
Cubic Model – Constant Mass (Figure 2.10)

```
clear
clc

M2=0.0014;
rho=0.347;
l=33; d=2.5;
rmin=0.5;
D=d/l;

A=rmin./l;
C=((-1/3)*A+sqrt((A.^2)/9-4*13/315*(A.^2-M2)))/(26/315);

R1=A+C/3;
R0=A;

MOM=(A.^2)/2+(7/30)*A.*C+(2/63)*C.^2;
Xbar=MOM/M2;
J0=(A.^2)/3+(8/45)*A.*C+(29/1134)*C.^2;
Jc=J0-M2.*Xbar.^2;
Jr=Jc+M2.*(Xbar+D).^2;

hold on
plot(R0,Xbar,'k')
```

MatLab File 9

R_o vs. Moment of Inertia about X=0
Cubic Model – Constant Mass (Figure 2.11)

```
clear
clc

M2=0.0014;
rho=0.347;
l=33; d=2.5;
rmin=0.5;
D=d/l;

A=rmin./l;
C=((-1/3)*A+sqrt((A.^2)/9-4*13/315*(A.^2-M2)))/(26/315);

R1=A+C/3;
R0=A;

MOM=(A.^2)/2+(7/30)*A.*C+(2/63)*C.^2;
Xbar=MOM/M2;
J0=(A.^2)/3+(8/45)*A.*C+(29/1134)*C.^2;
Jc=J0-M2.*Xbar.^2;
Jr=Jc+M2.*(Xbar+D).^2;

hold on
plot(R0,J0,'k')
```

MatLab File 10

R_o vs. R_1
Cubic Model – Constant Moment of Inertia about X=0 (Figure 2.12)

```
clear
clc
J0=.0008;

l=33;

Amax=sqrt(10229*J0/250);
if Amax<1.375/l
    Amax=sqrt(10229*J0/250)
else
    Amax=1.375/l;
end

A=0:.025/l:Amax;
C=((-8/45)*A+sqrt((8/45)^2*(A.^2)-4*29/1134*((A.^2)/3-J0)))/(58/1134);

R1=A+C/3;
R0=A;

M=A.^2+(1/3)*A.*C+(13/315)*C.^2;
MOM=(A.^2)/2+(7/30)*A.*C+(2/63)*C.^2;
Xbar=MOM./M;


hold on
plot(R0,R1,'k')
```

MatLab File 11

R_o vs. Center of Mass
Cubic Model – Constant Moment of Inertia about X=0 (Figure 2.13)

```
clear
clc
J0=.0008;

l=33;

Amax=sqrt(10229*J0/250);
if Amax<1.375/l
    Amax=sqrt(10229*J0/250)
else
    Amax=1.375/l;
end

A=0:.025/l:Amax;
C=((-8/45)*A+sqrt((8/45)^2*(A.^2)-4*29/1134*((A.^2)/3-J0)))/(58/1134);

R1=A+C/3;
R0=A;

M=A.^2+(1/3)*A.*C+(13/315)*C.^2;
MOM=(A.^2)/2+(7/30)*A.*C+(2/63)*C.^2;
Xbar=MOM./M;


hold on
plot(R0,Xbar,'k')
```

MatLab File 12

R_o vs. Mass
Cubic Model – Constant Moment of Inertia about X=0 (Figure 2.14)

```
clear
clc
J0=.0008;

l=33;

Amax=sqrt(10229*J0/250);
if Amax<1.375/l
    Amax=sqrt(10229*J0/250)
else
    Amax=1.375/l;
end

A=0:.025/l:Amax;
C=((-8/45)*A+sqrt((8/45)^2*(A.^2)-4*29/1134*((A.^2)/3-J0)))/(58/1134);

R1=A+C/3;
R0=A;

M=A.^2+(1/3)*A.*C+(13/315)*C.^2;
MOM=(A.^2)/2+(7/30)*A.*C+(2/63)*C.^2;
Xbar=MOM./M;


hold on
plot(R0,M,'k')
```

MatLab File 13

Outgoing Ball Velocity, V'2, versus location of impact, X (Figure 3.1)

```
x=0:.025:0.9144;
L=0.9144;
X=x/L;
A=0.0127;
p=600;
D=(A-.0349)/(0.5*L^3);

m1=p*pi.*((D.^2).*(L^7)/7-
(D.^2).*(L^7)/2+(9.*D.^2).*(L^7)/20+(A.*D).*(L^4)/2-
(A.*D.*L^4)+(A^2)*(L));

xbar=(p*pi./m1).*((D.^2).*(L^8)/8-
(3.*D.^2).*(L^8)/7+(9.*D.^2).*(L^8)/24+(2*A.*D).*(L^5)/5-
(3*A.*D).*(L^5)/4+(A^2)*(L^2)/2);

Io=(p*pi).*((D.^2).*(L^9)/9-
(3.*D.^2).*(L^9)/8+(9.*D.^2).*(L^9)/28+(A.*D).*(L^6)/3-
(3*A.*D).*(L^6)/5+(A^2)*(L^3)/3);

Ic=Io-m1.*(xbar.^2);

y=x-xbar;

M=m1./0.145;
v2=-40;
w=50;
d=0.0635;
e=0.5;

vc=w.*(d+xbar);

v2prime=v2+(M.*(1+e).*(vc+w.*y-v2))./(1+M+(m1.*y.^2)./Ic);

V2prime=v2prime./(-v2);

plot(X,V2prime);
```

MatLab File 14

Variance of the bat handle-end radius versus the barrel-end radius for a constant mass scenario for e=0.5, Ω=50 radians/second, and d=2.5 inches (Figure 3.2)

```
l=33; r0=0.5:0.025:1.375; d=2.5;
M2=0.00089245; M1=0.0001327;
OMEGA=1.071; e=0.5;
R0=r0/l; D=d/l; A=R0;

C=((-A/3)+sqrt((A/3).^2-4*(A.^2-M2)*(13/315)))/(26/315);

R1=R0+C/3;

MOM=(1/2)*A.^2+(7/30)*A.*C+(2/63)*C.^2;
XBAR=MOM/M2;
J=(1/3)*A.^2+(8/45)*A.*C+(29/1134)*C.^2;
I=J-M2*XBAR.^2;

VC=(D+XBAR)*OMEGA;
M=M2/M1;

YMAX=(1/OMEGA)*(-(1+VC)+sqrt((VC+1).^2+OMEGA^2*(1+M).*I));
XMAX=YMAX+XBAR;
VMAX=-1+((M.*(1+e).*(VC+OMEGA*YMAX+1))./(1+M+M.*YMAX.^2./I));

plot(R0,R1);
```

MatLab File 15

Location of the optimal impact point along the bat as the barrel-end radius changes for e=0.5, Ω=50 radians/second, and d=2.5 inches (Figure 3.3)

```
l=33; r0=0.5:0.025:1.375; d=2.5;
M2=0.00089245; M1=0.0001327;
OMEGA=1.071; e=0.5;
R0=r0/l; D=d/l; A=R0;

C=((-A/3)+sqrt((A/3).^2-4*(A.^2-M2)*(13/315)))/(26/315);

R1=R0+C/3;

MOM=(1/2)*A.^2+(7/30)*A.*C+(2/63)*C.^2;
XBAR=MOM/M2;
J=(1/3)*A.^2+(8/45)*A.*C+(29/1134)*C.^2;
I=J-M2*XBAR.^2;

VC=(D+XBAR)*OMEGA;
M=M2/M1;

YMAX=(1/OMEGA)*(-(1+VC)+sqrt((VC+1).^2+OMEGA^2*(1+M).*I));
XMAX=YMAX+XBAR;
VMAX=-1+((M.*(1+e).*(VC+OMEGA*YMAX+1))./(1+M+M.*YMAX.^2./I));

plot(R1,XMAX);
```

MatLab File 16

Maximum ball exit velocity as a function of the barrel-end radius for e=0.5, Ω=50 radians/second, and d=2.5 inches (Figure 3.4)

```
l=33; r0=0.5:0.025:1.375; d=2.5;
M2=0.00089245; M1=0.0001327;
OMEGA=1.071; e=0.5;
R0=r0/l; D=d/l; A=R0;

C=((-A/3)+sqrt((A/3).^2-4*(A.^2-M2)*(13/315)))/(26/315);

R1=R0+C/3;

MOM=(1/2)*A.^2+(7/30)*A.*C+(2/63)*C.^2;
XBAR=MOM/M2;
J=(1/3)*A.^2+(8/45)*A.*C+(29/1134)*C.^2;
I=J-M2*XBAR.^2;

VC=(D+XBAR)*OMEGA;
M=M2/M1;

YMAX=(1/OMEGA)*(-(1+VC)+sqrt((VC+1).^2+OMEGA^2*(1+M).*I));
XMAX=YMAX+XBAR;
VMAX=-1+((M.*(1+e).*(VC+OMEGA*YMAX+1))./(1+M+M.*YMAX.^2./I));

plot(R1,VMAX);
```

MatLab File 17

Non-dimensional bat mass vs. location of Max radius for e=0.5, Ω=50 radians/second, and d=2.5 inches (Figure 3.5)

```
clear
clc


L=23:0.1:33;
l=33; d=2.5;
rmin=0.5;  rmax=1.375;
e=0.5; omega=60; v1=-1575; rho=0.347;
m1=5;
P=0;

D=(2.*(P-L).*(rmax-rmin))./(L.^4-4*L.^3*P+8*L.*P^3-5*P^4-
6*L.*P^2+6*P^3);
C=(3*D.*(L.^2-P^2))./(2.*(P-L));
B=(3*D*P.*(P^2-L.^2-P))./(P-L);
A=rmin-B.*P-C.*P^2-D.*P^3;

m2=rho*pi*(A.^2*l+A.*B.*l^2+(2*A.*C+B.^2)*l^3/3+(2*A.*D+2*B.*C)*l^4/4+(
2*B.*D+C.^2)*l^5/5+2*C.*D*l^6/6+D.^2*l^7/7);
mom=rho*pi*(A.^2*l^2/2+2*A.*B.*l^3/3+(2*A.*C+B.^2)*l^4/4+(2*A.*D+2*B.*C
)*l^5/5+(2*B.*D+C.^2)*l^6/6+2*C.*D*l^7/7+D.^2*l^8/8);
J0=rho*pi*(A.^2*l^3/3+2*A.*B.*l^4/4+(2*A.*C+B.^2)*l^5/5+(2*A.*D+2*B.*C)
*l^6/6+(2*B.*D+C.^2)*l^7/7+2*C.*D*l^8/8+D.^2*l^9/9);
xbar=mom./m2;
Jc=J0-m2.*xbar.^2;

vc=(d+xbar)*omega;
m=m2/m1;

y=(1/omega)*(-(vc-v1)+sqrt((vc-v1).^2+omega^2*(1+m).*Jc./m2));
xmax=y+xbar;
vmax=v1+(m.*(1+e).*(vc+omega.*y-v1))./(1+m+m2.*y.^2./Jc);

Vmax=vmax/(-v1);
Xmax=xmax/l;
M1=m2/(rho*pi*l^3);
ndJ0=30*J0/(rho*pi*l^5);
ndJc=30*Jc/(rho*pi*l^5);
ndL=L/l;

hold on
plot(ndL,M1,'g')
```

MatLab File 18

Moment of Inertia about x=0 vs. location of Max radius for e=0.5, Ω=50 radians/second, and d=2.5 inches (Figure 3.6)

```
clear
clc


L=23:0.1:33;
l=33; d=2.5;
rmin=0.5;  rmax=1.375;
e=0.5; omega=60; v1=-1575; rho=0.347;
m1=5;
P=0;

D=(2.*(P-L).*(rmax-rmin))./(L.^4-4*L.^3*P+8*L.*P^3-5*P^4-
6*L.*P^2+6*P^3);
C=(3*D.*(L.^2-P^2))./(2.*(P-L));
B=(3*D*P.*(P^2-L.^2-P))./(P-L);
A=rmin-B.*P-C.*P^2-D.*P^3;

m2=rho*pi*(A.^2*l+A.*B.*l^2+(2*A.*C+B.^2)*l^3/3+(2*A.*D+2*B.*C)*l^4/4+(
2*B.*D+C.^2)*l^5/5+2*C.*D*l^6/6+D.^2*l^7/7);
mom=rho*pi*(A.^2*l^2/2+2*A.*B.*l^3/3+(2*A.*C+B.^2)*l^4/4+(2*A.*D+2*B.*C
)*l^5/5+(2*B.*D+C.^2)*l^6/6+2*C.*D*l^7/7+D.^2*l^8/8);
J0=rho*pi*(A.^2*l^3/3+2*A.*B.*l^4/4+(2*A.*C+B.^2)*l^5/5+(2*A.*D+2*B.*C)
*l^6/6+(2*B.*D+C.^2)*l^7/7+2*C.*D*l^8/8+D.^2*l^9/9);
xbar=mom./m2;
Jc=J0-m2.*xbar.^2;

vc=(d+xbar)*omega;
m=m2/m1;

y=(1/omega)*(-(vc-v1)+sqrt((vc-v1).^2+omega^2*(1+m).*Jc./m2));
xmax=y+xbar;
vmax=v1+(m.*(1+e).*(vc+omega.*y-v1))./(1+m+m2.*y.^2./Jc);

Vmax=vmax/(-v1);
Xmax=xmax/l;
M1=m2/(rho*pi*l^3);
ndJ0=30*J0/(rho*pi*l^5);
ndJc=30*Jc/(rho*pi*l^5);
ndL=L/l;

hold on
plot(ndL,ndJ0,'g')
```

MatLab File 19

Moment of Inertia about the center of mass vs. location of maximum radius for e=0.5, Ω=50 radians/second, and d=2.5 inches (Figure 3.7)

```
clear
clc


L=23:0.1:33;
l=33; d=2.5;
rmin=0.5;  rmax=1.375;
e=0.5; omega=60; v1=-1575; rho=0.347;
m1=5;
P=0;

D=(2.*(P-L).*(rmax-rmin))./(L.^4-4*L.^3*P+8*L.*P^3-5*P^4-
6*L.*P^2+6*P^3);
C=(3*D.*(L.^2-P^2))./(2.*(P-L));
B=(3*D*P.*(P^2-L.^2-P))./(P-L);
A=rmin-B.*P-C.*P^2-D.*P^3;

m2=rho*pi*(A.^2*l+A.*B.*l^2+(2*A.*C+B.^2)*l^3/3+(2*A.*D+2*B.*C)*l^4/4+(
2*B.*D+C.^2)*l^5/5+2*C.*D*l^6/6+D.^2*l^7/7);
mom=rho*pi*(A.^2*l^2/2+2*A.*B.*l^3/3+(2*A.*C+B.^2)*l^4/4+(2*A.*D+2*B.*C
)*l^5/5+(2*B.*D+C.^2)*l^6/6+2*C.*D*l^7/7+D.^2*l^8/8);
J0=rho*pi*(A.^2*l^3/3+2*A.*B.*l^4/4+(2*A.*C+B.^2)*l^5/5+(2*A.*D+2*B.*C)
*l^6/6+(2*B.*D+C.^2)*l^7/7+2*C.*D*l^8/8+D.^2*l^9/9);
xbar=mom./m2;
Jc=J0-m2.*xbar.^2;

vc=(d+xbar)*omega;
m=m2/m1;

y=(1/omega)*(-(vc-v1)+sqrt((vc-v1).^2+omega^2*(1+m).*Jc./m2));
xmax=y+xbar;
vmax=v1+(m.*(1+e).*(vc+omega.*y-v1))./(1+m+m2.*y.^2./Jc);

Vmax=vmax/(-v1);
Xmax=xmax/l;
M1=m2/(rho*pi*l^3);
ndJ0=30*J0/(rho*pi*l^5);
ndJc=30*Jc/(rho*pi*l^5);
ndL=L/l;

hold on
plot(ndL,ndJc,'g')
```

MatLab File 20

Non-dimensional VMAX vs. location of maximum radius (Figure 3.8)

```
clear
clc


L=23:0.1:33;
l=33; d=2.5;
rmin=0.5;  rmax=1.375;
e=0.5; omega=60; v1=-1575; rho=0.347;
m1=5;
P=0;

D=(2.*(P-L).*(rmax-rmin))./(L.^4-4*L.^3*P+8*L.*P^3-5*P^4-
6*L.*P^2+6*P^3);
C=(3*D.*(L.^2-P^2))./(2.*(P-L));
B=(3*D*P.*(P^2-L.^2-P))./(P-L);
A=rmin-B.*P-C.*P^2-D.*P^3;

m2=rho*pi*(A.^2*l+A.*B.*l^2+(2*A.*C+B.^2)*l^3/3+(2*A.*D+2*B.*C)*l^4/4+(
2*B.*D+C.^2)*l^5/5+2*C.*D*l^6/6+D.^2*l^7/7);
mom=rho*pi*(A.^2*l^2/2+2*A.*B.*l^3/3+(2*A.*C+B.^2)*l^4/4+(2*A.*D+2*B.*C
)*l^5/5+(2*B.*D+C.^2)*l^6/6+2*C.*D*l^7/7+D.^2*l^8/8);
J0=rho*pi*(A.^2*l^3/3+2*A.*B.*l^4/4+(2*A.*C+B.^2)*l^5/5+(2*A.*D+2*B.*C)
*l^6/6+(2*B.*D+C.^2)*l^7/7+2*C.*D*l^8/8+D.^2*l^9/9);
xbar=mom./m2;
Jc=J0-m2.*xbar.^2;

vc=(d+xbar)*omega;
m=m2/m1;

y=(1/omega)*(-(vc-v1)+sqrt((vc-v1).^2+omega^2*(1+m).*Jc./m2));
xmax=y+xbar;
vmax=v1+(m.*(1+e).*(vc+omega.*y-v1))./(1+m+m2.*y.^2./Jc);

Vmax=vmax/(-v1);
Xmax=xmax/l;
M1=m2/(rho*pi*l^3);
ndJ0=30*J0/(rho*pi*l^5);
ndJc=30*Jc/(rho*pi*l^5);
ndL=L/l;

hold on
plot(ndL,Vmax,'g')
```

MatLab File 21

Location at which maximum outgoing velocity occurs (xmax) vs. location of Max radius (Figure 3.9)

```
clear
clc


L=23:0.1:33;
l=33; d=2.5;
rmin=0.5;  rmax=1.375;
e=0.5; omega=60; v1=-1575; rho=0.347;
m1=5;
P=0;

D=(2.*(P-L).*(rmax-rmin))./(L.^4-4*L.^3*P+8*L.*P^3-5*P^4-
6*L.*P^2+6*P^3);
C=(3*D.*(L.^2-P^2))./(2.*(P-L));
B=(3*D*P.*(P^2-L.^2-P))./(P-L);
A=rmin-B.*P-C.*P^2-D.*P^3;

m2=rho*pi*(A.^2*l+A.*B.*l^2+(2*A.*C+B.^2)*l^3/3+(2*A.*D+2*B.*C)*l^4/4+(
2*B.*D+C.^2)*l^5/5+2*C.*D*l^6/6+D.^2*l^7/7);
mom=rho*pi*(A.^2*l^2/2+2*A.*B.*l^3/3+(2*A.*C+B.^2)*l^4/4+(2*A.*D+2*B.*C
)*l^5/5+(2*B.*D+C.^2)*l^6/6+2*C.*D*l^7/7+D.^2*l^8/8);
J0=rho*pi*(A.^2*l^3/3+2*A.*B.*l^4/4+(2*A.*C+B.^2)*l^5/5+(2*A.*D+2*B.*C)
*l^6/6+(2*B.*D+C.^2)*l^7/7+2*C.*D*l^8/8+D.^2*l^9/9);
xbar=mom./m2;
Jc=J0-m2.*xbar.^2;

vc=(d+xbar)*omega;
m=m2/m1;

y=(1/omega)*(-(vc-v1)+sqrt((vc-v1).^2+omega^2*(1+m).*Jc./m2));
xmax=y+xbar;
vmax=v1+(m.*(1+e).*(vc+omega.*y-v1))./(1+m+m2.*y.^2./Jc);

Vmax=vmax/(-v1);
Xmax=xmax/l;
M1=m2/(rho*pi*l^3);
ndJ0=30*J0/(rho*pi*l^5);
ndJc=30*Jc/(rho*pi*l^5);
ndL=L/l;

hold on
plot(ndL,Xmax,'g')
```

MatLab File 22

Non-dimensional minimum radius R_{MIN} versus location of maximum radius (Figure 3.10)

```
L=23:0.25:33;
l=33; d=2.5;
rmax=1.375;  m2=40;
e=0.5;  v1=-1575; rho=0.347;
m1=5; omega=50;
P=0;

a=l-2*l^3./L.^2+l^4./L.^3+9*l^5./(5*L.^4)-2*l^6./L.^5+4*l^7./(7*L.^6);
b=rmax*(2*l^3./L.^2-l^4./L.^3-18*l^5./(5*L.^4)+4*l^6./L.^5-
8*l^7./(7*L.^6));
c=rmax^2*(9*l^5./(5*L.^4)-2*l^6./L.^5+4*l^7./(7*L.^6))-m2/(rho*pi);

rmin=(-b+sqrt(b.^2-4*a.*c))./(2*a);

D=(2.*(P-L).*(rmax-rmin))./(L.^4-4*L.^3*P+8*L.*P^3-5*P^4-
6*L.*P^2+6*P^3);
C=(3*D.*(L.^2-P^2))./(2.*(P-L));
B=(3*D*P.*(P^2-L.^2-P))./(P-L);
A=rmin-B.*P-C.*P^2-D.*P^3;

mom=rho*pi*(A.^2*l^2/2+2*A.*B.*l^3/3+(2*A.*C+B.^2)*l^4/4+(2*A.*D+2*B.*C
)*l^5/5+(2*B.*D+C.^2)*l^6/6+2*C.*D*l^7/7+D.^2*l^8/8);
J0=rho*pi*(A.^2*l^3/3+2*A.*B.*l^4/4+(2*A.*C+B.^2)*l^5/5+(2*A.*D+2*B.*C)
*l^6/6+(2*B.*D+C.^2)*l^7/7+2*C.*D*l^8/8+D.^2*l^9/9);
xbar=mom./m2;
Jc=J0-m2.*xbar.^2;
Jr=Jc+m2.*(xbar+d).^2;

vc=(d+xbar).*omega;
m=m2/m1;

y=(1./omega).*(-(vc-v1)+sqrt((vc-v1).^2+omega.^2*(1+m).*Jc./m2));
xmax=y+xbar;
vmax=v1+(m.*(1+e).*(vc+omega.*y-v1))./(1+m+m2.*y.^2./Jc);

Vmax=vmax/(-v1);
Rmin=rmin/l;
Xmax=xmax/l;
ndJ0=30*J0/(rho*pi*l^5);
ndJc=30*Jc/(rho*pi*l^5);
ndL=L/l;

hold on
plot(ndL,Rmin,'b')
```

MatLab File 23

Moment of Inertia about x=0 versus the location of max radius (Figure 3.11)

```
L=23:0.25:33;
l=33; d=2.5;
rmax=1.375;  m2=40;
e=0.5;  v1=-1575; rho=0.347;
m1=5; omega=50;
P=0;

a=l-2*l^3./L.^2+l^4./L.^3+9*l^5./(5*L.^4)-2*l^6./L.^5+4*l^7./(7*L.^6);
b=rmax*(2*l^3./L.^2-l^4./L.^3-18*l^5./(5*L.^4)+4*l^6./L.^5-
8*l^7./(7*L.^6));
c=rmax^2*(9*l^5./(5*L.^4)-2*l^6./L.^5+4*l^7./(7*L.^6))-m2/(rho*pi);

rmin=(-b+sqrt(b.^2-4*a.*c))./(2*a);

D=(2.*(P-L).*(rmax-rmin))./(L.^4-4*L.^3*P+8*L.*P^3-5*P^4-
6*L.*P^2+6*P^3);
C=(3*D.*(L.^2-P^2))./(2.*(P-L));
B=(3*D*P.*(P^2-L.^2-P))./(P-L);
A=rmin-B.*P-C.*P^2-D.*P^3;

mom=rho*pi*(A.^2*l^2/2+2*A.*B.*l^3/3+(2*A.*C+B.^2)*l^4/4+(2*A.*D+2*B.*C
)*l^5/5+(2*B.*D+C.^2)*l^6/6+2*C.*D*l^7/7+D.^2*l^8/8);
J0=rho*pi*(A.^2*l^3/3+2*A.*B.*l^4/4+(2*A.*C+B.^2)*l^5/5+(2*A.*D+2*B.*C)
*l^6/6+(2*B.*D+C.^2)*l^7/7+2*C.*D*l^8/8+D.^2*l^9/9);
xbar=mom./m2;
Jc=J0-m2.*xbar.^2;
Jr=Jc+m2.*(xbar+d).^2;

vc=(d+xbar).*omega;
m=m2/m1;

y=(1./omega).*(-(vc-v1)+sqrt((vc-v1).^2+omega.^2*(1+m).*Jc./m2));
xmax=y+xbar;
vmax=v1+(m.*(1+e).*(vc+omega.*y-v1))./(1+m+m2.*y.^2./Jc);

Vmax=vmax/(-v1);
Rmin=rmin/l;
Xmax=xmax/l;
ndJ0=30*J0/(rho*pi*l^5);
ndJc=30*Jc/(rho*pi*l^5);
ndL=L/l;

hold on
plot(ndL,ndJ0,'b')
```

MatLab File 24

Moment of Inertia about the center of mass versus the location of max radius (Figure 3.12)

```
L=23:0.25:33;
l=33; d=2.5;
rmax=1.375;  m2=40;
e=0.5;  v1=-1575; rho=0.347;
m1=5; omega=50;
P=0;

a=l-2*l^3./L.^2+l^4./L.^3+9*l^5./(5*L.^4)-2*l^6./L.^5+4*l^7./(7*L.^6);
b=rmax*(2*l^3./L.^2-l^4./L.^3-18*l^5./(5*L.^4)+4*l^6./L.^5-
8*l^7./(7*L.^6));
c=rmax^2*(9*l^5./(5*L.^4)-2*l^6./L.^5+4*l^7./(7*L.^6))-m2/(rho*pi);

rmin=(-b+sqrt(b.^2-4*a.*c))./(2*a);

D=(2.*(P-L).*(rmax-rmin))./(L.^4-4*L.^3*P+8*L.*P^3-5*P^4-
6*L.*P^2+6*P^3);
C=(3*D.*(L.^2-P^2))./(2.*(P-L));
B=(3*D*P.*(P^2-L.^2-P))./(P-L);
A=rmin-B.*P-C.*P^2-D.*P^3;

mom=rho*pi*(A.^2*l^2/2+2*A.*B.*l^3/3+(2*A.*C+B.^2)*l^4/4+(2*A.*D+2*B.*C
)*l^5/5+(2*B.*D+C.^2)*l^6/6+2*C.*D*l^7/7+D.^2*l^8/8);
J0=rho*pi*(A.^2*l^3/3+2*A.*B.*l^4/4+(2*A.*C+B.^2)*l^5/5+(2*A.*D+2*B.*C)
*l^6/6+(2*B.*D+C.^2)*l^7/7+2*C.*D*l^8/8+D.^2*l^9/9);
xbar=mom./m2;
Jc=J0-m2.*xbar.^2;
Jr=Jc+m2.*(xbar+d).^2;

vc=(d+xbar).*omega;
m=m2/m1;

y=(1./omega).*(-(vc-v1)+sqrt((vc-v1).^2+omega.^2*(1+m).*Jc./m2));
xmax=y+xbar;
vmax=v1+(m.*(1+e).*(vc+omega.*y-v1))./(1+m+m2.*y.^2./Jc);

Vmax=vmax/(-v1);
Rmin=rmin/l;
Xmax=xmax/l;
ndJ0=30*J0/(rho*pi*l^5);
ndJc=30*Jc/(rho*pi*l^5);
ndL=L/l;

hold on
plot(ndL,ndJc,'b')
```

MatLab File 25

Location at which maximum outgoing velocity occurs X_{MAX} vs. location of Max radius (Figure 3.13)

```
L=23:0.25:33;
l=33; d=2.5;
rmax=1.375;  m2=40;
e=0.5;  v1=-1575; rho=0.347;
m1=5; omega=50;
P=0;

a=l-2*l^3./L.^2+l^4./L.^3+9*l^5./(5*L.^4)-2*l^6./L.^5+4*l^7./(7*L.^6);
b=rmax*(2*l^3./L.^2-l^4./L.^3-18*l^5./(5*L.^4)+4*l^6./L.^5-
8*l^7./(7*L.^6));
c=rmax^2*(9*l^5./(5*L.^4)-2*l^6./L.^5+4*l^7./(7*L.^6))-m2/(rho*pi);

rmin=(-b+sqrt(b.^2-4*a.*c))./(2*a);

D=(2.*(P-L).*(rmax-rmin))./(L.^4-4*L.^3*P+8*L.*P^3-5*P^4-
6*L.*P^2+6*P^3);
C=(3*D.*(L.^2-P^2))./(2.*(P-L));
B=(3*D*P.*(P^2-L.^2-P))./(P-L);
A=rmin-B.*P-C.*P^2-D.*P^3;

mom=rho*pi*(A.^2*l^2/2+2*A.*B.*l^3/3+(2*A.*C+B.^2)*l^4/4+(2*A.*D+2*B.*C
)*l^5/5+(2*B.*D+C.^2)*l^6/6+2*C.*D*l^7/7+D.^2*l^8/8);
J0=rho*pi*(A.^2*l^3/3+2*A.*B.*l^4/4+(2*A.*C+B.^2)*l^5/5+(2*A.*D+2*B.*C)
*l^6/6+(2*B.*D+C.^2)*l^7/7+2*C.*D*l^8/8+D.^2*l^9/9);
xbar=mom./m2;
Jc=J0-m2.*xbar.^2;
Jr=Jc+m2.*(xbar+d).^2;

vc=(d+xbar).*omega;
m=m2/m1;

y=(1./omega).*(-(vc-v1)+sqrt((vc-v1).^2+omega.^2*(1+m).*Jc./m2));
xmax=y+xbar;
vmax=v1+(m.*(1+e).*(vc+omega.*y-v1))./(1+m+m2.*y.^2./Jc);

Vmax=vmax/(-v1);
Rmin=rmin/l;
Xmax=xmax/l;
ndJ0=30*J0/(rho*pi*l^5);
ndJc=30*Jc/(rho*pi*l^5);
ndL=L/l;

hold on
plot(ndL,Xmax,'b')
```

MatLab File 26

Non-dimensional V_{MAX} vs. location of maximum radius (Figure 3.14)

```
L=23:0.25:33;
l=33; d=2.5;
rmax=1.375;  m2=40;
e=0.5;  v1=-1575; rho=0.347;
m1=5; omega=50;
P=0;

a=l-2*l^3./L.^2+l^4./L.^3+9*l^5./(5*L.^4)-2*l^6./L.^5+4*l^7./(7*L.^6);
b=rmax*(2*l^3./L.^2-l^4./L.^3-18*l^5./(5*L.^4)+4*l^6./L.^5-
8*l^7./(7*L.^6));
c=rmax^2*(9*l^5./(5*L.^4)-2*l^6./L.^5+4*l^7./(7*L.^6))-m2/(rho*pi);

rmin=(-b+sqrt(b.^2-4*a.*c))./(2*a);

D=(2.*(P-L).*(rmax-rmin))./(L.^4-4*L.^3*P+8*L.*P^3-5*P^4-
6*L.*P^2+6*P^3);
C=(3*D.*(L.^2-P^2))./(2.*(P-L));
B=(3*D*P.*(P^2-L.^2-P))./(P-L);
A=rmin-B.*P-C.*P^2-D.*P^3;

mom=rho*pi*(A.^2*l^2/2+2*A.*B.*l^3/3+(2*A.*C+B.^2)*l^4/4+(2*A.*D+2*B.*C
)*l^5/5+(2*B.*D+C.^2)*l^6/6+2*C.*D*l^7/7+D.^2*l^8/8);
J0=rho*pi*(A.^2*l^3/3+2*A.*B.*l^4/4+(2*A.*C+B.^2)*l^5/5+(2*A.*D+2*B.*C)
*l^6/6+(2*B.*D+C.^2)*l^7/7+2*C.*D*l^8/8+D.^2*l^9/9);
xbar=mom./m2;
Jc=J0-m2.*xbar.^2;
Jr=Jc+m2.*(xbar+d).^2;

vc=(d+xbar).*omega;
m=m2/m1;

y=(1./omega).*(-(vc-v1)+sqrt((vc-v1).^2+omega.^2*(1+m).*Jc./m2));
xmax=y+xbar;
vmax=v1+(m.*(1+e).*(vc+omega.*y-v1))./(1+m+m2.*y.^2./Jc);

Vmax=vmax/(-v1);
Rmin=rmin/l;
Xmax=xmax/l;
ndJ0=30*J0/(rho*pi*l^5);
ndJc=30*Jc/(rho*pi*l^5);
ndL=L/l;

hold on
plot(ndL,Vmax,'b')
```

MatLab File 27

Ω'/ Ω vs Location of impact, Y, with e = 0.3, 0.5, 0.7 (Figure 3.15)

```
M=6.90872;
D=0.0756;
X=0.672907;
e=0.3;
J=0.405646;

Omega=1.067;

Vc=Omega.*(D+X);
Y=-0.672907:0.01:0.327093;
x=Y+X;
V2=Vc+Y.*Omega;
V1=-1;

V1p=(V1.*Y.*Y+J.*Omega.*Y+e.*J.*(V2-V1)+V1.*J./M+Vc.*J)/(Y.*Y+J+J./M);
V2p=V1p+(V1-V2).*e;
Omegap=Omega+(Y./J).*(V1-V1p);
Vcp=V2p-Omegap.*Y;
Dp=-X+Vcp./Omegap;
F=Omegap./Omega;
plot(Y,F,'r');
hold on

e=0.5;
V1p=(V1.*Y.*Y+J.*Omega.*Y+e.*J.*(V2-V1)+V1.*J./M+Vc.*J)/(Y.*Y+J+J./M);
V2p=V1p+(V1-V2).*e;
Omegap=Omega+(Y./J).*(V1-V1p);
Vcp=V2p-Omegap.*Y;
Dp=-X+Vcp./Omegap;
F=Omegap./Omega;
plot(Y,F,'m');
hold on

e=0.7;
V1p=(V1.*Y.*Y+J.*Omega.*Y+e.*J.*(V2-V1)+V1.*J./M+Vc.*J)/(Y.*Y+J+J./M);
V2p=V1p+(V1-V2).*e;
Omegap=Omega+(Y./J).*(V1-V1p);
Vcp=V2p-Omegap.*Y;
Dp=-X+Vcp./Omegap;
F=Omegap./Omega;
plot(Y,F,'b');
hold on

r=0;
plot(Y,r,'k.');

legend('e=0.3','e=0.5','e=0.7');
```

MatLab File 28

D'/D vs. coefficient of restitution, e, with Y= -0.2, -0.1, 0, 0.1, 0.2, and 0.3 (Figure 3.16)

```
%Set all constants
M=6;
D=0.0756;
X=0.667;
Omega=1.071;
J=0.547;
%We are varying e
e=0.1:0.01:1;
%now find all valiables dependent on those constants
Vc=Omega.*(D+X);
%pick a value of Y to find V1 and V2 at.  Does not need to be max
Y=0.3;
V2=Vc+Y.*Omega;
V1=-1;
%now find all the prime values
V1p=(V1.*Y.*Y+J.*Omega.*Y+e.*J.*(V2-V1)+V1.*J./M+Vc.*J)/(Y.*Y+J+J./M);
V2p=V1p+(V1-V2).*e;
Omegap=Omega+(Y./J).*(V1-V1p);
Vcp=V2p-Omegap.*Y;
Dp=-X+Vcp./Omegap;
F=Dp./D;
plot(e,F,'r');
hold on

%pick a value of Y to find V1 and V2 at.  Does not need to be max
Y=0.2;
V2=Vc+Y.*Omega;
V1=-1;
%now find all the prime values
V1p=(V1.*Y.*Y+J.*Omega.*Y+e.*J.*(V2-V1)+V1.*J./M+Vc.*J)/(Y.*Y+J+J./M);
V2p=V1p+(V1-V2).*e;
Omegap=Omega+(Y./J).*(V1-V1p);
Vcp=V2p-Omegap.*Y;
Dp=-X+Vcp./Omegap;
F=Dp./D;
plot(e,F,'m');
hold on

%pick a value of Y to find V1 and V2 at.  Does not need to be max
Y=0.1;
V2=Vc+Y.*Omega;
V1=-1;
%now find all the prime values
V1p=(V1.*Y.*Y+J.*Omega.*Y+e.*J.*(V2-V1)+V1.*J./M+Vc.*J)/(Y.*Y+J+J./M);
V2p=V1p+(V1-V2).*e;
Omegap=Omega+(Y./J).*(V1-V1p);
Vcp=V2p-Omegap.*Y;
Dp=-X+Vcp./Omegap;
F=Dp./D;
plot(e,F,'g');
hold on
```

```
%pick a value of Y to find V1 and V2 at.  Does not need to be max
Y=0;
V2=Vc+Y.*Omega;
V1=-1;
%now find all the prime values
V1p=(V1.*Y.*Y+J.*Omega.*Y+e.*J.*(V2-V1)+V1.*J./M+Vc.*J)/(Y.*Y+J+J./M);
V2p=V1p+(V1-V2).*e;
Omegap=Omega+(Y./J).*(V1-V1p);
Vcp=V2p-Omegap.*Y;
Dp=-X+Vcp./Omegap;
F=Dp./D;
plot(e,F,'b');
hold on

%pick a value of Y to find V1 and V2 at.  Does not need to be max
Y=-0.1;
V2=Vc+Y.*Omega;
V1=-1;
%now find all the prime values
V1p=(V1.*Y.*Y+J.*Omega.*Y+e.*J.*(V2-V1)+V1.*J./M+Vc.*J)/(Y.*Y+J+J./M);
V2p=V1p+(V1-V2).*e;
Omegap=Omega+(Y./J).*(V1-V1p);
Vcp=V2p-Omegap.*Y;
Dp=-X+Vcp./Omegap;
F=Dp./D;
plot(e,F,'k');
hold on

%pick a value of Y to find V1 and V2 at.  Does not need to be max
Y=-0.2;
V2=Vc+Y.*Omega;
V1=-1;
%now find all the prime values
V1p=(V1.*Y.*Y+J.*Omega.*Y+e.*J.*(V2-V1)+V1.*J./M+Vc.*J)/(Y.*Y+J+J./M);
V2p=V1p+(V1-V2).*e;
Omegap=Omega+(Y./J).*(V1-V1p);
Vcp=V2p-Omegap.*Y;
Dp=-X+Vcp./Omegap;
F=Dp./D;
plot(e,F,'c');
hold on

Legend('Y=0.3','Y=0.2','Y=0.1','Y=0','Y=-0.1','Y=-0.2');
```

MatLab File 29

V1'max versus coefficient of restitution, e, with M=3, 4, 5, 6, and 7 (Figure 3.17)

```
M=3;
e=0.1:0.01:1;
D=0.0756;
X=0.667;
Omega=1.071;
J=0.547;
x=0:0.01:1;
Vc=(D+X)*Omega;
V1max=-
1.+(M.*(1+e).*sqrt((Vc+1)*(Vc+1)+Omega*Omega*(1+M)*J/M))./(1.+M+(M/(Ome
ga*J)).*(-1-Vc+sqrt((Vc+1)*(Vc+1)+Omega*Omega*(1+M)*J/M)).*(-1-
Vc+sqrt((Vc+1)*(Vc+1)+Omega*Omega*(1+M)*J/M)));
plot(e,V1max,'r');
hold on
M=4;
V1max=-
1.+(M.*(1+e).*sqrt((Vc+1)*(Vc+1)+Omega*Omega*(1+M)*J/M))./(1.+M+(M/(Ome
ga*J)).*(-1-Vc+sqrt((Vc+1)*(Vc+1)+Omega*Omega*(1+M)*J/M)).*(-1-
Vc+sqrt((Vc+1)*(Vc+1)+Omega*Omega*(1+M)*J/M)));
plot(e,V1max,'b');
hold on
M=5;
V1max=-
1.+(M.*(1+e).*sqrt((Vc+1)*(Vc+1)+Omega*Omega*(1+M)*J/M))./(1.+M+(M/(Ome
ga*J)).*(-1-Vc+sqrt((Vc+1)*(Vc+1)+Omega*Omega*(1+M)*J/M)).*(-1-
Vc+sqrt((Vc+1)*(Vc+1)+Omega*Omega*(1+M)*J/M)));
plot(e,V1max,'m');
hold on
M=6;
V1max=-
1.+(M.*(1+e).*sqrt((Vc+1)*(Vc+1)+Omega*Omega*(1+M)*J/M))./(1.+M+(M/(Ome
ga*J)).*(-1-Vc+sqrt((Vc+1)*(Vc+1)+Omega*Omega*(1+M)*J/M)).*(-1-
Vc+sqrt((Vc+1)*(Vc+1)+Omega*Omega*(1+M)*J/M)));
plot(e,V1max,'c');
hold on
M=7;
V1max=-
1.+(M.*(1+e).*sqrt((Vc+1)*(Vc+1)+Omega*Omega*(1+M)*J/M))./(1.+M+(M/(Ome
ga*J)).*(-1-Vc+sqrt((Vc+1)*(Vc+1)+Omega*Omega*(1+M)*J/M)).*(-1-
Vc+sqrt((Vc+1)*(Vc+1)+Omega*Omega*(1+M)*J/M)));
plot(e,V1max,'k');
hold on
legend('M=3','M=4','M=5','M=6','M=7');
```

MatLab File 30

D'/D vs. Ω, with Y= -0.2, -0.1, 0, 0.1, 0.2, and 0.3 (Figure 3.18)

```
%Set all constants
M=6;
D=0.0756;
X=0.667;
e=0.5;
J=0.547;
%We are varying Omega
Omega=0.5:0.01:1.5;
%now find all valiables dependent on those constants
Vc=Omega.*(D+X);
%pick a value of Y to find V1 and V2 at.  Does not need to be max
Y=0.3;
V2=Vc+Y.*Omega;
V1=-1;
%now find all the prime values
V1p=(V1.*Y.*Y+J.*Omega.*Y+e.*J.*(V2-V1)+V1.*J./M+Vc.*J)/(Y.*Y+J+J./M);
V2p=V1p+(V1-V2).*e;
Omegap=Omega+(Y./J).*(V1-V1p);
Vcp=V2p-Omegap.*Y;
Dp=-X+Vcp./Omegap;
F=Dp./D;
plot(Omega,F,'r');
hold on

%pick a value of Y to find V1 and V2 at.  Does not need to be max
Y=0.2;
V2=Vc+Y.*Omega;
V1=-1;
%now find all the prime values
V1p=(V1.*Y.*Y+J.*Omega.*Y+e.*J.*(V2-V1)+V1.*J./M+Vc.*J)/(Y.*Y+J+J./M);
V2p=V1p+(V1-V2).*e;
Omegap=Omega+(Y./J).*(V1-V1p);
Vcp=V2p-Omegap.*Y;
Dp=-X+Vcp./Omegap;
F=Dp./D;
plot(Omega,F,'m');
hold on

%pick a value of Y to find V1 and V2 at.  Does not need to be max
Y=0.1;
V2=Vc+Y.*Omega;
V1=-1;
%now find all the prime values
V1p=(V1.*Y.*Y+J.*Omega.*Y+e.*J.*(V2-V1)+V1.*J./M+Vc.*J)/(Y.*Y+J+J./M);
V2p=V1p+(V1-V2).*e;
Omegap=Omega+(Y./J).*(V1-V1p);
Vcp=V2p-Omegap.*Y;
Dp=-X+Vcp./Omegap;
F=Dp./D;
plot(Omega,F,'g');
hold on
```

```
%pick a value of Y to find V1 and V2 at.  Does not need to be max
Y=0;
V2=Vc+Y.*Omega;
V1=-1;
%now find all the prime values
V1p=(V1.*Y.*Y+J.*Omega.*Y+e.*J.*(V2-V1)+V1.*J./M+Vc.*J)/(Y.*Y+J+J./M);
V2p=V1p+(V1-V2).*e;
Omegap=Omega+(Y./J).*(V1-V1p);
Vcp=V2p-Omegap.*Y;
Dp=-X+Vcp./Omegap;
F=Dp./D;
plot(Omega,F,'b');
hold on

%pick a value of Y to find V1 and V2 at.  Does not need to be max
Y=-0.1;
V2=Vc+Y.*Omega;
V1=-1;
%now find all the prime values
V1p=(V1.*Y.*Y+J.*Omega.*Y+e.*J.*(V2-V1)+V1.*J./M+Vc.*J)/(Y.*Y+J+J./M);
V2p=V1p+(V1-V2).*e;
Omegap=Omega+(Y./J).*(V1-V1p);
Vcp=V2p-Omegap.*Y;
Dp=-X+Vcp./Omegap;
F=Dp./D;
plot(Omega,F,'k');
hold on

%pick a value of Y to find V1 and V2 at.  Does not need to be max
Y=-0.2;
V2=Vc+Y.*Omega;
V1=-1;
%now find all the prime values
V1p=(V1.*Y.*Y+J.*Omega.*Y+e.*J.*(V2-V1)+V1.*J./M+Vc.*J)/(Y.*Y+J+J./M);
V2p=V1p+(V1-V2).*e;
Omegap=Omega+(Y./J).*(V1-V1p);
Vcp=V2p-Omegap.*Y;
Dp=-X+Vcp./Omegap;
F=Dp./D;
plot(Omega,F,'c');
hold on

Legend('Y=0.3','Y=0.2','Y=0.1','Y=0','Y=-0.1','Y=-0.2');
```

MatLab File 31

V'max versus Ω, with M= 3, 4, 5, 6, and 7 (Figure 3.19)

```
M=3;
e=0.5;
D=0.0756;
X=0.667;
Omega=0.5:0.01:1.5;
J=0.547;
x=0:0.01:1;
Vc=(D+X)*Omega;
V1max=-
1+(M*(1+e)*sqrt((Vc+1).*(Vc+1)+Omega.*Omega.*(1+M)*J/M))./(1+M+(M./(Ome
ga.*J)).*(-1-Vc+sqrt((Vc+1).*(Vc+1)+Omega.*Omega.*(1+M)*J/M)).*(-1-
Vc+sqrt((Vc+1).*(Vc+1)+Omega.*Omega.*(1+M)*J/M)));
plot(Omega,V1max,'r');
hold on
M=4;
V1max=-
1+(M*(1+e)*sqrt((Vc+1).*(Vc+1)+Omega.*Omega.*(1+M)*J/M))./(1+M+(M./(Ome
ga.*J)).*(-1-Vc+sqrt((Vc+1).*(Vc+1)+Omega.*Omega.*(1+M)*J/M)).*(-1-
Vc+sqrt((Vc+1).*(Vc+1)+Omega.*Omega.*(1+M)*J/M)));
plot(Omega,V1max,'b');
hold on
M=5;
V1max=-
1+(M*(1+e)*sqrt((Vc+1).*(Vc+1)+Omega.*Omega.*(1+M)*J/M))./(1+M+(M./(Ome
ga.*J)).*(-1-Vc+sqrt((Vc+1).*(Vc+1)+Omega.*Omega.*(1+M)*J/M)).*(-1-
Vc+sqrt((Vc+1).*(Vc+1)+Omega.*Omega.*(1+M)*J/M)));
plot(Omega,V1max,'m');
hold on
M=6;
V1max=-
1+(M*(1+e)*sqrt((Vc+1).*(Vc+1)+Omega.*Omega.*(1+M)*J/M))./(1+M+(M./(Ome
ga.*J)).*(-1-Vc+sqrt((Vc+1).*(Vc+1)+Omega.*Omega.*(1+M)*J/M)).*(-1-
Vc+sqrt((Vc+1).*(Vc+1)+Omega.*Omega.*(1+M)*J/M)));
plot(Omega,V1max,'c');
hold on
M=7;
V1max=-
1+(M*(1+e)*sqrt((Vc+1).*(Vc+1)+Omega.*Omega.*(1+M)*J/M))./(1+M+(M./(Ome
ga.*J)).*(-1-Vc+sqrt((Vc+1).*(Vc+1)+Omega.*Omega.*(1+M)*J/M)).*(-1-
Vc+sqrt((Vc+1).*(Vc+1)+Omega.*Omega.*(1+M)*J/M)));
xmax=X+(1./Omega).*(-1-Vc+sqrt((Vc+1).*(Vc+1)+Omega.*(1+M)*(J/M)));
plot(Omega,V1max,'k');
hold on
legend('M=3','M=4','M=5','M=6','M=7');
```

MatLab File 32

X'max versus Ω, with M= 3, 4, 5, 6, and 7 (Figure 3.20)

```
M=3;
e=0.5;
D=0.0756;
X=0.667;
Omega=0.5:0.01:1.5;
J=0.547;
x=0:0.01:1;
Vc=(D+X)*Omega;
xmax=X+(1./Omega).*(-1-
Vc+sqrt((Vc+1).*(Vc+1)+Omega.*Omega.*(1+M)*(J/M)));
plot(Omega,xmax,'r');
hold on
M=4;
xmax=X+(1./Omega).*(-1-
Vc+sqrt((Vc+1).*(Vc+1)+Omega.*Omega.*(1+M)*(J/M)));
plot(Omega,xmax,'b');
hold on
M=5;
xmax=X+(1./Omega).*(-1-
Vc+sqrt((Vc+1).*(Vc+1)+Omega.*Omega.*(1+M)*(J/M)));
plot(Omega,xmax,'m');
hold on
M=6;
xmax=X+(1./Omega).*(-1-
Vc+sqrt((Vc+1).*(Vc+1)+Omega.*Omega.*(1+M)*(J/M)));
plot(Omega,xmax,'c');
hold on
M=7;
xmax=X+(1./Omega).*(-1-
Vc+sqrt((Vc+1).*(Vc+1)+Omega.*Omega.*(1+M)*(J/M)));
plot(Omega,xmax,'k');
hold on
legend('M=3','M=4','M=5','M=6','M=7');
```

MatLab File 33

Omega versus non-dimensional max radius R1 for T=49, 61 and 73 Nm (Figure 4.1)

```
l=33; d=2.5;
rmin=0.5:0.0125:1.375;
e=0.5; v1=-1575; rho=0.347;
m1=5; T=4000000; m2=35;
M2=m2/(rho*pi*l^3);
P=0; L=l;
M=m2/m1;

A=rmin/l;
C=((-1/3)*A+sqrt((A.^2)/9-4*13/315*(A.^2-M2)))/(26/315);

R1=A+C/3;

rmax=R1*l;

MOM=(A.^2)/2+(7/30)*A.*C+(2/63)*C.^2;
Xbar=MOM/M2;
ndJ0=(A.^2)/3+(8/45)*A.*C+(29/1134)*C.^2;
J0=ndJ0*rho*pi*l^5;

xbar=Xbar*l;
Jc=J0-m2.*xbar.^2;
Jr=Jc+m2.*(xbar+d).^2;

omeganaught=20;
theta=pi;
omega=omeganaught+sqrt(2*T*theta./Jr);

vc=(d+xbar).*omega;
m=m2/m1;

y=(1./omega).*(-(vc-v1)+sqrt((vc-v1).^2+omega.^2.*(1+m).*Jc./m2));
xmax=y+xbar;
vmax=v1+(m.*(1+e).*(vc+omega.*y-v1))./(1+m+m2.*y.^2./Jc);

Vmax=vmax/(-v1);
Xmax=xmax/l;
ndJ0=30*J0/(rho*pi*l^5);
ndJc=30*Jc/(rho*pi*l^5);
ndL=L/l;

hold on
plot(R1,omega,'r')
```

MatLab File 34

Non-dimensional maximum outgoing velocity versus non-dimensional max radius R1 for T=49, 61 and 73 Nm (Figure 4.2)

```
l=33; d=2.5;
rmin=0.5:0.0125:1.375;
e=0.5; v1=-1575; rho=0.347;
m1=5; T=4000000; m2=35;
M2=m2/(rho*pi*l^3);
P=0; L=l;
M=m2/m1;

A=rmin/l;
C=((-1/3)*A+sqrt((A.^2)/9-4*13/315*(A.^2-M2)))/(26/315);

R1=A+C/3;

rmax=R1*l;

MOM=(A.^2)/2+(7/30)*A.*C+(2/63)*C.^2;
Xbar=MOM/M2;
ndJ0=(A.^2)/3+(8/45)*A.*C+(29/1134)*C.^2;
J0=ndJ0*rho*pi*l^5;

xbar=Xbar*l;
Jc=J0-m2.*xbar.^2;
Jr=Jc+m2.*(xbar+d).^2;

omeganaught=20;
theta=pi;
omega=omeganaught+sqrt(2*T*theta./Jr);

vc=(d+xbar).*omega;
m=m2/m1;

y=(1./omega).*(-(vc-v1)+sqrt((vc-v1).^2+omega.^2.*(1+m).*Jc./m2));
xmax=y+xbar;
vmax=v1+(m.*(1+e).*(vc+omega.*y-v1))./(1+m+m2.*y.^2./Jc);

Vmax=vmax/(-v1);
Xmax=xmax/l;
ndJ0=30*J0/(rho*pi*l^5);
ndJc=30*Jc/(rho*pi*l^5);
ndL=L/l;

hold on
plot(R1,Vmax,'r')
```

MatLab File 35

Non-dimensional X_{MAX} versus non-dimensional max radius R1 for T=49, 61 and 73 Nm (Figure 4.3)

```
l=33; d=2.5;
rmin=0.5:0.0125:1.375;
e=0.5; v1=-1575; rho=0.347;
m1=5; T=4000000; m2=35;
M2=m2/(rho*pi*l^3);
P=0; L=l;
M=m2/m1;

A=rmin/l;
C=((-1/3)*A+sqrt((A.^2)/9-4*13/315*(A.^2-M2)))/(26/315);

R1=A+C/3;

rmax=R1*l;

MOM=(A.^2)/2+(7/30)*A.*C+(2/63)*C.^2;
Xbar=MOM/M2;
ndJ0=(A.^2)/3+(8/45)*A.*C+(29/1134)*C.^2;
J0=ndJ0*rho*pi*l^5;

xbar=Xbar*l;
Jc=J0-m2.*xbar.^2;
Jr=Jc+m2.*(xbar+d).^2;

omeganaught=20;
theta=pi;
omega=omeganaught+sqrt(2*T*theta./Jr);

vc=(d+xbar).*omega;
m=m2/m1;

y=(1./omega).*(-(vc-v1)+sqrt((vc-v1).^2+omega.^2.*(1+m).*Jc./m2));
xmax=y+xbar;
vmax=v1+(m.*(1+e).*(vc+omega.*y-v1))./(1+m+m2.*y.^2./Jc);

Vmax=vmax/(-v1);
Xmax=xmax/l;
ndJ0=30*J0/(rho*pi*l^5);
ndJc=30*Jc/(rho*pi*l^5);
ndL=L/l;

hold on
plot(R1,Xmax,'r')
```

MatLab File 36

Non-dimensional V_{MAX} versus non-dimensional location of max radius for T=49, 61 and 73 Nm (Figure 4.4)

```
l=33; d=2.5;
rmin=0.5;  rmax=1.375;
e=0.5; v1=-1575; rho=0.347;
m1=5; T=4000000;
P=0; L=23:0.1:l;

D=(2.*(P-L).*(rmax-rmin))./(L.^4-4*L.^3*P+8*L.*P^3-5*P^4-
6*L.*P^2+6*P^3);
C=(3*D.*(L.^2-P^2))./(2.*(P-L));
B=(3*D*P.*(P^2-L.^2-P))./(P-L);
A=rmin-B.*P-C.*P^2-D.*P^3;

m2=rho*pi*(A.^2*l+A.*B.*l^2+(2*A.*C+B.^2)*l^3/3+(2*A.*D+2*B.*C)*l^4/4+(
2*B.*D+C.^2)*l^5/5+2*C.*D*l^6/6+D.^2*l^7/7);
mom=rho*pi*(A.^2*l^2/2+2*A.*B.*l^3/3+(2*A.*C+B.^2)*l^4/4+(2*A.*D+2*B.*C
)*l^5/5+(2*B.*D+C.^2)*l^6/6+2*C.*D*l^7/7+D.^2*l^8/8);
J0=rho*pi*(A.^2*l^3/3+2*A.*B.*l^4/4+(2*A.*C+B.^2)*l^5/5+(2*A.*D+2*B.*C)
*l^6/6+(2*B.*D+C.^2)*l^7/7+2*C.*D*l^8/8+D.^2*l^9/9);
xbar=mom./m2;
Jc=J0-m2.*xbar.^2;
Jr=Jc+m2.*(xbar+d).^2;

omeganaught=20;
theta=pi;
omega=omeganaught+sqrt(2*T*theta./Jr);

vc=(d+xbar).*omega;
m=m2/m1;

y=(1./omega).*(-(vc-v1)+sqrt((vc-v1).^2+omega.^2.*(1+m).*Jc./m2));
xmax=y+xbar;
vmax=v1+(m.*(1+e).*(vc+omega.*y-v1))./(1+m+m2.*y.^2./Jc);

Vmax=vmax/(-v1);
Xmax=xmax/l;
M1=m2/(rho*pi*l^3);
ndJ0=30*J0/(rho*pi*l^5);
ndJc=30*Jc/(rho*pi*l^5);
ndL=L/l;

hold on
plot(ndL,Vmax,'r')
```

MatLab File 37

Angular velocity ω versus non-dimensional location of max radius for T=49, 61 and 73 Nm (Figure 4.5)

```
l=33; d=2.5;
rmin=0.5;  rmax=1.375;
e=0.5; v1=-1575; rho=0.347;
m1=5; T=4000000;
P=0; L=23:0.1:l;

D=(2.*(P-L).*(rmax-rmin))./(L.^4-4*L.^3*P+8*L.*P^3-5*P^4-
6*L.*P^2+6*P^3);
C=(3*D.*(L.^2-P^2))./(2.*(P-L));
B=(3*D*P.*(P^2-L.^2-P))./(P-L);
A=rmin-B.*P-C.*P^2-D.*P^3;

m2=rho*pi*(A.^2*l+A.*B.*l^2+(2*A.*C+B.^2)*l^3/3+(2*A.*D+2*B.*C)*l^4/4+(
2*B.*D+C.^2)*l^5/5+2*C.*D*l^6/6+D.^2*l^7/7);
mom=rho*pi*(A.^2*l^2/2+2*A.*B.*l^3/3+(2*A.*C+B.^2)*l^4/4+(2*A.*D+2*B.*C
)*l^5/5+(2*B.*D+C.^2)*l^6/6+2*C.*D*l^7/7+D.^2*l^8/8);
J0=rho*pi*(A.^2*l^3/3+2*A.*B.*l^4/4+(2*A.*C+B.^2)*l^5/5+(2*A.*D+2*B.*C)
*l^6/6+(2*B.*D+C.^2)*l^7/7+2*C.*D*l^8/8+D.^2*l^9/9);
xbar=mom./m2;
Jc=J0-m2.*xbar.^2;
Jr=Jc+m2.*(xbar+d).^2;

omeganaught=20;
theta=pi;
omega=omeganaught+sqrt(2*T*theta./Jr);

vc=(d+xbar).*omega;
m=m2/m1;

y=(1./omega).*(-(vc-v1)+sqrt((vc-v1).^2+omega.^2.*(1+m).*Jc./m2));
xmax=y+xbar;
vmax=v1+(m.*(1+e).*(vc+omega.*y-v1))./(1+m+m2.*y.^2./Jc);

Vmax=vmax/(-v1);
Xmax=xmax/l;
M1=m2/(rho*pi*l^3);
ndJ0=30*J0/(rho*pi*l^5);
ndJc=30*Jc/(rho*pi*l^5);
ndL=L/l;

hold on
plot(ndL,omega,'r')
```

MatLab File 38

Non-dimensional maximum outgoing velocity V_{MAX} versus non-dimensional location of max radius for constant mass and T=49, 61 and 73 Nm (Figure 4.6)

```
l=33; d=2.5;
rmin=0.5:0.0125:1.375;
e=0.5; v1=-1575; rho=0.347;
m1=5; T=2660000; m2=35;
M2=m2/(rho*pi*l^3);
P=0; L=l;
M=m2/m1;

A=rmin/l;
C=((-1/3)*A+sqrt((A.^2)/9-4*13/315*(A.^2-M2)))/(26/315);

R1=A+C/3;

rmax=R1*l;

MOM=(A.^2)/2+(7/30)*A.*C+(2/63)*C.^2;
Xbar=MOM/M2;
ndJ0=(A.^2)/3+(8/45)*A.*C+(29/1134)*C.^2;
J0=ndJ0*rho*pi*l^5;

xbar=Xbar*l;
Jc=J0-m2.*xbar.^2;
Jr=Jc+m2.*(xbar+d).^2;

omeganaught=20;
theta=pi;
omega=omeganaught+sqrt(2*T*theta./Jr);

vc=(d+xbar).*omega;
m=m2/m1;

y=(1./omega).*(-(vc-v1)+sqrt((vc-v1).^2+omega.^2.*(1+m).*Jc./m2));
xmax=y+xbar;
vmax=v1+(m.*(1+e).*(vc+omega.*y-v1))./(1+m+m2.*y.^2./Jc);

Vmax=vmax/(-v1);
Xmax=xmax/l;
ndJ0=30*J0/(rho*pi*l^5);
ndJc=30*Jc/(rho*pi*l^5);
ndL=L/l;

hold on
plot(R1,Vmax,'r')
```

MatLab File 39

Angular velocity ω versus non-dimensional location of max radius for constant mass and T=49, 61 and 73 Nm (Figure 4.7)

```
l=33; d=2.5;
rmin=0.5:0.0125:1.375;
e=0.5; v1=-1575; rho=0.347;
m1=5; T=2660000; m2=35;
M2=m2/(rho*pi*l^3);
P=0; L=l;
M=m2/m1;

A=rmin/l;
C=((-1/3)*A+sqrt((A.^2)/9-4*13/315*(A.^2-M2)))/(26/315);

R1=A+C/3;

rmax=R1*l;

MOM=(A.^2)/2+(7/30)*A.*C+(2/63)*C.^2;
Xbar=MOM/M2;
ndJ0=(A.^2)/3+(8/45)*A.*C+(29/1134)*C.^2;
J0=ndJ0*rho*pi*l^5;

xbar=Xbar*l;
Jc=J0-m2.*xbar.^2;
Jr=Jc+m2.*(xbar+d).^2;

omeganaught=20;
theta=pi;
omega=omeganaught+sqrt(2*T*theta./Jr);

vc=(d+xbar).*omega;
m=m2/m1;

y=(1./omega).*(-(vc-v1)+sqrt((vc-v1).^2+omega.^2.*(1+m).*Jc./m2));
xmax=y+xbar;
vmax=v1+(m.*(1+e).*(vc+omega.*y-v1))./(1+m+m2.*y.^2./Jc);

Vmax=vmax/(-v1);
Xmax=xmax/l;
ndJ0=30*J0/(rho*pi*l^5);
ndJc=30*Jc/(rho*pi*l^5);
ndL=L/l;

hold on
plot(R1,omega,'r')
```

MatLab File 40

Moment of Inertia about the center of rotation I_R versus cup depth h (Figure 4.8)

```
l=33; d=2.5;
rmin=0.5;  rmax=1.375;
e=0.5; v1=-1575; rho=0.347;
m1=5; T=3494000;
P=0; L=l;

Rc=1; h=0:.01:1;

D=(2.*(P-L).*(rmax-rmin))./(L.^4-4*L.^3*P+8*L.*P^3-5*P^4-
6*L.*P^2+6*P^3);
C=(3*D.*(L.^2-P^2))./(2.*(P-L));
B=(3*D*P.*(P^2-L.^2-P))./(P-L);
A=rmin-B.*P-C.*P^2-D.*P^3;

m2=rho*pi*(A.^2*l+A.*B.*l^2+(2*A.*C+B.^2)*l^3/3+(2*A.*D+2*B.*C)*l^4/4+(
2*B.*D+C.^2)*l^5/5+2*C.*D*l^6/6+D.^2*l^7/7);
mom=rho*pi*(A.^2*l^2/2+2*A.*B.*l^3/3+(2*A.*C+B.^2)*l^4/4+(2*A.*D+2*B.*C
)*l^5/5+(2*B.*D+C.^2)*l^6/6+2*C.*D*l^7/7+D.^2*l^8/8);
J0=rho*pi*(A.^2*l^3/3+2*A.*B.*l^4/4+(2*A.*C+B.^2)*l^5/5+(2*A.*D+2*B.*C)
*l^6/6+(2*B.*D+C.^2)*l^7/7+2*C.*D*l^8/8+D.^2*l^9/9);

mi=rho*pi*Rc^2*h/2;
momi=rho*pi*Rc^2*(l*h/2-h.^2/6);
J0i=rho*pi*Rc^2*(h.^3/12+l^2*h/2-l*h.^2/3);

xbar=(mom-momi)./m2;
Jc=(J0-J0i)-m2.*xbar.^2;
Jr=Jc+m2.*(xbar+d).^2;

omeganaught=20;
theta=pi;
omega=omeganaught+sqrt(2*T*theta./Jr);

vc=(d+xbar).*omega;
m=m2/m1;

y=(1./omega).*(-(vc-v1)+sqrt((vc-v1).^2+omega.^2.*(1+m).*Jc./m2));
xmax=y+xbar;
vmax=v1+(m.*(1+e).*(vc+omega.*y-v1))./(1+m+m2.*y.^2./Jc);

Vmax=vmax/(-v1);
Xmax=xmax/l;
M1=m2/(rho*pi*l^3);
ndJ0=30*J0/(rho*pi*l^5);
ndJc=30*Jc/(rho*pi*l^5);
ndL=L/l;

hold on
plot(h,Jr,'k')
```

MatLab File 41

Mass of the bat m_1 versus cup depth h (Figure 4.9)

```
l=33; d=2.5;
rmin=0.5;  rmax=1.375;
e=0.5; v1=-1575; rho=0.347;
m1=5; T=3494000;
P=0; L=l;

Rc=1; h=0:.01:1;

D=(2.*(P-L).*(rmax-rmin))./(L.^4-4*L.^3*P+8*L.*P^3-5*P^4-
6*L.*P^2+6*P^3);
C=(3*D.*(L.^2-P^2))./(2.*(P-L));
B=(3*D*P.*(P^2-L.^2-P))./(P-L);
A=rmin-B.*P-C.*P^2-D.*P^3;

m2=rho*pi*(A.^2*l+A.*B.*l^2+(2*A.*C+B.^2)*l^3/3+(2*A.*D+2*B.*C)*l^4/4+(
2*B.*D+C.^2)*l^5/5+2*C.*D*l^6/6+D.^2*l^7/7);
mom=rho*pi*(A.^2*l^2/2+2*A.*B.*l^3/3+(2*A.*C+B.^2)*l^4/4+(2*A.*D+2*B.*C
)*l^5/5+(2*B.*D+C.^2)*l^6/6+2*C.*D*l^7/7+D.^2*l^8/8);
J0=rho*pi*(A.^2*l^3/3+2*A.*B.*l^4/4+(2*A.*C+B.^2)*l^5/5+(2*A.*D+2*B.*C)
*l^6/6+(2*B.*D+C.^2)*l^7/7+2*C.*D*l^8/8+D.^2*l^9/9);

mi=rho*pi*Rc^2*h/2;
momi=rho*pi*Rc^2*(l*h/2-h.^2/6);
J0i=rho*pi*Rc^2*(h.^3/12+l^2*h/2-l*h.^2/3);

xbar=(mom-momi)./m2;
Jc=(J0-J0i)-m2.*xbar.^2;
Jr=Jc+m2.*(xbar+d).^2;

omeganaught=20;
theta=pi;
omega=omeganaught+sqrt(2*T*theta./Jr);

vc=(d+xbar).*omega;
m=m2/m1;

y=(1./omega).*(-(vc-v1)+sqrt((vc-v1).^2+omega.^2.*(1+m).*Jc./m2));
xmax=y+xbar;
vmax=v1+(m.*(1+e).*(vc+omega.*y-v1))./(1+m+m2.*y.^2./Jc);

Vmax=vmax/(-v1);
Xmax=xmax/l;
M1=m2/(rho*pi*l^3);
ndJ0=30*J0/(rho*pi*l^5);
ndJc=30*Jc/(rho*pi*l^5);
ndL=L/l;

hold on
plot(h,(m2-mi),'k')
```

MatLab File 42

Angular velocity ω versus cup depth h (Figure 4.10)

```
l=33; d=2.5;
rmin=0.5;  rmax=1.375;
e=0.5; v1=-1575; rho=0.347;
m1=5; T=3494000;
P=0; L=l;

Rc=1; h=0:.01:1;

D=(2.*(P-L).*(rmax-rmin))./(L.^4-4*L.^3*P+8*L.*P^3-5*P^4-
6*L.*P^2+6*P^3);
C=(3*D.*(L.^2-P^2))./(2.*(P-L));
B=(3*D*P.*(P^2-L.^2-P))./(P-L);
A=rmin-B.*P-C.*P^2-D.*P^3;

m2=rho*pi*(A.^2*l+A.*B.*l^2+(2*A.*C+B.^2)*l^3/3+(2*A.*D+2*B.*C)*l^4/4+(
2*B.*D+C.^2)*l^5/5+2*C.*D*l^6/6+D.^2*l^7/7);
mom=rho*pi*(A.^2*l^2/2+2*A.*B.*l^3/3+(2*A.*C+B.^2)*l^4/4+(2*A.*D+2*B.*C
)*l^5/5+(2*B.*D+C.^2)*l^6/6+2*C.*D*l^7/7+D.^2*l^8/8);
J0=rho*pi*(A.^2*l^3/3+2*A.*B.*l^4/4+(2*A.*C+B.^2)*l^5/5+(2*A.*D+2*B.*C)
*l^6/6+(2*B.*D+C.^2)*l^7/7+2*C.*D*l^8/8+D.^2*l^9/9);

mi=rho*pi*Rc^2*h/2;
momi=rho*pi*Rc^2*(l*h/2-h.^2/6);
J0i=rho*pi*Rc^2*(h.^3/12+l^2*h/2-l*h.^2/3);

xbar=(mom-momi)./m2;
Jc=(J0-J0i)-m2.*xbar.^2;
Jr=Jc+m2.*(xbar+d).^2;

omeganaught=20;
theta=pi;
omega=omeganaught+sqrt(2*T*theta./Jr);

vc=(d+xbar).*omega;
m=m2/m1;

y=(1./omega).*(-(vc-v1)+sqrt((vc-v1).^2+omega.^2.*(1+m).*Jc./m2));
xmax=y+xbar;
vmax=v1+(m.*(1+e).*(vc+omega.*y-v1))./(1+m+m2.*y.^2./Jc);

Vmax=vmax/(-v1);
Xmax=xmax/l;
M1=m2/(rho*pi*l^3);
ndJ0=30*J0/(rho*pi*l^5);
ndJc=30*Jc/(rho*pi*l^5);
ndL=L/l;

hold on
plot(h,omega,'k')
```

MatLab File 43

Non-dimensional maximum outgoing velocity V_{MAX} versus cup depth h (Figure 4.11)

```
l=33; d=2.5;
rmin=0.5;  rmax=1.375;
e=0.5; v1=-1575; rho=0.347;
m1=5; T=3494000;
P=0; L=l;

Rc=1; h=0:.01:1;

D=(2.*(P-L).*(rmax-rmin))./(L.^4-4*L.^3*P+8*L.*P^3-5*P^4-
6*L.*P^2+6*P^3);
C=(3*D.*(L.^2-P^2))./(2.*(P-L));
B=(3*D*P.*(P^2-L.^2-P))./(P-L);
A=rmin-B.*P-C.*P^2-D.*P^3;

m2=rho*pi*(A.^2*l+A.*B.*l^2+(2*A.*C+B.^2)*l^3/3+(2*A.*D+2*B.*C)*l^4/4+(
2*B.*D+C.^2)*l^5/5+2*C.*D*l^6/6+D.^2*l^7/7);
mom=rho*pi*(A.^2*l^2/2+2*A.*B.*l^3/3+(2*A.*C+B.^2)*l^4/4+(2*A.*D+2*B.*C
)*l^5/5+(2*B.*D+C.^2)*l^6/6+2*C.*D*l^7/7+D.^2*l^8/8);
J0=rho*pi*(A.^2*l^3/3+2*A.*B.*l^4/4+(2*A.*C+B.^2)*l^5/5+(2*A.*D+2*B.*C)
*l^6/6+(2*B.*D+C.^2)*l^7/7+2*C.*D*l^8/8+D.^2*l^9/9);

mi=rho*pi*Rc^2*h/2;
momi=rho*pi*Rc^2*(l*h/2-h.^2/6);
J0i=rho*pi*Rc^2*(h.^3/12+l^2*h/2-l*h.^2/3);

xbar=(mom-momi)./m2;
Jc=(J0-J0i)-m2.*xbar.^2;
Jr=Jc+m2.*(xbar+d).^2;

omeganaught=20;
theta=pi;
omega=omeganaught+sqrt(2*T*theta./Jr);

vc=(d+xbar).*omega;
m=m2/m1;

y=(1./omega).*(-(vc-v1)+sqrt((vc-v1).^2+omega.^2.*(1+m).*Jc./m2));
xmax=y+xbar;
vmax=v1+(m.*(1+e).*(vc+omega.*y-v1))./(1+m+m2.*y.^2./Jc);

Vmax=vmax/(-v1);
Xmax=xmax/l;
M1=m2/(rho*pi*l^3);
ndJ0=30*J0/(rho*pi*l^5);
ndJc=30*Jc/(rho*pi*l^5);
ndL=L/l;

hold on
plot(h,Vmax,'k')
```

MatLab File 44

Non-dimensional location of maximum outgoing velocity X_{MAX} versus cup depth h (Figure 4.12)

```
l=33; d=2.5;
rmin=0.5;  rmax=1.375;
e=0.5; v1=-1575; rho=0.347;
m1=5; T=3494000;
P=0; L=l;

Rc=1; h=0:.01:1;

D=(2.*(P-L).*(rmax-rmin))./(L.^4-4*L.^3*P+8*L.*P^3-5*P^4-
6*L.*P^2+6*P^3);
C=(3*D.*(L.^2-P^2))./(2.*(P-L));
B=(3*D*P.*(P^2-L.^2-P))./(P-L);
A=rmin-B.*P-C.*P^2-D.*P^3;

m2=rho*pi*(A.^2*l+A.*B.*l^2+(2*A.*C+B.^2)*l^3/3+(2*A.*D+2*B.*C)*l^4/4+(
2*B.*D+C.^2)*l^5/5+2*C.*D*l^6/6+D.^2*l^7/7);
mom=rho*pi*(A.^2*l^2/2+2*A.*B.*l^3/3+(2*A.*C+B.^2)*l^4/4+(2*A.*D+2*B.*C
)*l^5/5+(2*B.*D+C.^2)*l^6/6+2*C.*D*l^7/7+D.^2*l^8/8);
J0=rho*pi*(A.^2*l^3/3+2*A.*B.*l^4/4+(2*A.*C+B.^2)*l^5/5+(2*A.*D+2*B.*C)
*l^6/6+(2*B.*D+C.^2)*l^7/7+2*C.*D*l^8/8+D.^2*l^9/9);

mi=rho*pi*Rc^2*h/2;
momi=rho*pi*Rc^2*(l*h/2-h.^2/6);
J0i=rho*pi*Rc^2*(h.^3/12+l^2*h/2-l*h.^2/3);

xbar=(mom-momi)./m2;
Jc=(J0-J0i)-m2.*xbar.^2;
Jr=Jc+m2.*(xbar+d).^2;

omeganaught=20;
theta=pi;
omega=omeganaught+sqrt(2*T*theta./Jr);

vc=(d+xbar).*omega;
m=m2/m1;

y=(1./omega).*(-(vc-v1)+sqrt((vc-v1).^2+omega.^2.*(1+m).*Jc./m2));
xmax=y+xbar;
vmax=v1+(m.*(1+e).*(vc+omega.*y-v1))./(1+m+m2.*y.^2./Jc);

Vmax=vmax/(-v1);
Xmax=xmax/l;
M1=m2/(rho*pi*l^3);
ndJ0=30*J0/(rho*pi*l^5);
ndJc=30*Jc/(rho*pi*l^5);
ndL=L/l;

hold on
plot(h,Xmax,'k')
```